GGI School on Astroparticle physics
11-22 March 2024

TUTORIAL FOR AXION LECTURES

Alessandro Mirizzi
(Bari Univ. & INFN BARI)
e-mail: alessandro.mirizzi@ba.infn.it

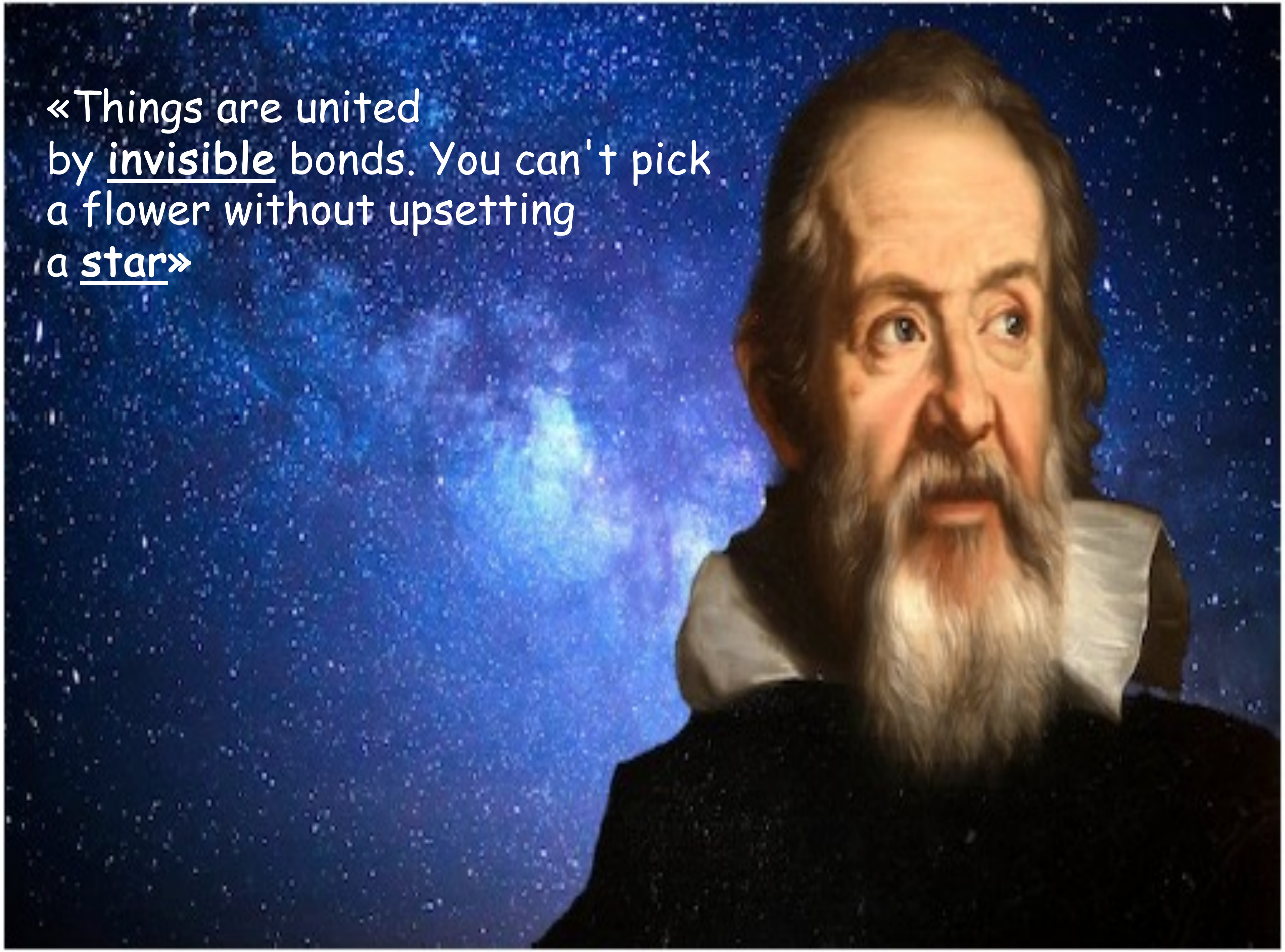
«Things are united
by invisible bonds. You can't pick
a flower without upsetting
a star»

REFERENCES

Axion Theory

- R.D. Peccei «The Axions and the Strong CP problem», hep-ph/0607268

- Di Luzio, Giannotti, Nardi, Visinelli «The landscape of QCD axion models», 2003.01100

Axion Cosmology

- P. Sikivie, «Axion Cosmology», astro-ph/0610440

- L. Di Luzio, M. Giannotti, E. Nardi, L. Visinelli «The landscape of QCD axion models», 2003.01100

Axion Astrophysics

- A. Caputo, G. Raffelt, «Astrophysical Axion Bounds: the 2024 Edition», 2401.13728

Axion Experiments

- I. Irastorza, J. Redondo, «New experimental approaches in the searches for axion-like particles», 1801.08127

THE STRONG CP PROBLEM

The QCD Lagrangian includes a term which violates CP (and T)

$$\mathcal{L}_{CP} \propto \theta \frac{\alpha_s}{8\pi} G \cdot \tilde{G}$$

where $\theta \equiv \theta_{QCD} - \arg \det M_q$

Prediction of an electric dipole moment for the neutron:

$$|d_n| < 2.4(1.0) \times 10^{-16} \theta \; e\, cm$$

Present experimental limit : $|d_n| < 1.8 \times 10^{-26} \; e\, cm$

[Abel et al., 2001.1196]

$$|\theta| \lesssim 10^{-10}$$ Why so small ?

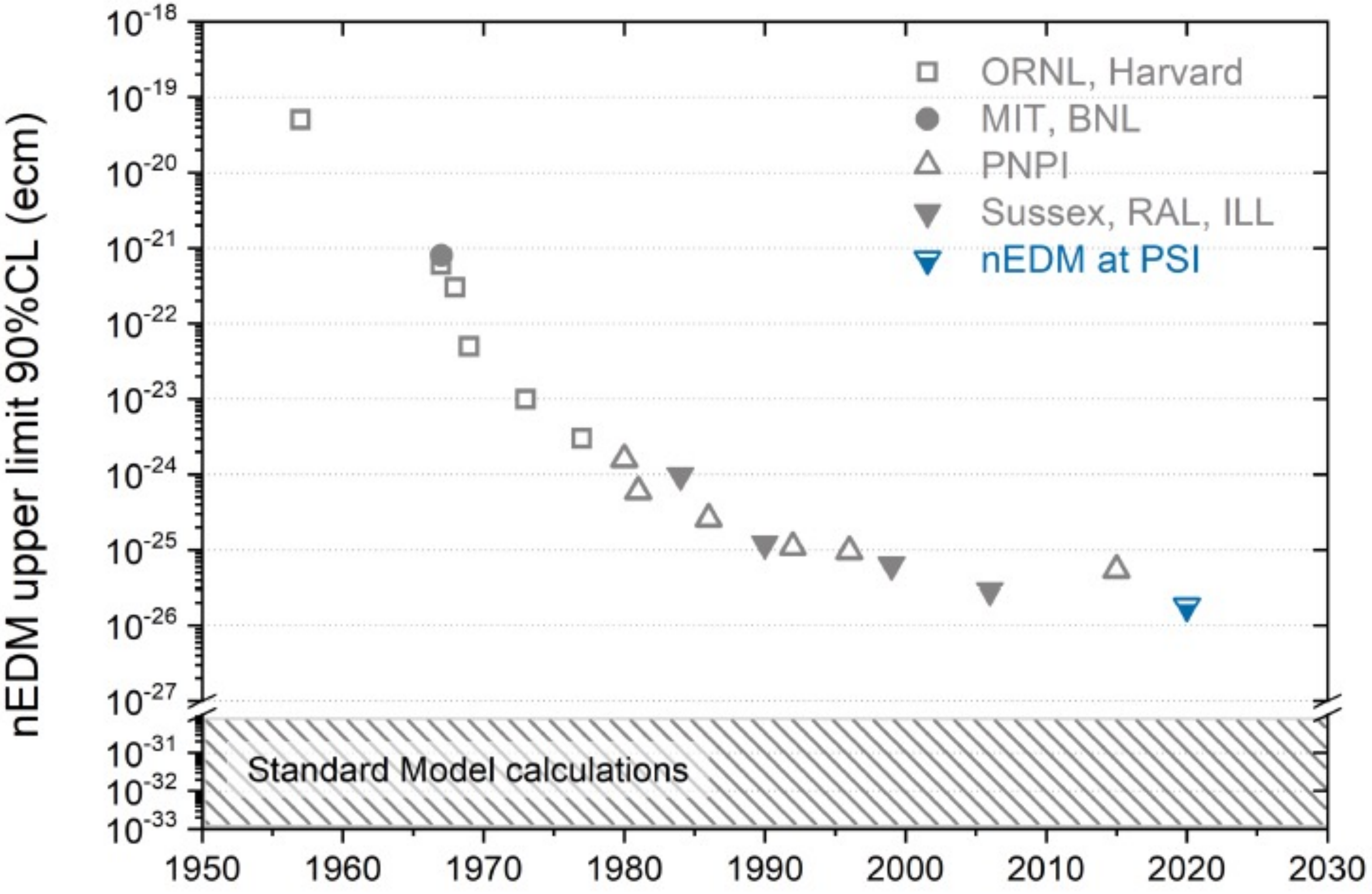
nEDM upper limit 90%CL (ecm)
10^-18
10^-19
10^-20
10^-21
10^-22
10^-23
10^-24
10^-25
10^-26
10^-27
10^-31
10^-32
10^-33
1950
1960
1970
1980
1990
2000
2010
2020
2030
ORNL, Harvard
MIT, BNL
PNPI
Sussex, RAL, ILL
nEDM at PSI
Standard Model calculations

THE PECCEI-QUINN MECHANISM

[Peccei & Quinn 1977, Wilczek 1978, Weinberg 1978]

- **PQ Symmetry**

Introduce a symmetry that results in a term which **dynamically minimize** θ.

Introduction of a new global $U(1)_{PQ}$ simmetry, spontaneously broken at a scale f_a.

⇒ **Existence of a massless pseudoscalar field a(x), the axion, interacting with the gluon field.**

Re-interpret θ as a dynamical variable: $\theta \to \frac{a(x)}{f_a}$

$$\mathcal{L}_\theta \to \mathcal{L}_a = \frac{1}{2}\left(\partial_\mu a\right)^2 - \frac{\alpha_s}{8\pi f_a} a\, G\cdot\tilde{G}$$

AXION POTENTIAL

[Grilli Cortona et al, 1511.02867]

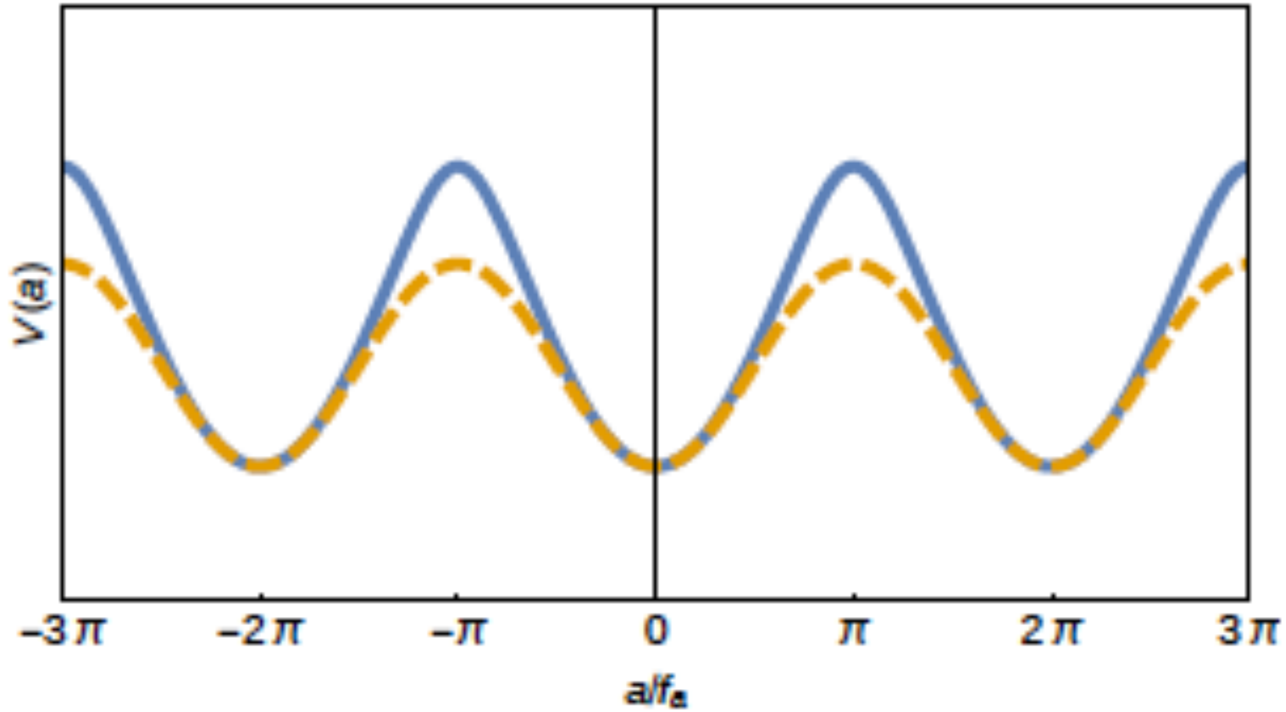

Figure 1: Comparison between the axion potential predicted by chiral Lagrangians, eq. (10) (continuous line) and the single cosine instanton one, $V^{inst}(a) = -m_a^2 f_a^2 \cos(a/f_a)$ (dashed line).

At low energy (Λ_{QCD}) the *gga* vertex generates the potential *V(a)* which has its minimun at $a_0=0$, restoring dynamically CP-simmetry.

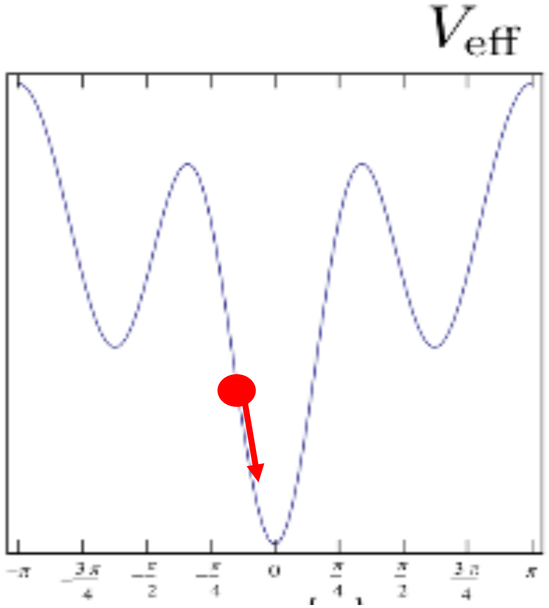

Potential (mass term) induced by L_a drives a(x) to CP-conserving minimum

CP-symmetry dynamically restored

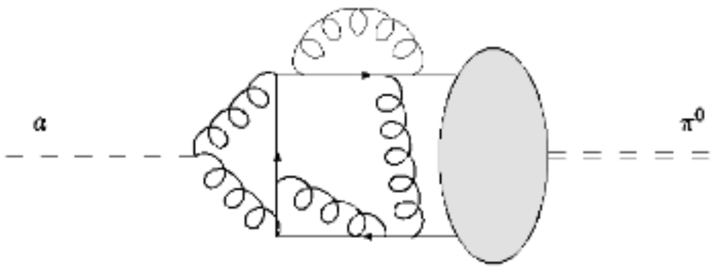

Axions generically couple to gluons and mix with π^0

Axions pick up a small mass

Recent precise determination (ChPT, Lattice QCD)

$$m_a = 5.691(51) \left(\frac{10^9\ GeV}{f_a}\right) meV$$

[Grilli Cortona et al, 2016
Borsanyi et al., 2016
Gorghetto, Villadoro 2019]

AXION PROPERTIES

Gluon coupling (Generic property)	$L_{aG} = \frac{\alpha_s}{8\pi f_a} G\tilde{G}a$	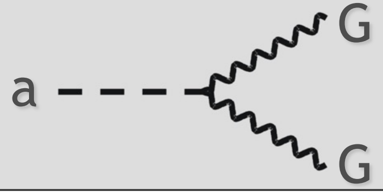
Photon coupling	$L_{a\gamma} = -\frac{g_{a\gamma}}{4} F\tilde{F}a = g_{a\gamma}\vec{E}\cdot\vec{B}a$ $g_{a\gamma} = \frac{\alpha}{2\pi f_a}\left(\frac{E}{N} - 1.92\right)$	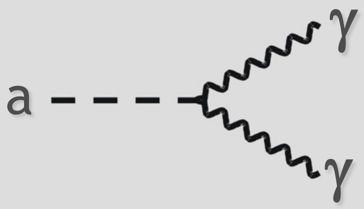
Pion coupling	$L_{a\pi} = \frac{C_{a\pi}}{f_a f_\pi}(\pi^0\pi^+\partial_\mu\pi^- + \ldots)\partial^\mu a$	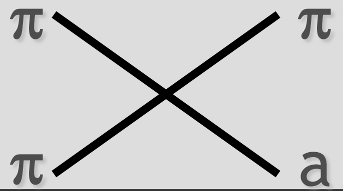
Nucleon coupling (axial vector)	$L_{aN} = \frac{C_N}{2f_a}\overline{\Psi}_N\gamma^\mu\gamma_5\Psi_N\,\partial_\mu a$	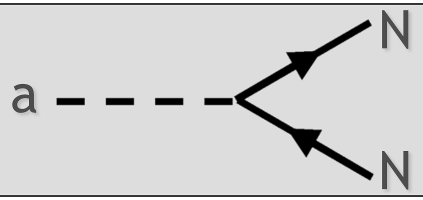
Electron coupling (optional absent for hadronic axions)	$L_{ae} = \frac{C_e}{2f_a}\overline{\Psi}_e\gamma^\mu\gamma_5\Psi_e\,\partial_\mu a$	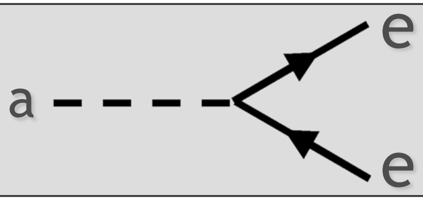

Slide by G. Raffelt

MAIN AXION MODELS

[see Di Luzio, Giannotti, Nardi & Visinelli, Phys. Rept. 870, 1-117 (2020), 2003.0110 [hep-ph]]

- DFSZ (Dine, Fischler, Srednicki, Zhitniskii) model

  ✓ Axions coupling to fermions and photons

- KSVZ (Kim, Shifman, Vainshetein, Zakharov) model (hadronic axions)

  ✓ tree-level coupling to quarks and leptons suppressed
  ✓ Nucleon and photon couplings still possible
  ✓ Evades bounds of DFSZ model

AXION BAND

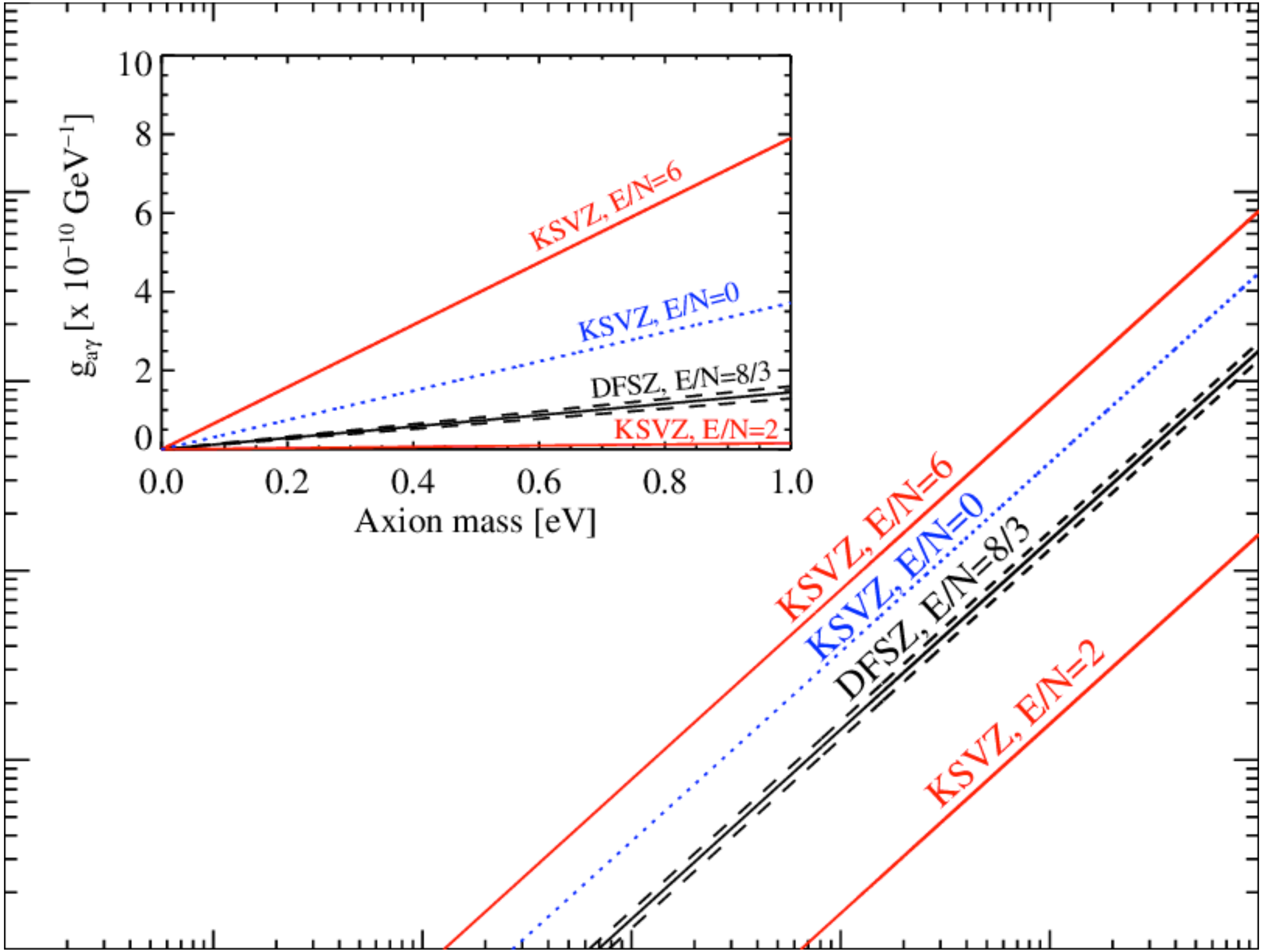

KSVZ, E/N=6
KSVZ, E/N=0
DFSZ, E/N=8/3
KSVZ, E/N=2
$g_{a\gamma}$ [x 10^{-10} GeV^{-1}]
Axion mass [eV]
0
2
4
6
8
10
0.0
0.2
0.4
0.6
0.8
1.0

STRING AXIVERSE

- Spectrum of low-energy effective theory in (3+1)-dimensions is supersymmetric and possibly contains several kinds of very weakly interacting slim particles (WISPs): Axion, ALPs (Axion-Like Particles)

- An axiverse - QCD axion plus possibly many ultra-light ALPs whose mass spectrum is logarithmically hierarchical – may naturally arise from strings [*Arvanitaki et al., arXiV: 0905.4702*]

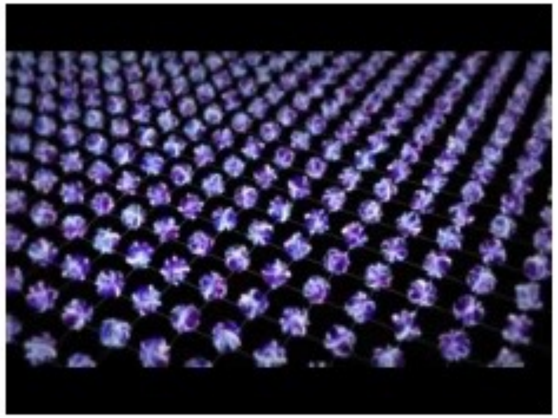

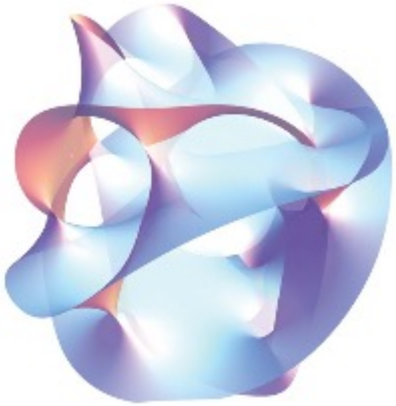

ALPs FROM STRING THEORY

[Witten '87, Conlon '06, Svrcek, Witten '06,….]

- String theory needs Extra Dimensions

Must compactify

- Shape and size deformations of Extra-D correspond to fields: Moduli and Axions
  Connected to the fundamental scale string scale

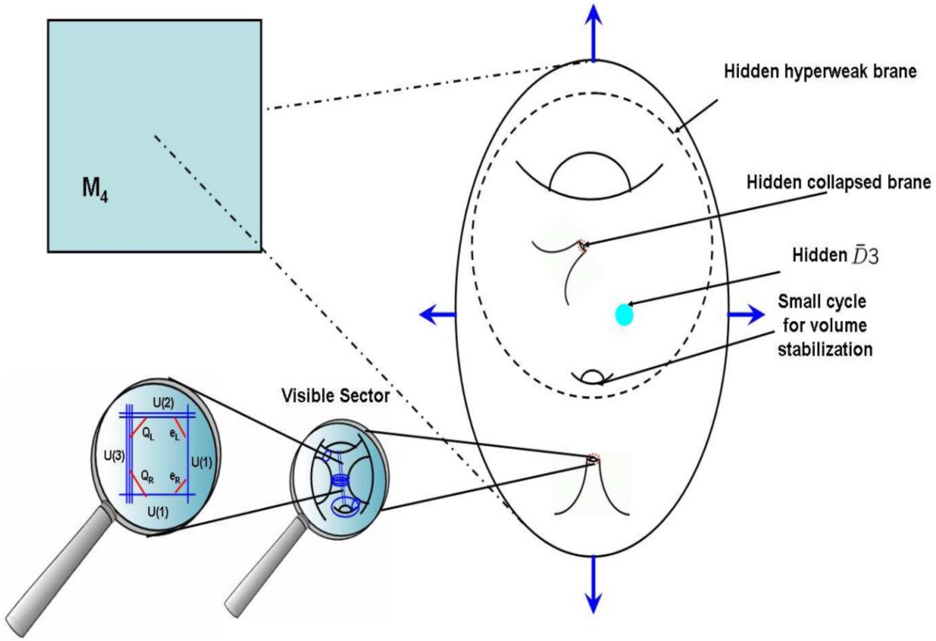

Compactification of type II string theories

- *[See J. Jaeckel & A. Ringwald, arXiv:1002.0329 for a review]*
- *[See M. Cicoli, M. Goodsell & A. Ringwald, arXiv:1206.0819 for a specific model in type IIB string]*

AXIONS AND MODULI

- Gauge field terms

$$\mathcal{L} = -\frac{1}{4g^2}F^2 - \frac{\theta}{32\pi^2}F\tilde{F}$$

+ Supersymmetry/supergravity

$$\mathcal{L} = \mathrm{Re}[f(\Phi)]F^2 + \mathrm{Im}[f(\Phi)]F\tilde{F}$$

Scalar moduli coupling — Pseudoscalar ALP coupling

- Gauge couplings always field dependent
  (no free coupling constants)
- Axions + Moduli always present in String theory

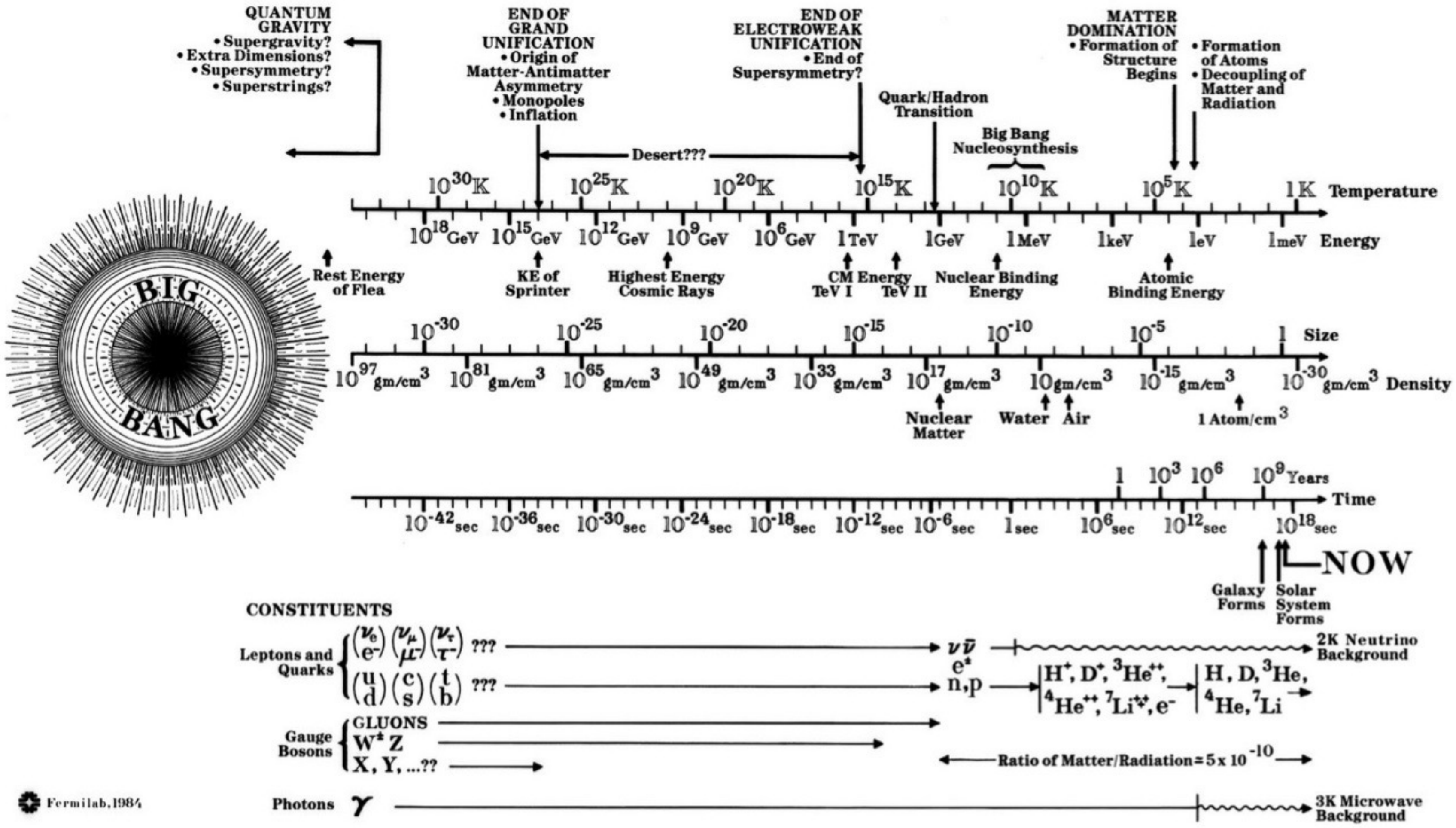

QUANTUM GRAVITY
• Supergravity?
• Extra Dimensions?
• Supersymmetry?
• Superstrings?
END OF GRAND UNIFICATION
• Origin of Matter-Antimatter Asymmetry
• Monopoles
• Inflation
Desert???
END OF ELECTROWEAK UNIFICATION
• End of Supersymmetry?
Quark/Hadron Transition
Big Bang Nucleosynthesis
MATTER DOMINATION
• Formation of Structure Begins
• Formation of Atoms
• Decoupling of Matter and Radiation
10^{30}K
10^{25}K
10^{20}K
10^{15}K
10^{10}K
10^{5}K
1 K
Temperature
10^{18}GeV
10^{15}GeV
10^{12}GeV
10^{9}GeV
10^{6}GeV
1 TeV
1 GeV
1 MeV
1 keV
1 eV
1 meV
Energy
BIG BANG
Rest Energy of Flea
KE of Sprinter
Highest Energy Cosmic Rays
CM Energy
TeV I
TeV II
Nuclear Binding Energy
Atomic Binding Energy
10^{-30}
10^{-25}
10^{-20}
10^{-15}
10^{-10}
10^{-5}
1
Size
10^{97} gm/cm^3
10^{81} gm/cm^3
10^{65} gm/cm^3
10^{49} gm/cm^3
10^{33} gm/cm^3
10^{17} gm/cm^3
10 gm/cm^3
10^{-15} gm/cm^3
10^{-30} gm/cm^3
Density
Nuclear Matter
Water
Air
1 Atom/cm^3
1
10^{3}
10^{6}
10^{9} Years
Time
10^{-42}sec
10^{-36}sec
10^{-30}sec
10^{-24}sec
10^{-18}sec
10^{-12}sec
10^{-6}sec
1 sec
10^{6}sec
10^{12}sec
10^{18}sec
NOW
Galaxy Forms
Solar System Forms
CONSTITUENTS
Leptons and Quarks
$\binom{\nu_e}{e^-}\binom{\nu_\mu}{\mu^-}\binom{\nu_\tau}{\tau^-}$???
$\binom{u}{d}\binom{c}{s}\binom{t}{b}$???
$\nu\bar{\nu}$
$e^{\pm}$
n,p
H^+, D^+, $^3He^{++}$, $^4He^{++}$, $^7Li^{+++}$, e^-
H, D, ^{3}He, ^{4}He, ^{7}Li
2K Neutrino Background
Gauge Bosons
GLUONS
$W^{\pm}$ Z
X, Y, ...??
Ratio of Matter/Radiation = 5×10^{-10}
Photons γ
3K Microwave Background
Fermilab, 1984

Event	time t	redshift z	temperature T
Inflation	10^{-34} s (?)	–	–
Baryogenesis	?	?	?
EW phase transition	20 ps	10^{15}	100 GeV
QCD phase transition	20 μs	10^{12}	150 MeV
Dark matter freeze-out	?	?	?
Neutrino decoupling	1 s	6×10^9	1 MeV
Electron-positron annihilation	6 s	2×10^9	500 keV
Big Bang nucleosynthesis	3 min	4×10^8	100 keV
Matter-radiation equality	60 kyr	3400	0.75 eV
Recombination	260–380 kyr	1100–1400	0.26–0.33 eV
Photon decoupling	380 kyr	1000–1200	0.23–0.28 eV
Reionization	100–400 Myr	11–30	2.6–7.0 meV
Dark energy-matter equality	9 Gyr	0.4	0.33 meV
Present	13.8 Gyr	0	0.24 meV

Table 3.1: *Key events in the thermal history of the universe.*

$T \sim 1\ eV$

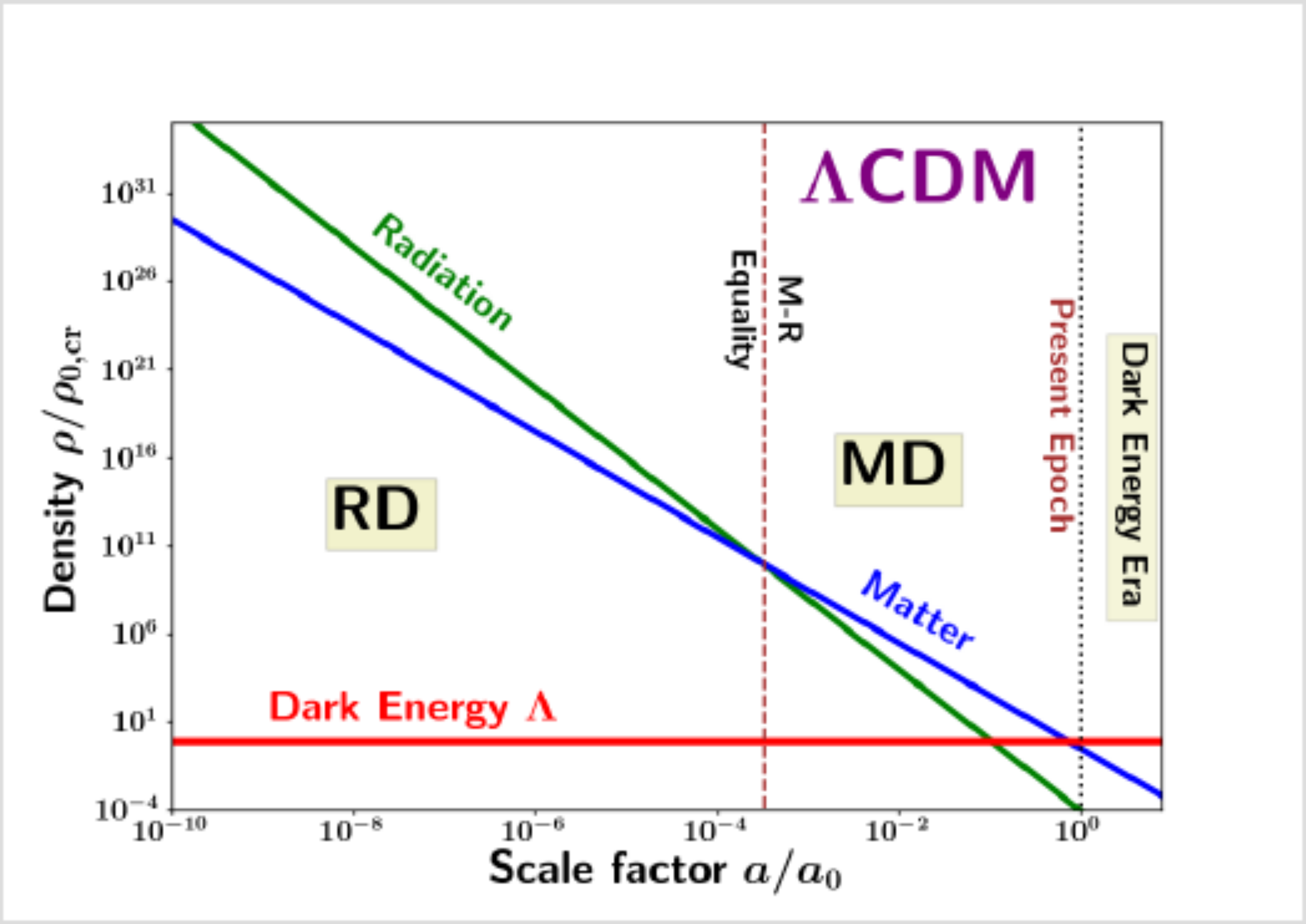

ΛCDM
Radiation
Matter
Dark Energy Λ
M-R Equality
Present Epoch
Dark Energy Era
RD
MD
Density $\rho/\rho_{0,\mathrm{cr}}$
Scale factor a/a_0
10^{31}
10^{26}
10^{21}
10^{16}
10^{11}
10^{6}
10^{1}
10^{-4}
10^{-10}
10^{-8}
10^{-6}
10^{-4}
10^{-2}
10^{0}

Standard Model Degrees of Freedom

- Since the masses and spin states of the particles of the Standard Model are known, we can easily calculate $g_\star(T)$
- At early times and high temperatures $T \gtrsim 100\,\mathrm{GeV}$

$$g_\star = g_b + \frac{7}{8} g_f \;=\; 106.75$$

type		mass	spin	g
quarks	$t, \bar{t}$	173 GeV	$\frac{1}{2}$	$2 \cdot 2 \cdot 3 = 12$
	$b, \bar{b}$	4 GeV		
	$c, \bar{c}$	1 GeV		
	$s, \bar{s}$	100 MeV		
	$d, \bar{s}$	5 MeV		
	$u, \bar{u}$	2 MeV		
gluons	g_i	0	1	$8 \cdot 2 = 16$
leptons	$\tau^\pm$	1777 MeV	$\frac{1}{2}$	$2 \cdot 2 = 4$
	$\mu^\pm$	106 MeV		
	$e^\pm$	511 keV		
	$\nu_\tau, \bar{\nu}_\tau$	< 0.6 eV	$\frac{1}{2}$	$2 \cdot 1 = 2$
	$\nu_\mu, \bar{\nu}_\mu$	< 0.6 eV		
	$\nu_e, \bar{\nu}_e$	< 0.6 eV		
gauge bosons	W^+	80 GeV	1	3
	W^-	80 GeV		
	Z^0	91 GeV		
	γ	0		2
Higgs boson	H^0	125 GeV	0	1

$g_b = 28$ photons (2), $W^\pm$ and Z^0 $(3 \cdot 3)$, gluons $(8 \cdot 2)$, and Higgs (1)

$g_f = 90$ quarks $(6 \cdot 12)$, charged leptons $(3 \cdot 4)$, and neutrinos $(3 \cdot 2)$

Table Credit: Baumann

Standard Model Thermal History

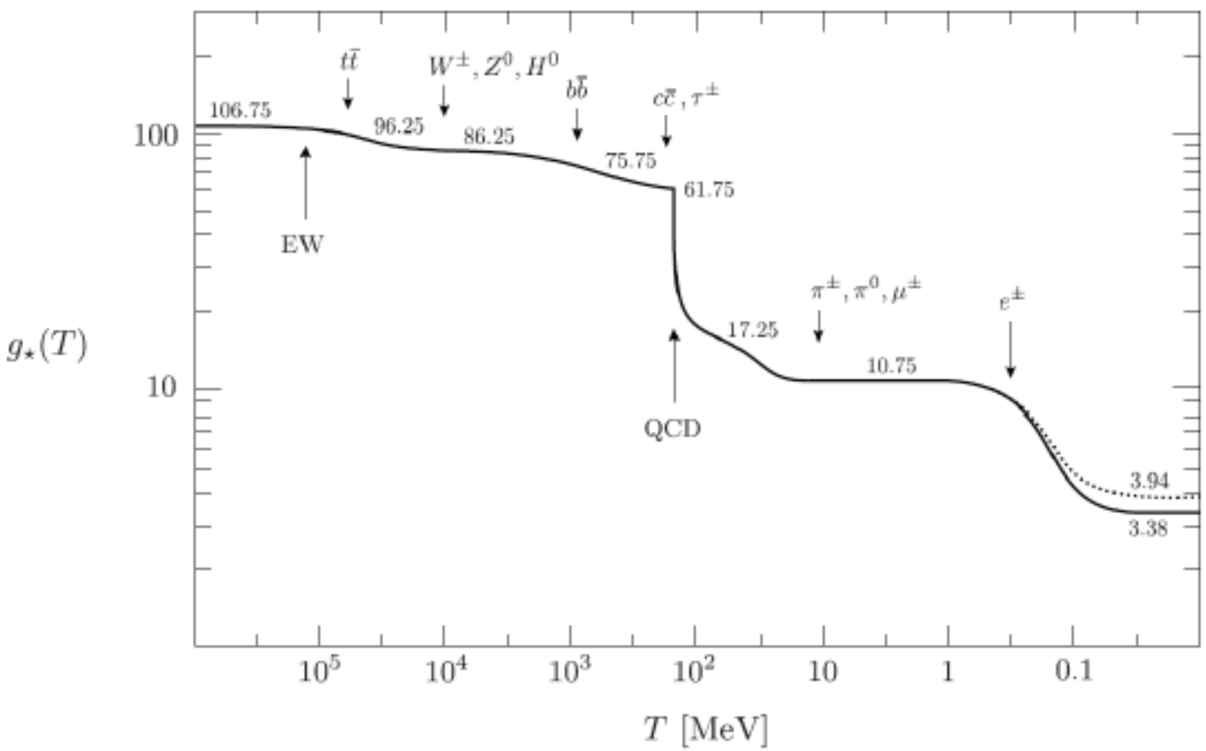

- As the temperature drops below particle masses, those particles fall out of equilibrium and $g_\star(T)$ decreases
- There is a large drop in $g_\star(T)$ at the QCD phase transition, when the degrees of freedom change from quarks and gluons to mesons and baryons

$$g_\star(T > \Lambda_{\rm QCD}) = 2 + 2 \times 8 + \frac{7}{8}(3 \times 12 + 4 + 4 + 3 \times 2) = 61.75$$

photons gluons u, d, s e μ ν

$$g_\star(T < \Lambda_{\rm QCD}) = 2 + 3 + \frac{7}{8}(4 + 4 + 3 \times 2) = 17.25$$

photons π e μ ν

Image Credit: Baumann

AXION THERMALIZATION

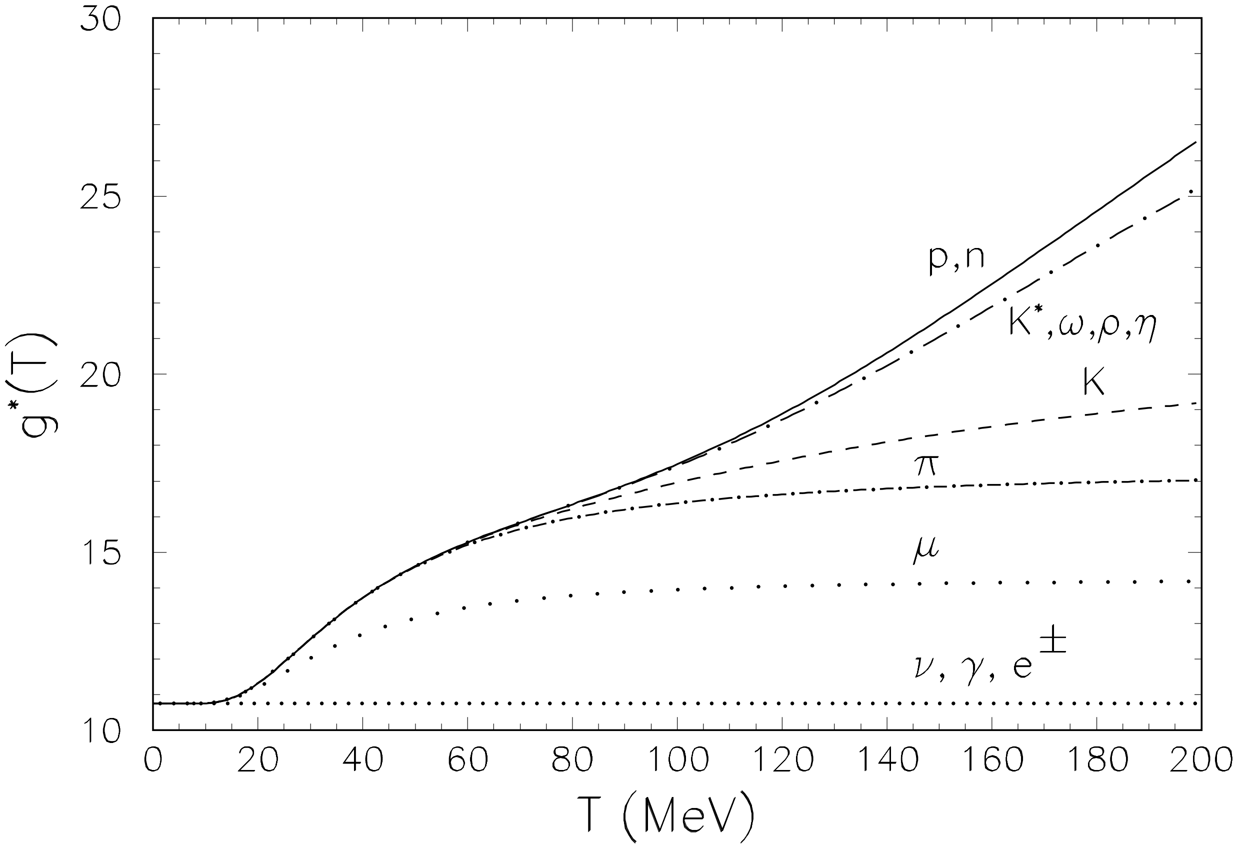

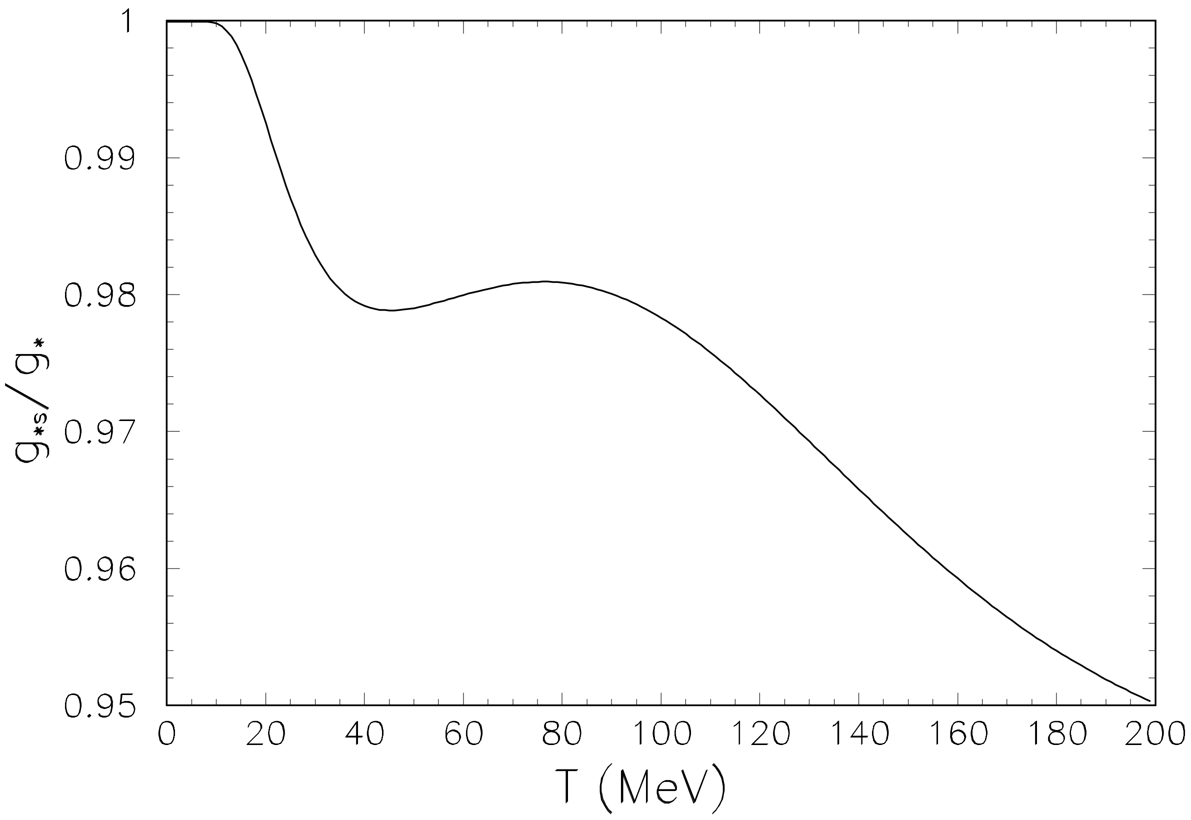

hep-ph/0504059

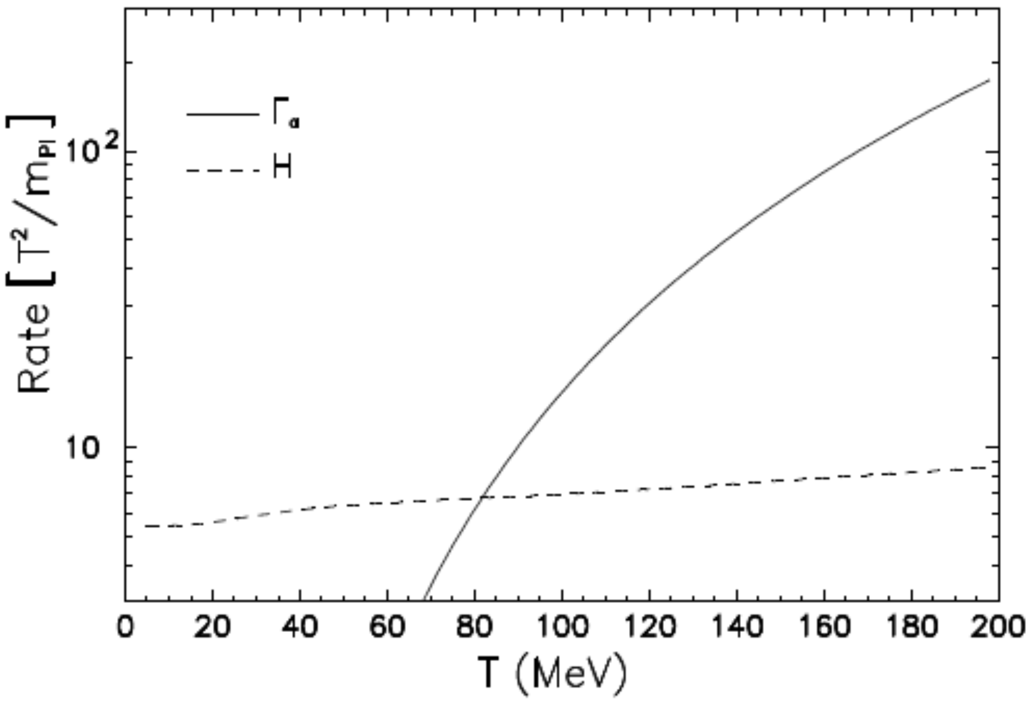

Figure 3. Average axion absorption rate for $f_a = 10^7$ GeV and cosmic expansion rate as a function of the cosmic temperature. Rates are in units of $T^2/m_{\rm Pl}$.

hep-ph/0504059

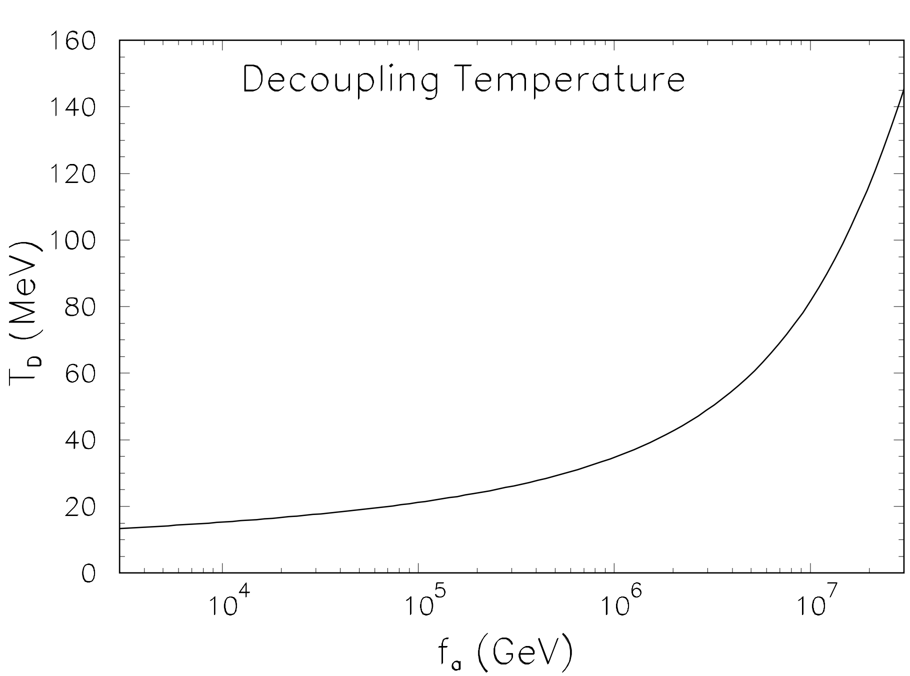

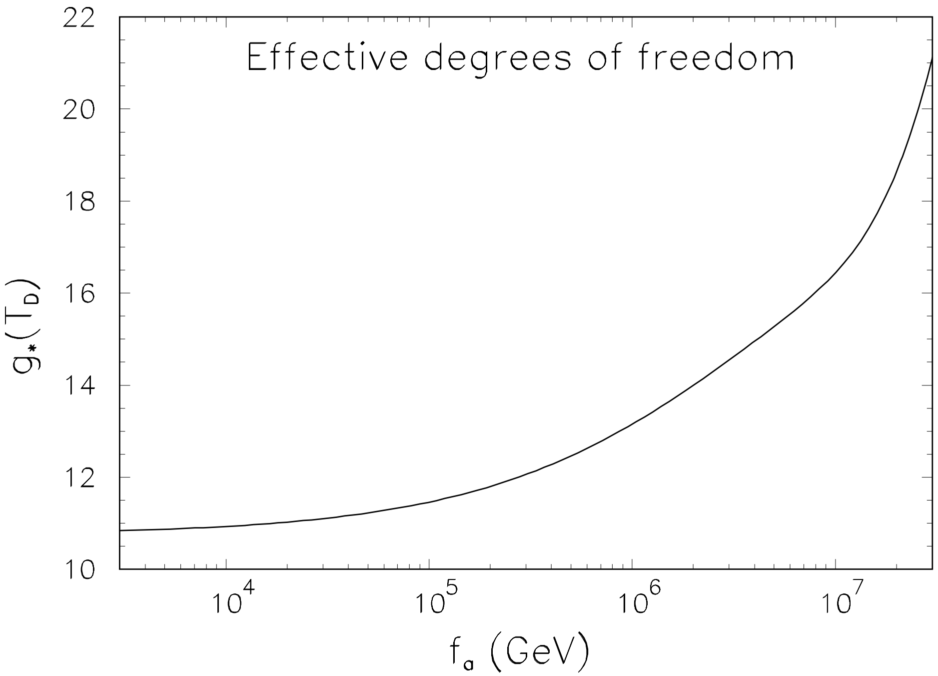

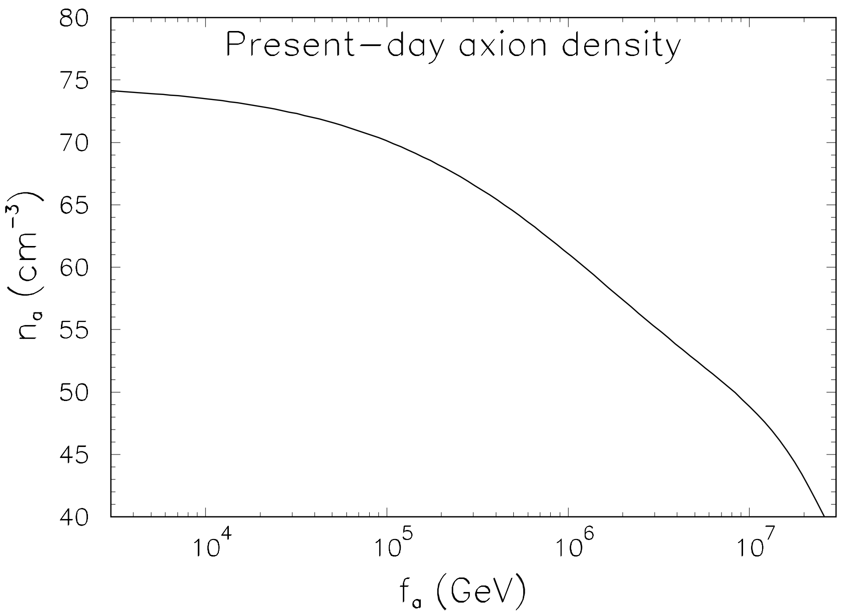

hep-ph/0504059

FORMATION OF STRUCTURE

$m_{\nu} = 0$ $\qquad$ $m_{\nu} = 1.9$ eV

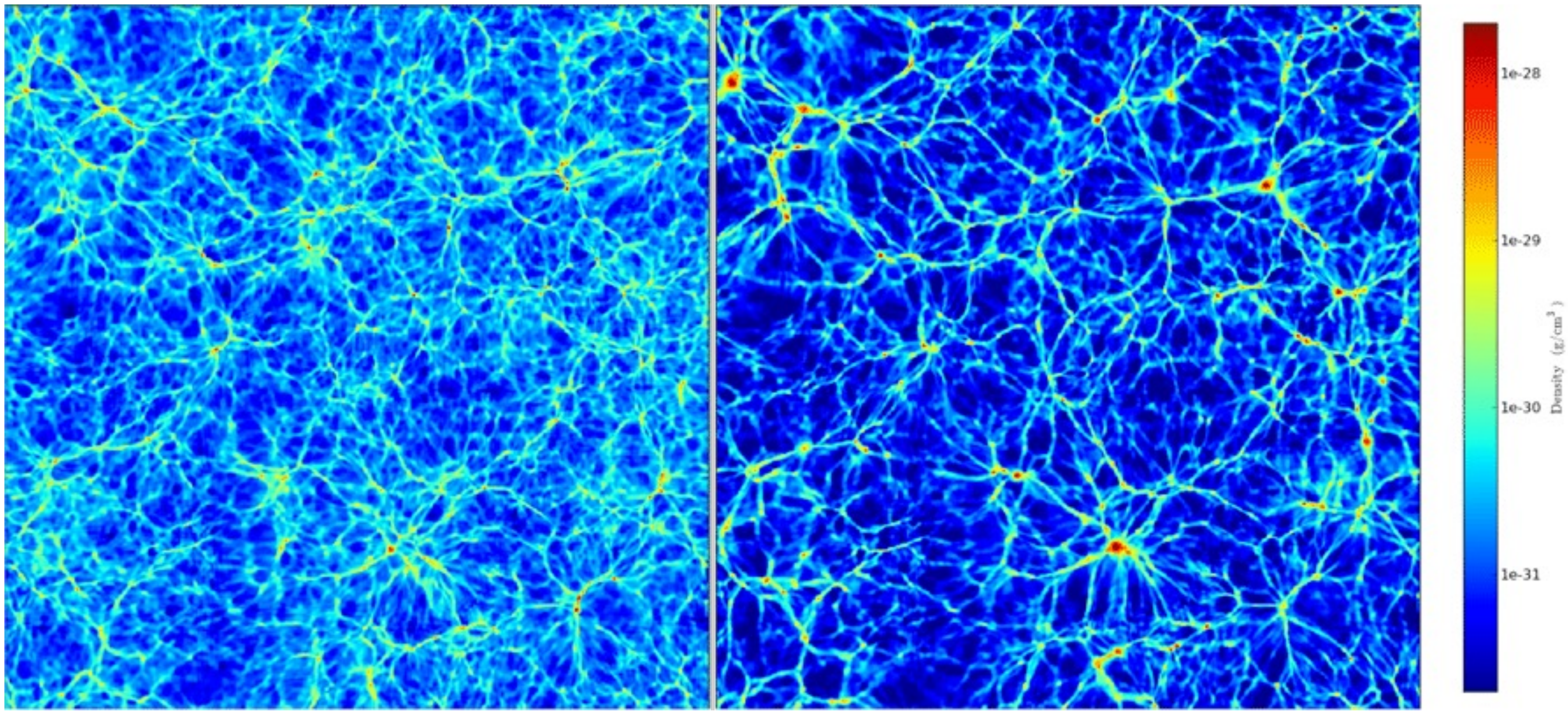

A fraction of HDM suppresses small scale structures

POWER SPECTRUM OF MATTER DENSITY FLUCTUATIONS

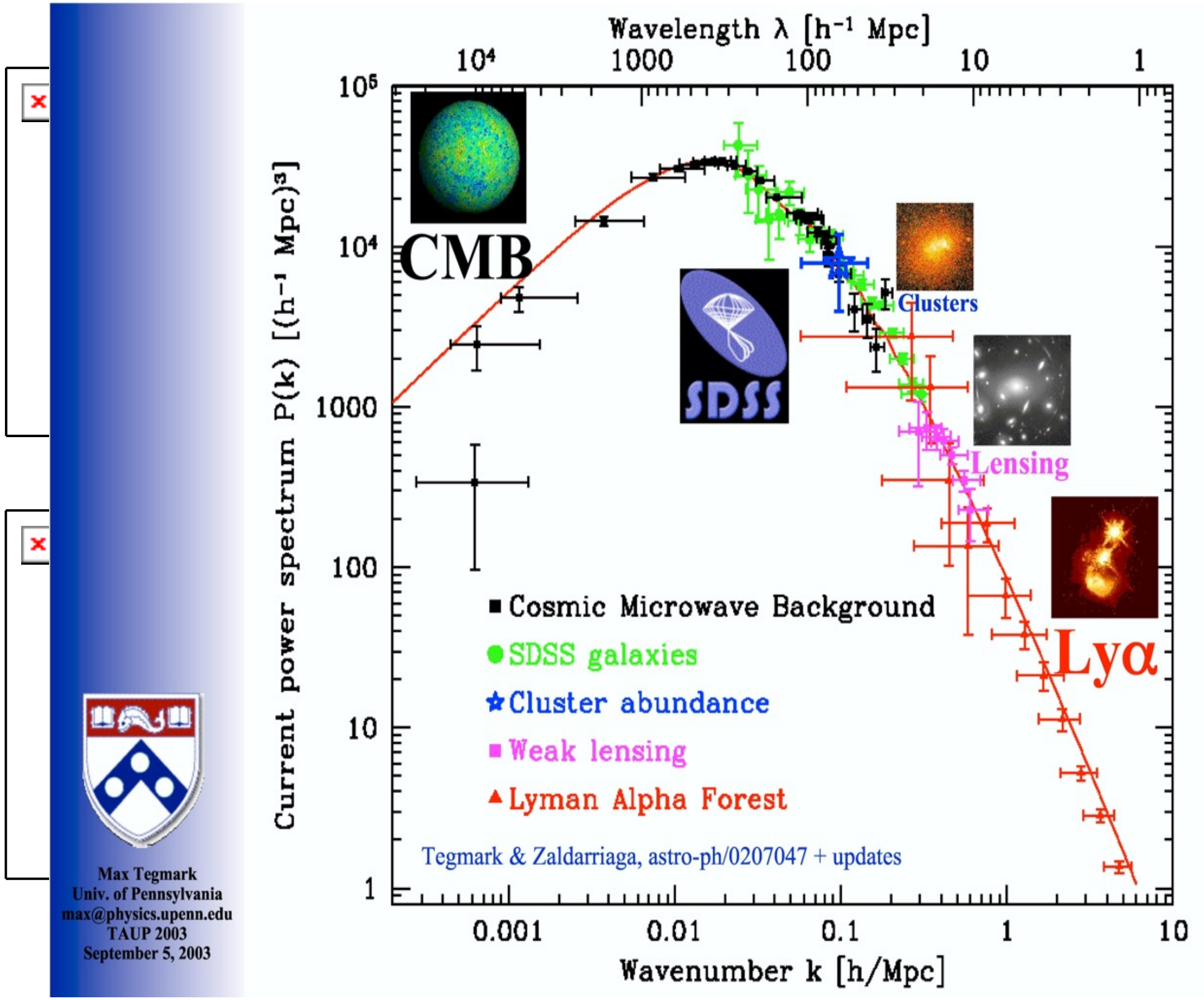

Power spectrum

$$P(k) \propto \left|\delta_k\right|^2$$

Density contrast

$$\delta(\vec{x}) = \frac{\rho(\vec{x}) - \bar{\rho}}{\bar{\rho}}$$

NEUTRINO FREE-STREAMING TRANSFER FUNCTION

Power suppression for $\lambda_{FS} \leq 100$ Mpc/h

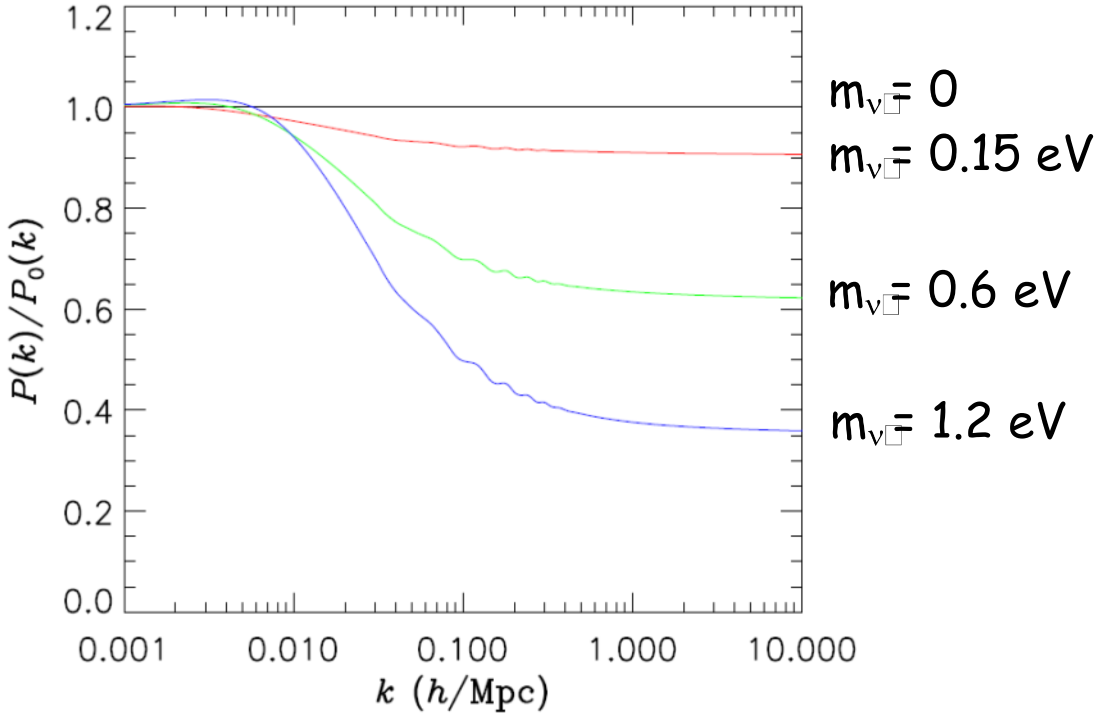

[Hannestad, 1007.0658]

Hot dark matter axions

If they are heavy enough then the thermal axion background contributes a form of **hot dark matter** (similar to neutrinos) which is heavily constrained by LSS+CMB

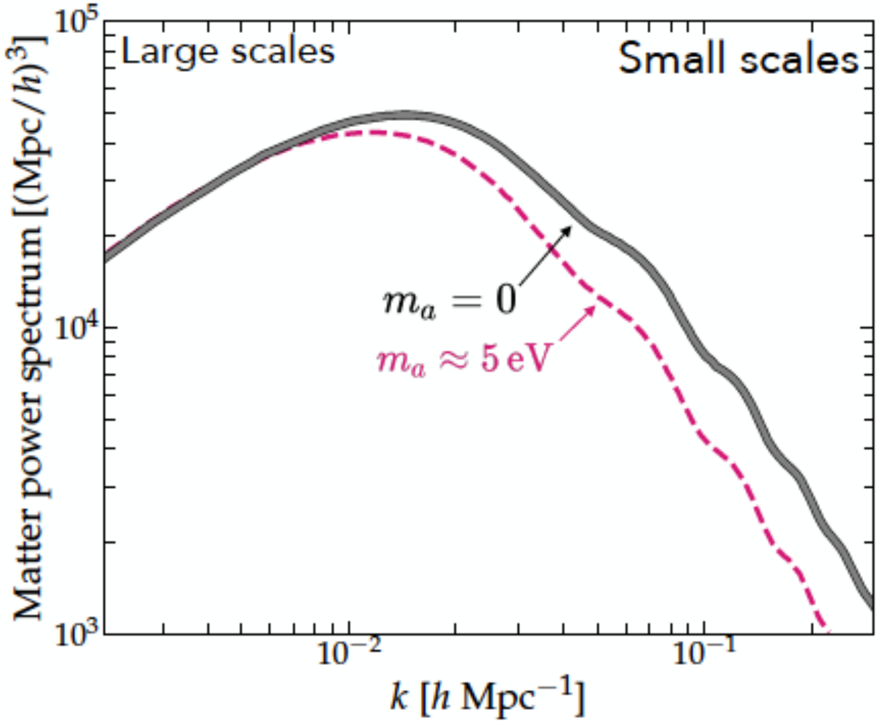

D'Eramo+ [2205.07849]

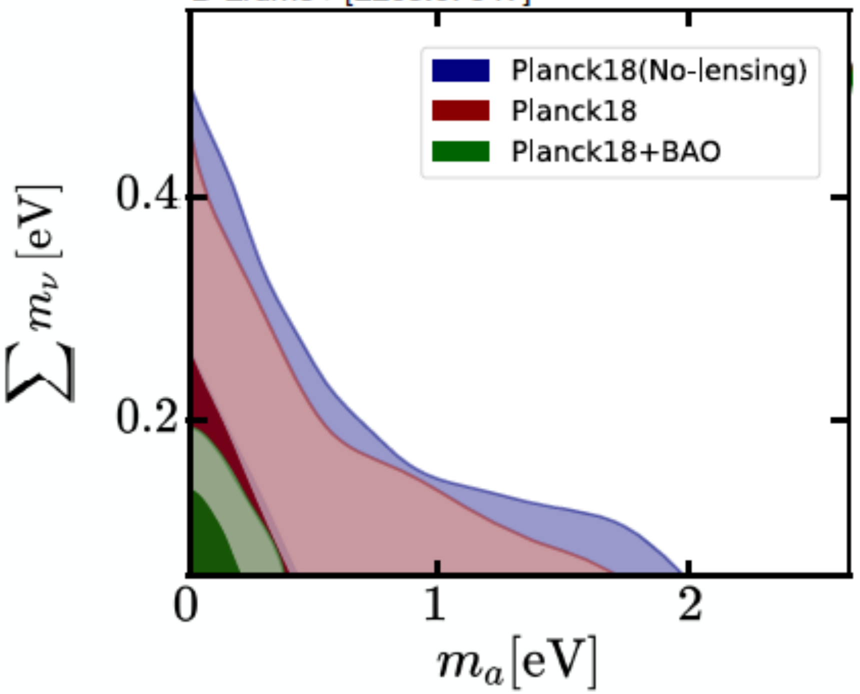

NEUTRINOS AND AXIONS HOT DM LIMIT AFTER PLANCK

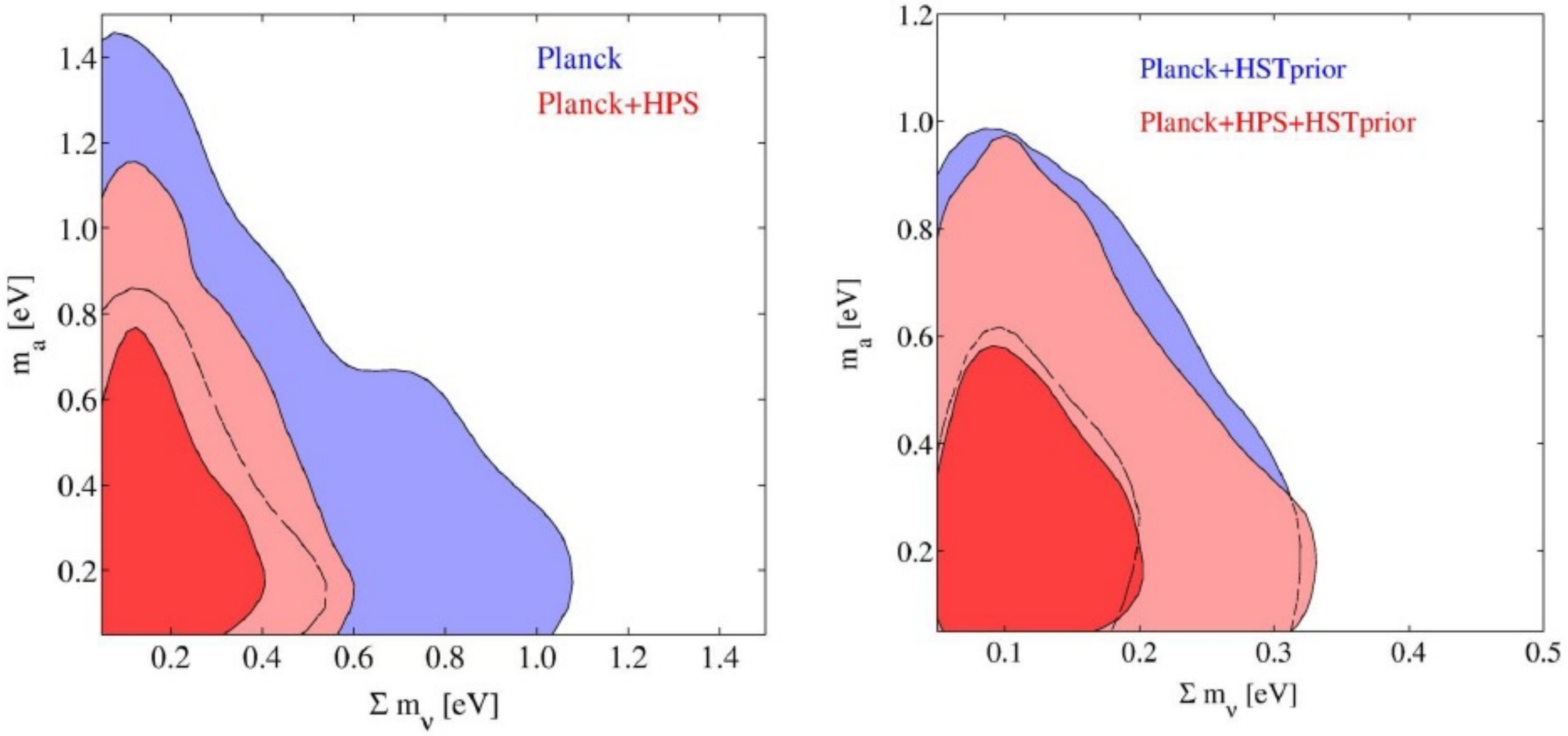

Archidiacono, Hannestad, Mirizzi, Raffelt & Wong, arXiv:1307.0615

(see also Giare', Di Valentino, Melchiorri, Mena, 2011.14704 for a recent update with Planck 2018 data)

Future EUCLID survey would be sensitive to $m_a \sim 0.2\ eV$

[Archidiacono et al., 1502.03325]

Γ vs H , NLO

- $m_a = 1$ eV: the most conservative HDM bound
- $m_a = 0.1$ eV: typical reach of future CMB-S4 experiments
- $T_\chi \sim 62$ MeV: boundary of validity of the chiral expansion

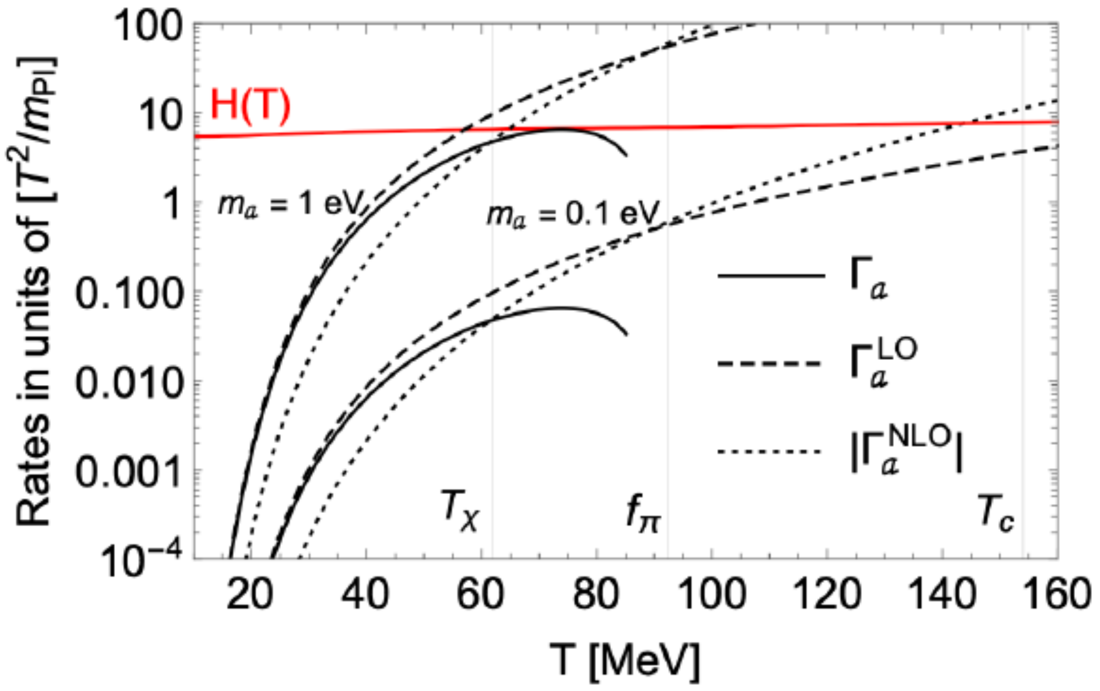

(see Di Luzio, Martinelli, Piazza, 2101.10330)

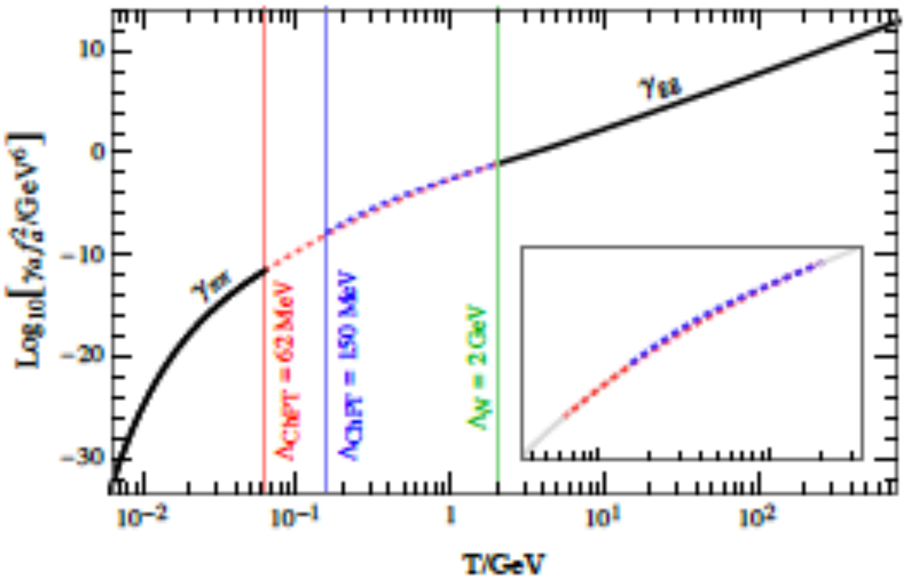

Figure 2. Axion production rate across the QCDPT. At high temperatures ($T > \Lambda_N$), the production is driven by thermal gluon scatterings whereas pion binary collisions are the main source of axions at low temperatures ($T < \Lambda_{ChPT}$). We interpolate between the two regimes (see text for details).

D' Eramo et al., 2108.04259

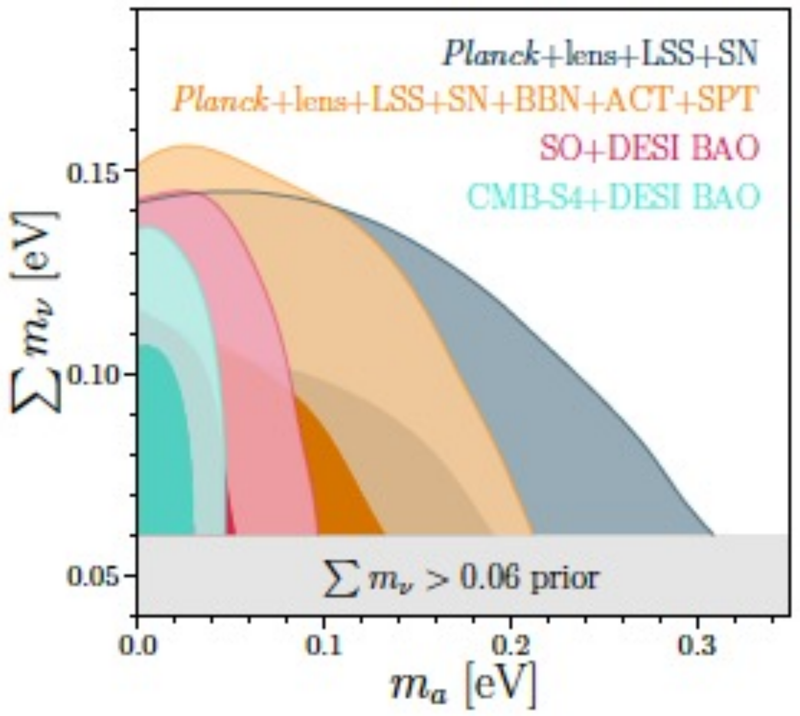

FIG. 3. 68% and 95% joint HDI for the axion mass and the sum of neutrino masses from current cosmological data (blue and orange contours) and future CMB/LSS surveys (magenta and turquoise contours). See text for details on the forecast.

Bianchini et al., 2310.08169

Thermal axions and $N_{\rm eff}$

Quantify effects of new relativistic species on early-Universe expansion rate via energy density in units of a single neutrino ($\Delta N_{\rm eff}$)

$$\rho_r = \left[1 + \frac{7}{8}\left(\frac{4}{11}\right)^{4/3}(N_{\rm eff}^{\rm SM} + \Delta N_{\rm eff})\right]\rho_\gamma$$

$N_{\rm eff}^{\rm SM} = 3.044$

- CMB-Stage 4 is targeting $\Delta N_{\rm eff} = 0.03$
- Could constrain axions decoupling before EWPT
- Quite plausible we could detect a relic population of thermal axions

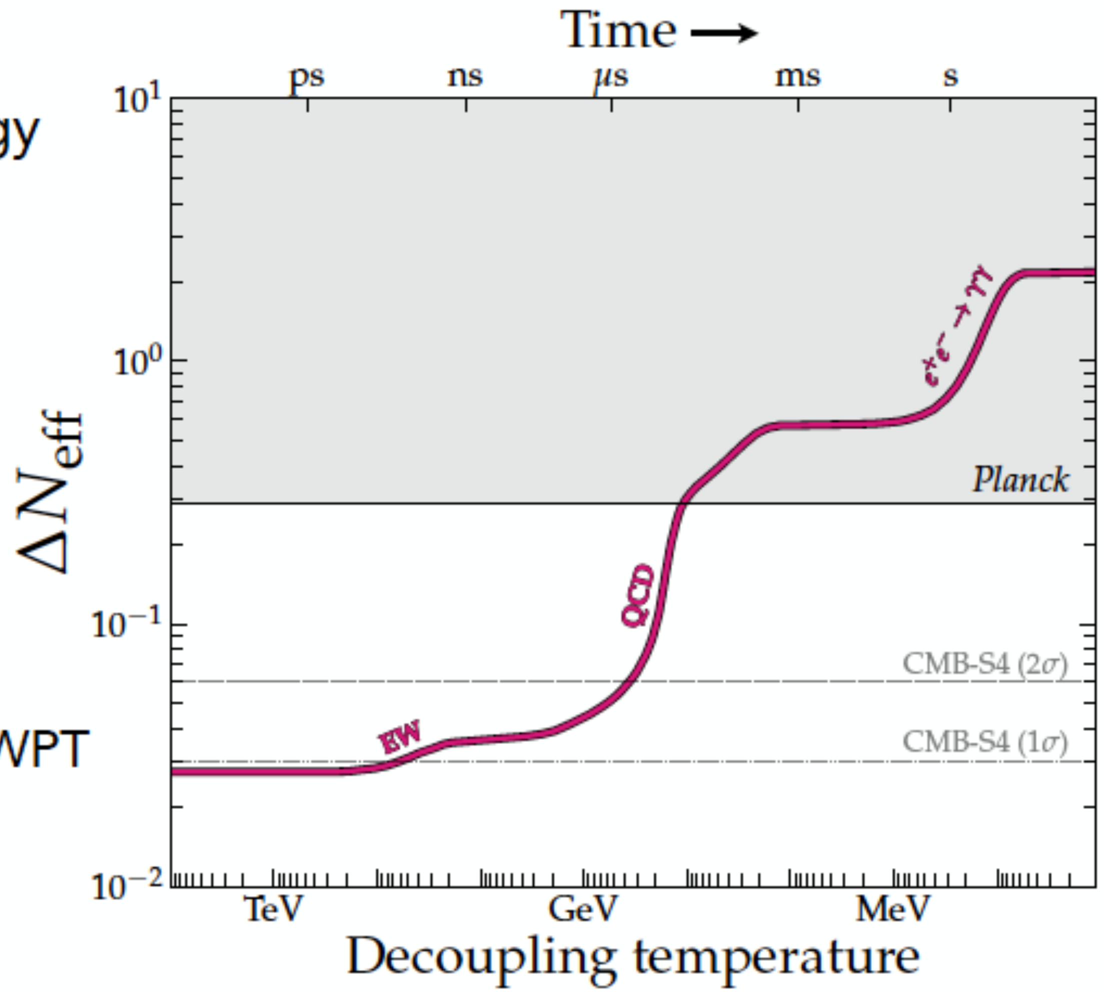

CREATION OF COSMOLOGICAL AXIONS

$T \sim f_a$ (very early universe)

- U_{PQ} (1) spontaneously broken
- Axion fields settles in the "Mexican hat"
- Axion field frozen at initial value $a(t_i) = \theta_i f_a$

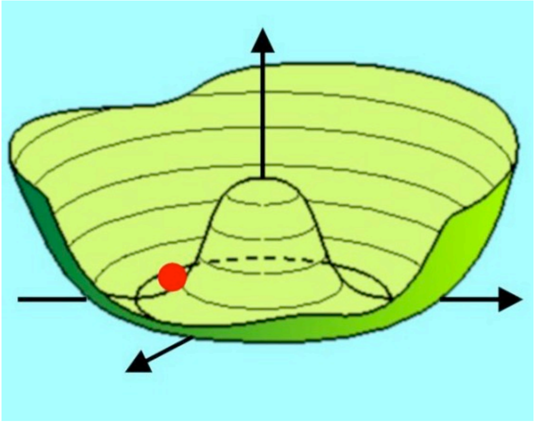

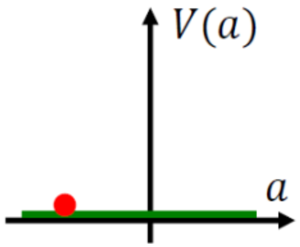

$T \sim 1$ GeV ($H \sim 10^{-9}$ eV)

- Axion mass turns on quickly
- Field start oscillating when $m_a \geq 3H$
- Classical field oscillations (axion at rest)

Vacuum realignment

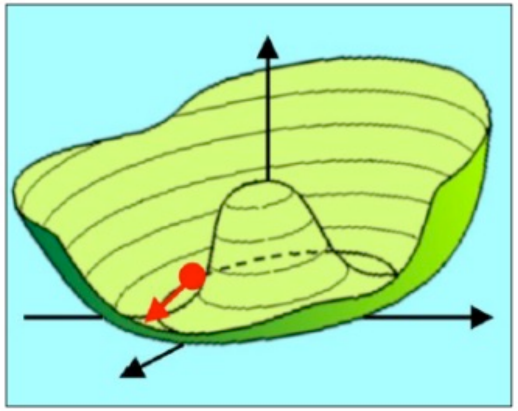

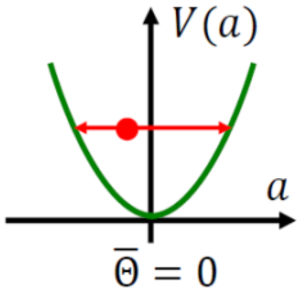

Coherent state of extremely non-relativistic DM, i.e. cold DM.

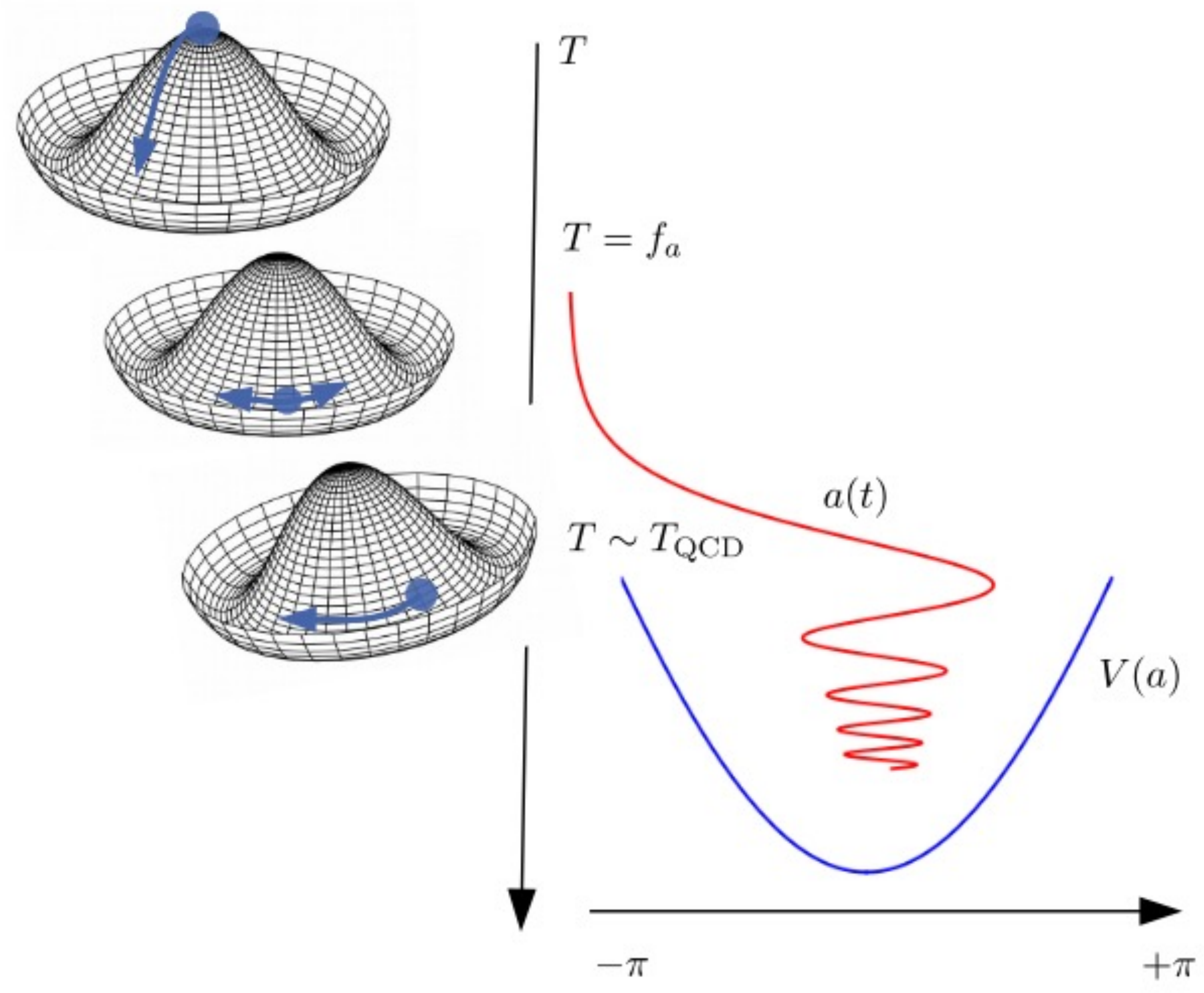

T
$T = f_a$
$a(t)$
$T \sim T_{\rm QCD}$
$V(a)$
$-\pi$
$+\pi$

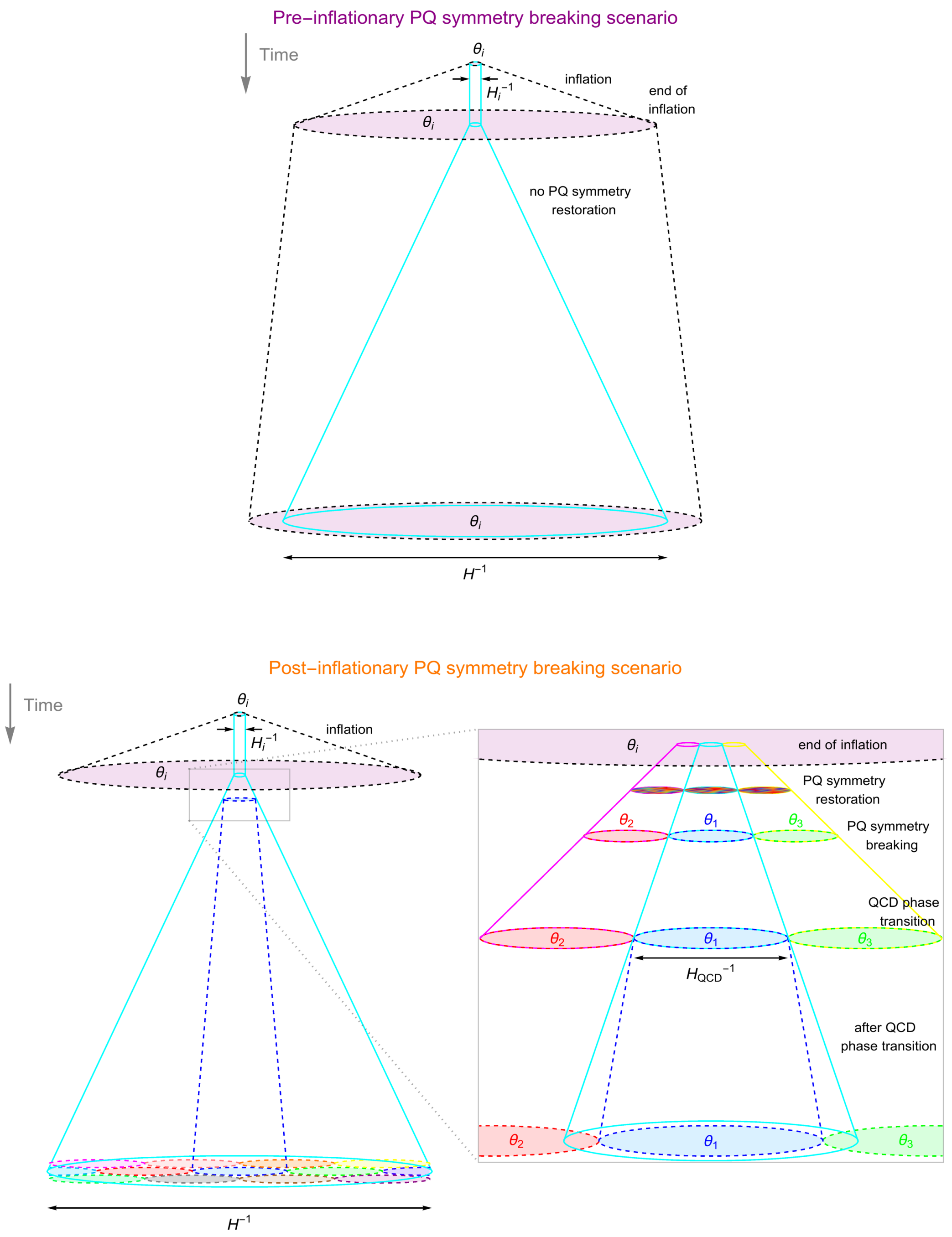

Pre–inflationary PQ symmetry breaking scenario
Time
θ_i
H_i^{-1}
inflation
end of inflation
θ_i
no PQ symmetry restoration
θ_i
H^{-1}
Post–inflationary PQ symmetry breaking scenario
Time
θ_i
H_i^{-1}
inflation
θ_i
H^{-1}
θ_i
end of inflation
PQ symmetry restoration
θ_2
θ_1
θ_3
PQ symmetry breaking
QCD phase transition
θ_2
θ_1
θ_3
H_{QCD}^{-1}
after QCD phase transition
θ_2
θ_1
θ_3

Misalignment mechanism for a generic scalar

At late times, the damping takes place over cosmological timescales, while the oscillations are fast
→ Make a WKB approximation $\dot{\phi}_{\rm env}/\phi_{\rm env} < m$

$$\phi(t) = \phi_{\rm env}(t) \cos mt$$

$$\rightarrow \; \phi \propto \underbrace{\phi_i a(t)^{-3/2}}_{\text{Envelope decays as } a^{-3/2}} \cos(mt)$$

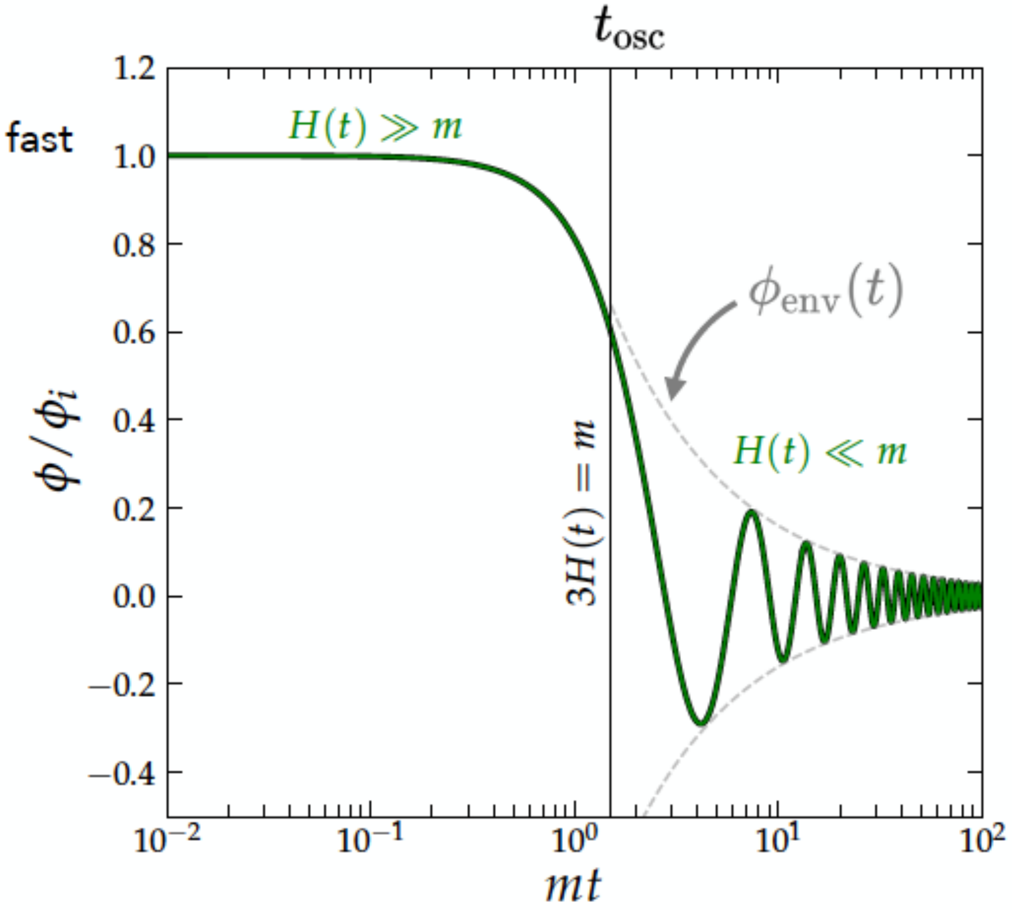

Slide dy Ciaran O'Haare

Misalignment mechanism for a generic scalar

At late times, the damping takes place over cosmological timescales, while the oscillations are f
→ Make a WKB approximation $\dot{\phi}_{\rm env}/\phi_{\rm env} < m$

$$\phi(t) = \phi_{\rm env}(t)\cos mt$$

$$\rightarrow \phi \propto \underbrace{\phi_i a(t)^{-3/2}}_{\text{Envelope decays as } a^{-3/2}} \cos(mt)$$

Look at the energy density in the scalar field

$$\rho_\phi = \frac{1}{2}\dot{\phi}^2 + \frac{1}{2}m^2\phi^2 \implies \rho_\phi \propto a^{-3}$$

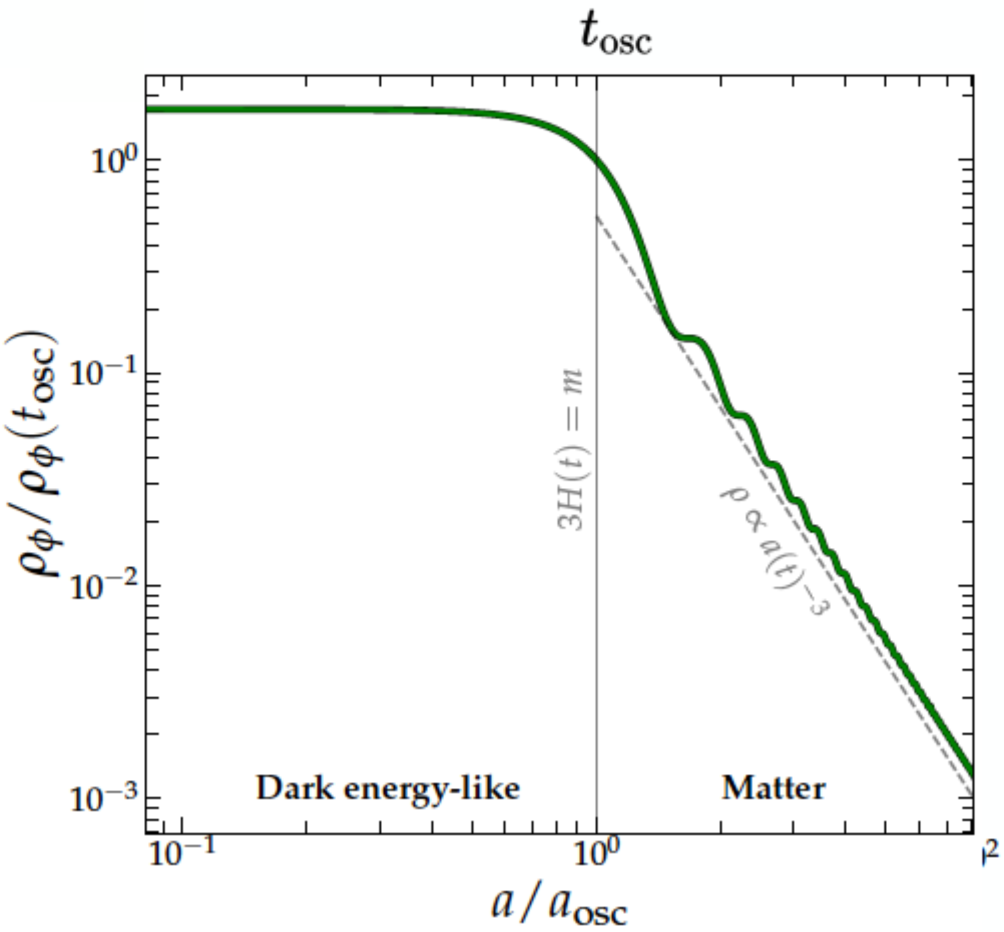

Slide dy Ciaran O'Haare

The QCD axion

Mass is generated by instantons whose effects are temperature-dependent

In the literature this dependence is called the “topological susceptibility”, $\chi(T)$

$$V(\theta) \approx \chi(T)(1 - \cos\theta) = m_a^2(T) f_a^2 (1 - \cos\theta)$$

Axion mass grows as temperature drops, reaching a constant when $T < T_{\rm QCD}$

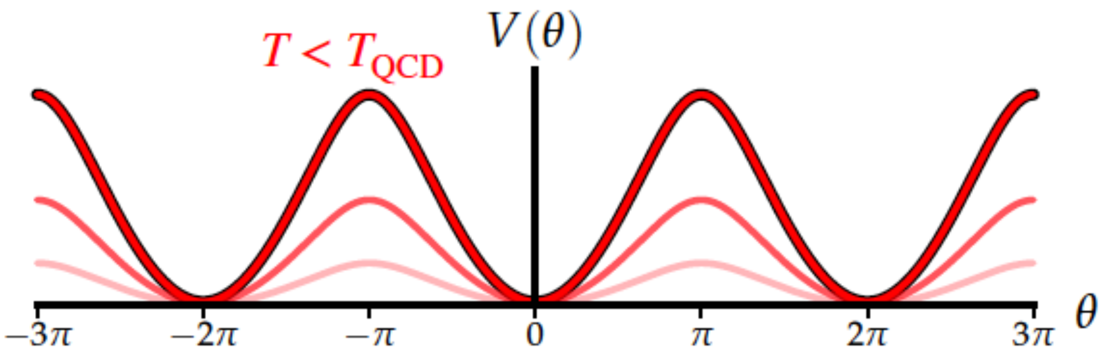

Lattice QCD calculation, Borsanyi+ [1606.07494]

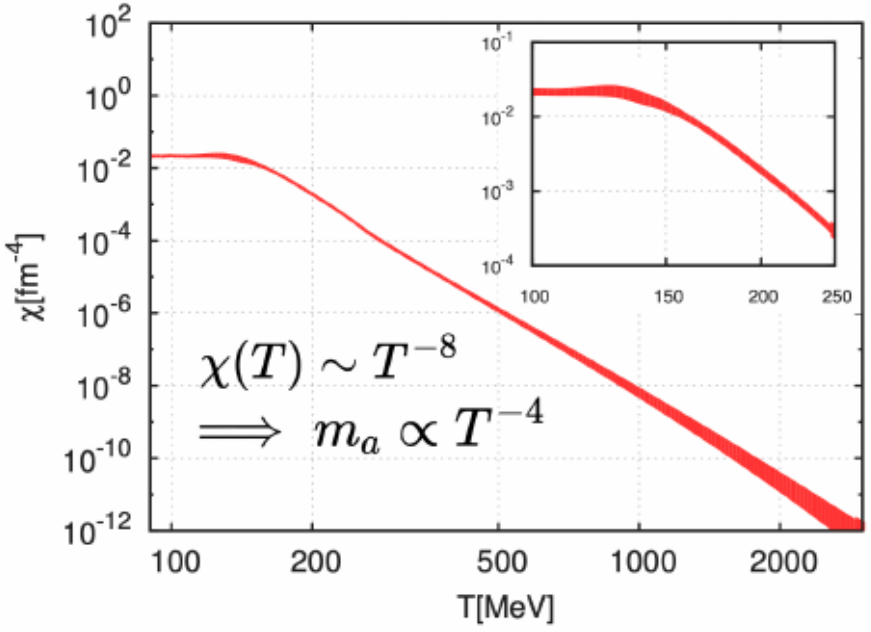

Slide dy Ciaran O’Haare

The QCD axion mass

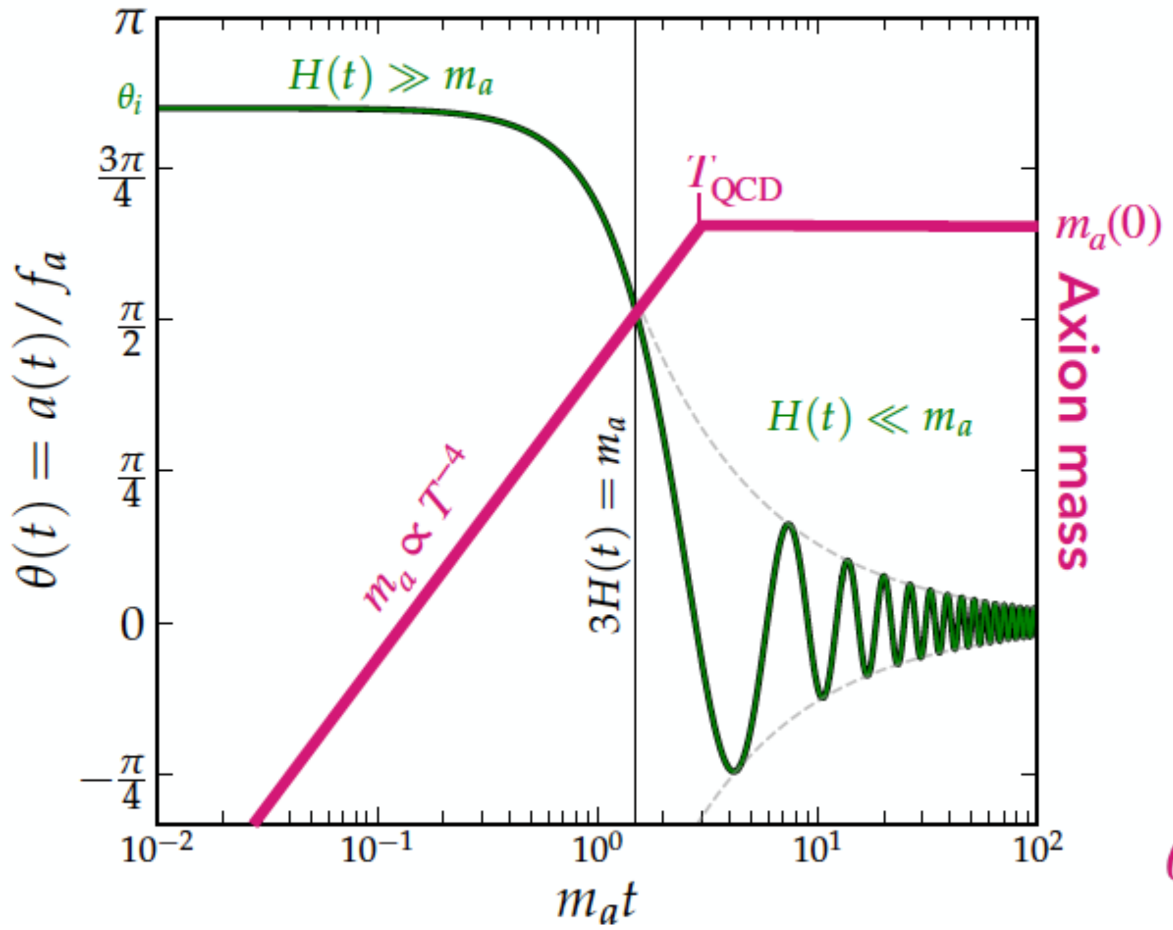

The tilt comes on gradually as the temperature drops

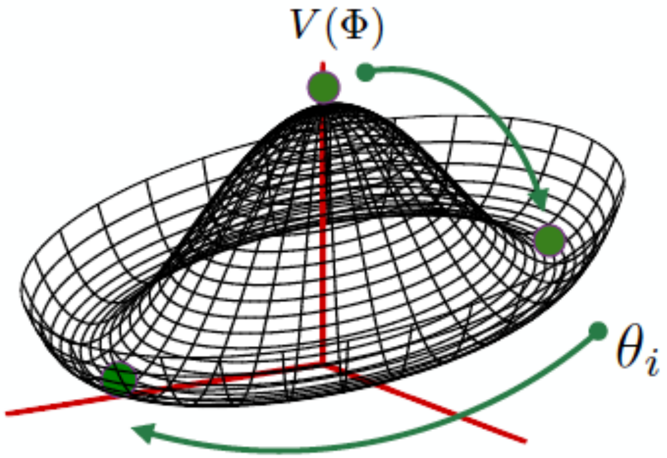

$$\ddot{\theta} + 3H\dot{\theta} + m_a^2\theta = 0$$

$$\ddot{\theta} + 3H\dot{\theta} + m_a(T)^2\sin(\theta) = 0$$

Slide dy Ciaran O'Haare

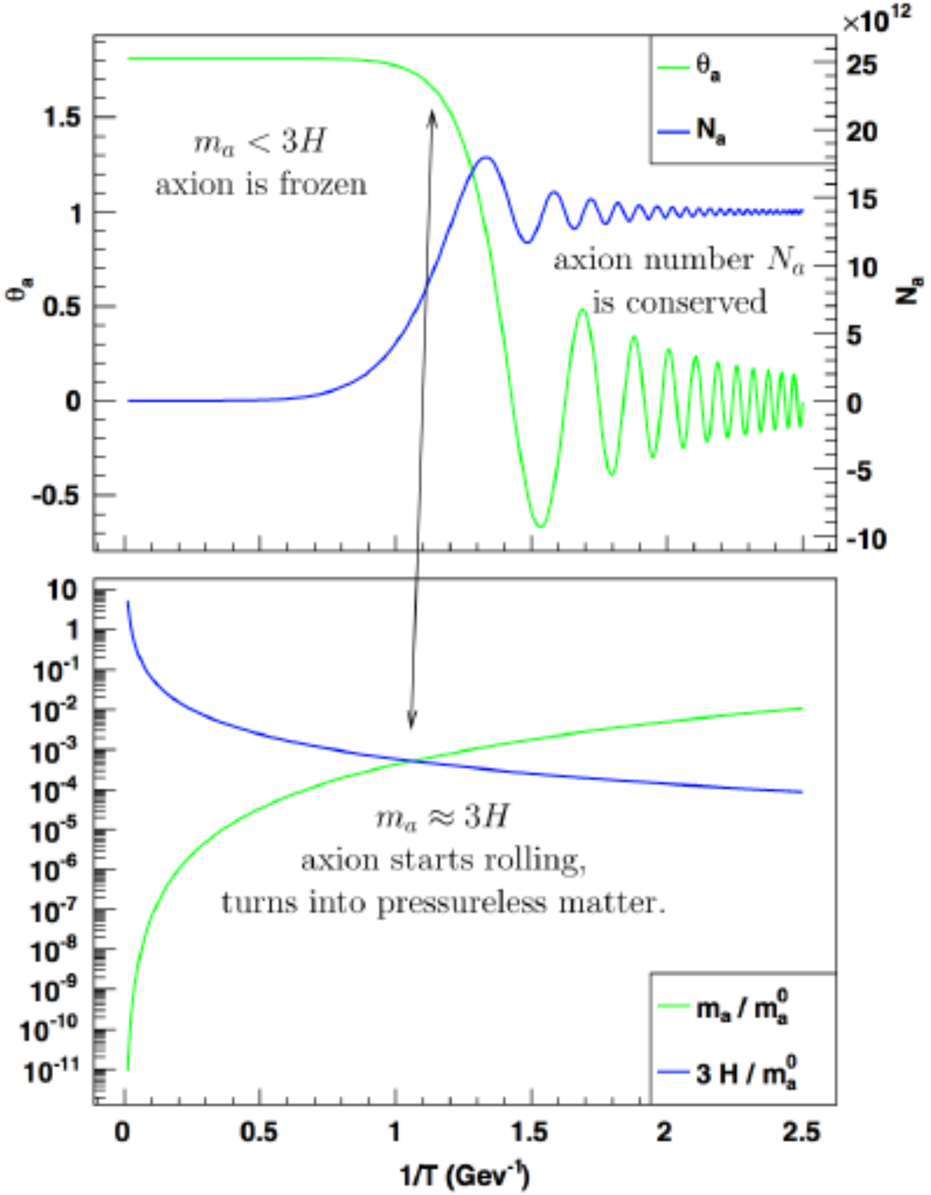

[Wantz,Shellard `09]

QCD axion abundance

- Full calculation leads to:

$$\Omega_a h^2 \approx 0.12\,\theta_i^2 \left(\frac{7.26\,\mu\text{eV}}{m_a}\right)^{\frac{n+6}{n+4}}$$

where $n \sim 8$

- Seems to prefer the "classic QCD axion window": $\mathcal{O}(1\text{—}10)\ \mu$eV

→ **but what should we pick for θ_i ?**

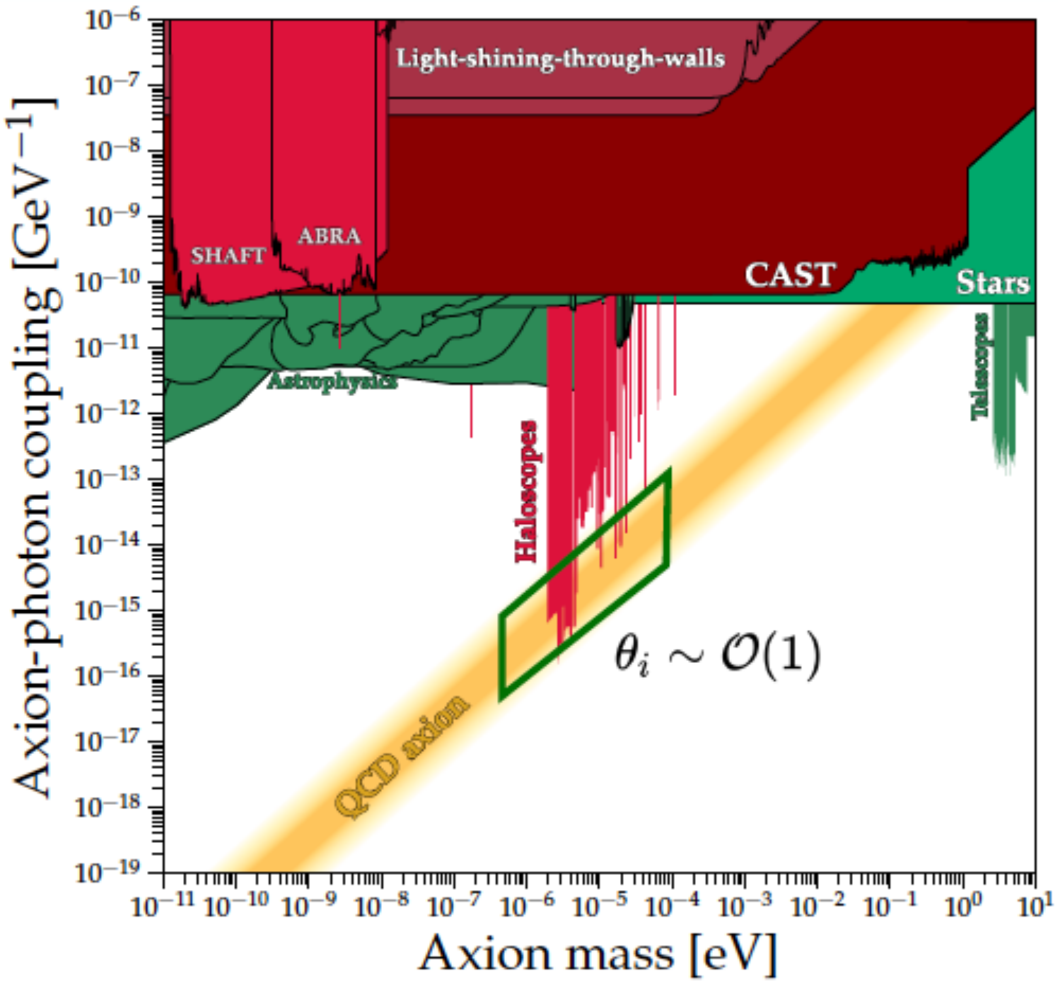

Slide dy Ciaran O'Haare

Axion Dark Matter

Production via vacuum misalignment

[Preskill,Wise,Wilczek 83; Abbott,Sikivie 83; Dine,Fischler 83,....]

- PQ phase transition takes place when $T \lesssim T_c^{\rm PQ} \sim v_{\rm PQ} = N_{\rm DW} f_a$
- Axion takes random initial values in causally connected domains

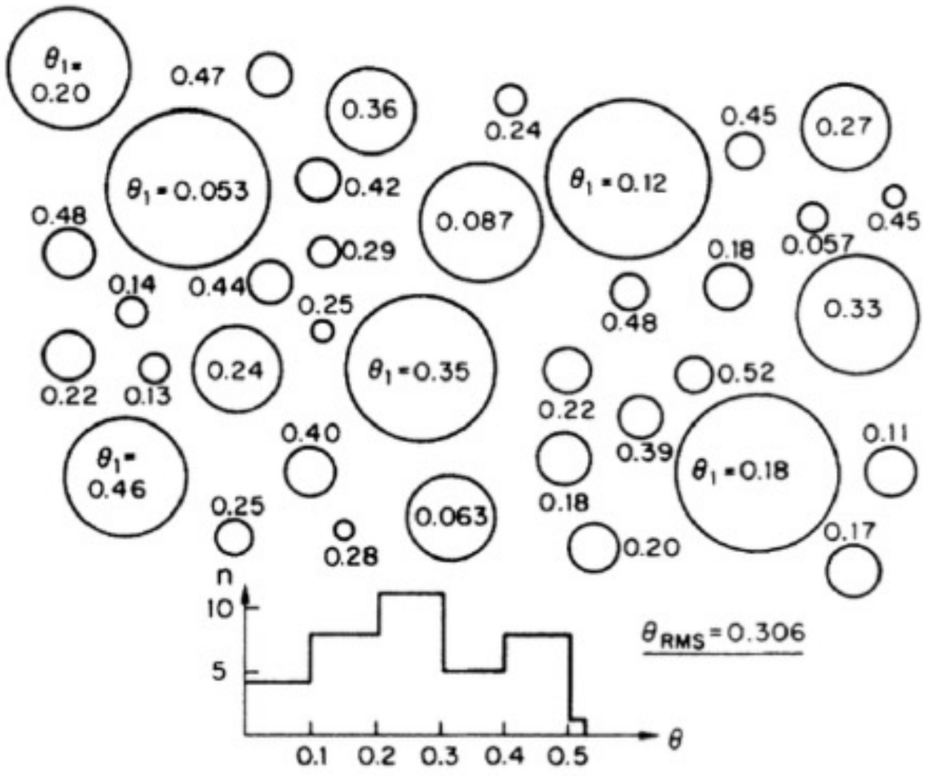

[Turner `86]

Pre-inflationary axions $\Omega_a h^2 \approx 0.12\,\theta_i^2 \left(\frac{7.26\,\mu\text{eV}}{m_a}\right)^{\frac{n+6}{n+4}}$

Our Universe could have been given any value of $\theta_i \in [-\pi, \pi]$. So we can make any axion mass work as long as we choose the θ_i that gives $\Omega_a h^2 = 0.12$

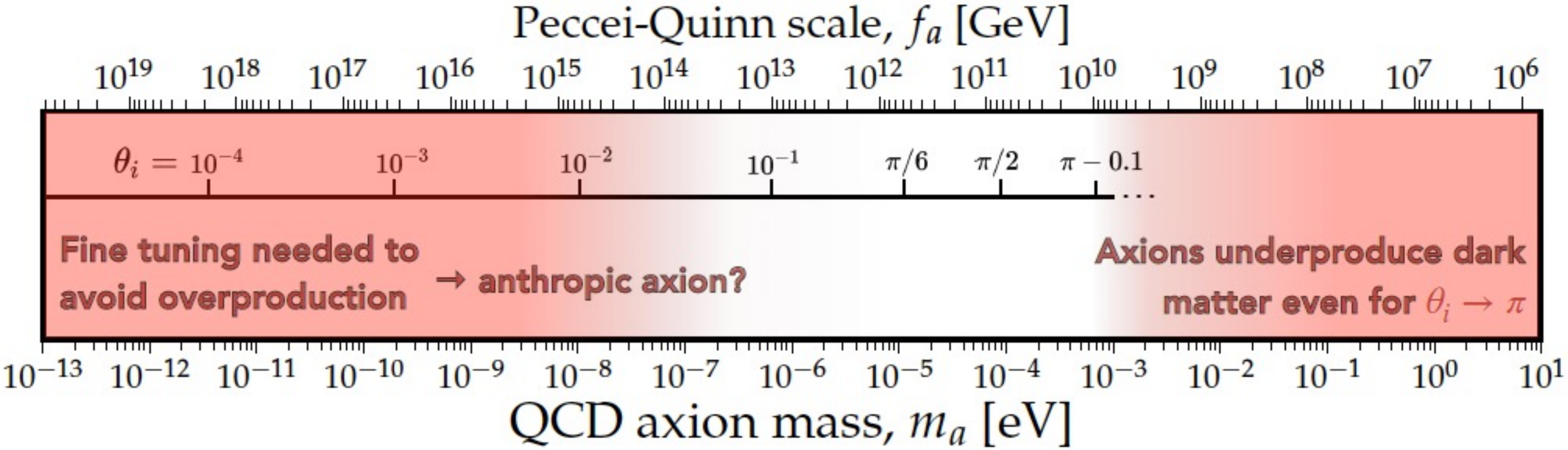

Slide dy Ciaran O’Haare

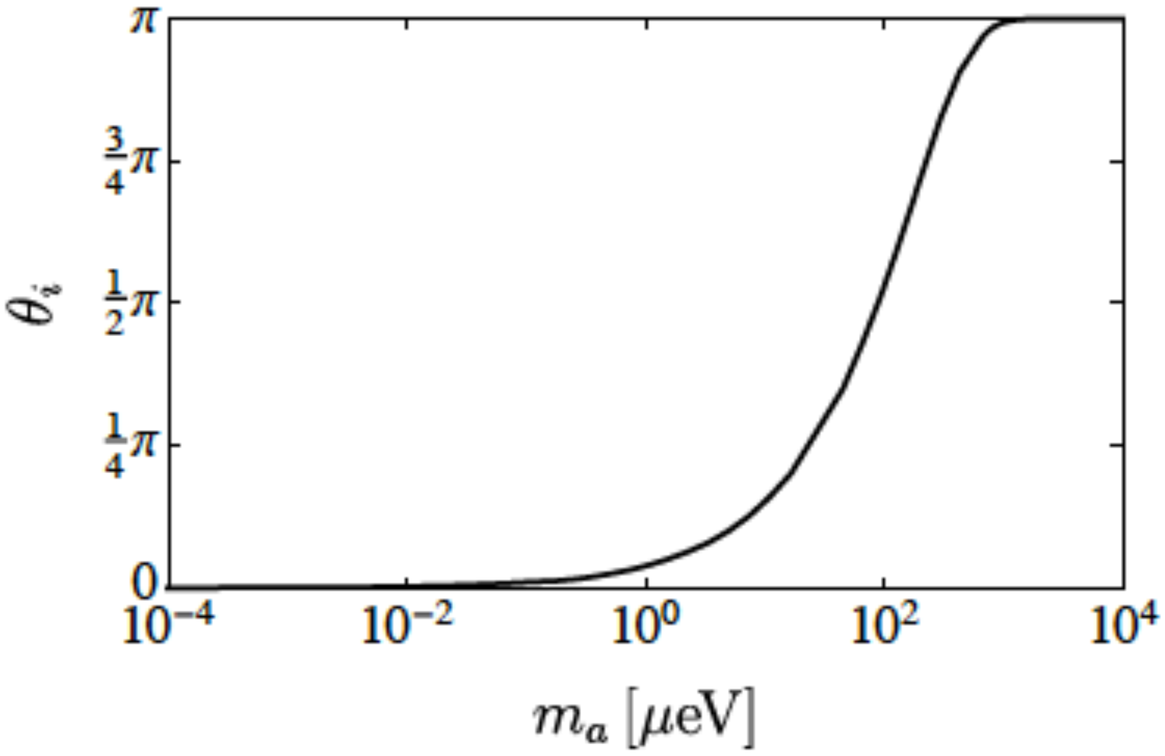

Figure 2: The relation between the DM axion mass and the initial misalignment angle in the pre-inflationary scenario.

Di Luzio et al., 2003.01100

Pre-inflationary axions: isocurvature

- Axion exists as scalar d.o.f *during* inflation
  → quantum fluctuations are also inflated

$$\sigma_{\text{axion}} \sim H_I/2\pi$$

- Fluctuations eventually become matter perturbations when the axion gets a mass
- This is bad: they will be *uncorrelated* with curvature fluctuations from inflaton. Such fluctuations are called **isocurvature**
- *Planck* bounds power in isocurvature to be less than <4% compared to primordial curvature perturbations.

$$\beta(k_0) \equiv \frac{\Delta_a^2(k_0)}{\Delta_{\mathcal{R}}^2(k_0) + \Delta_a^2(k_0)} < 0.038$$

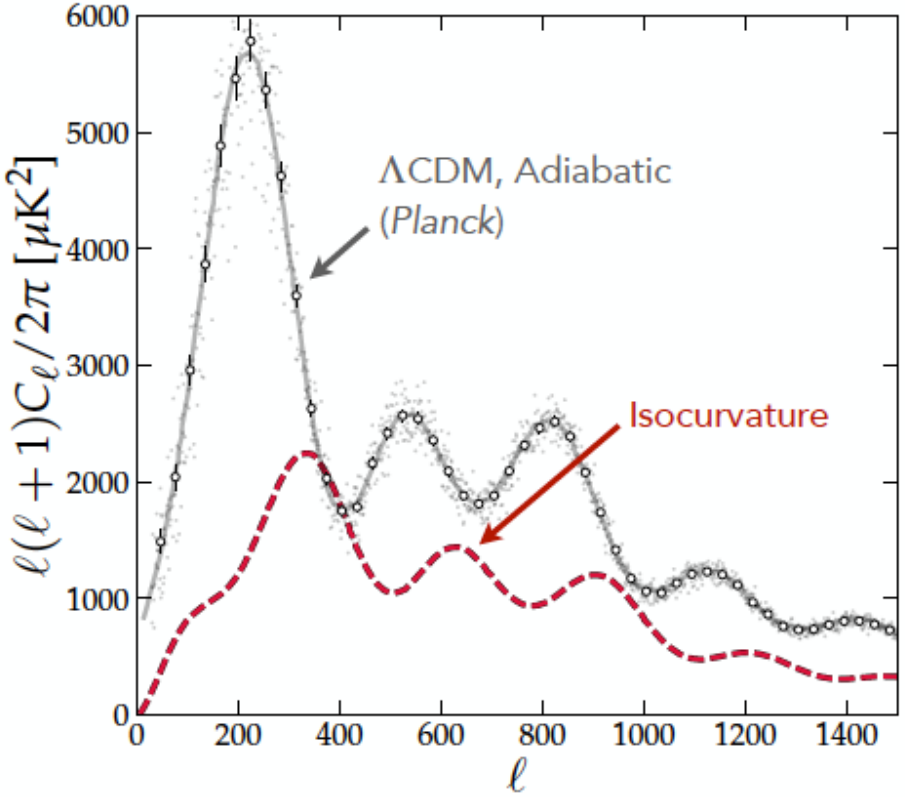

Slide dy Ciaran O’Haare

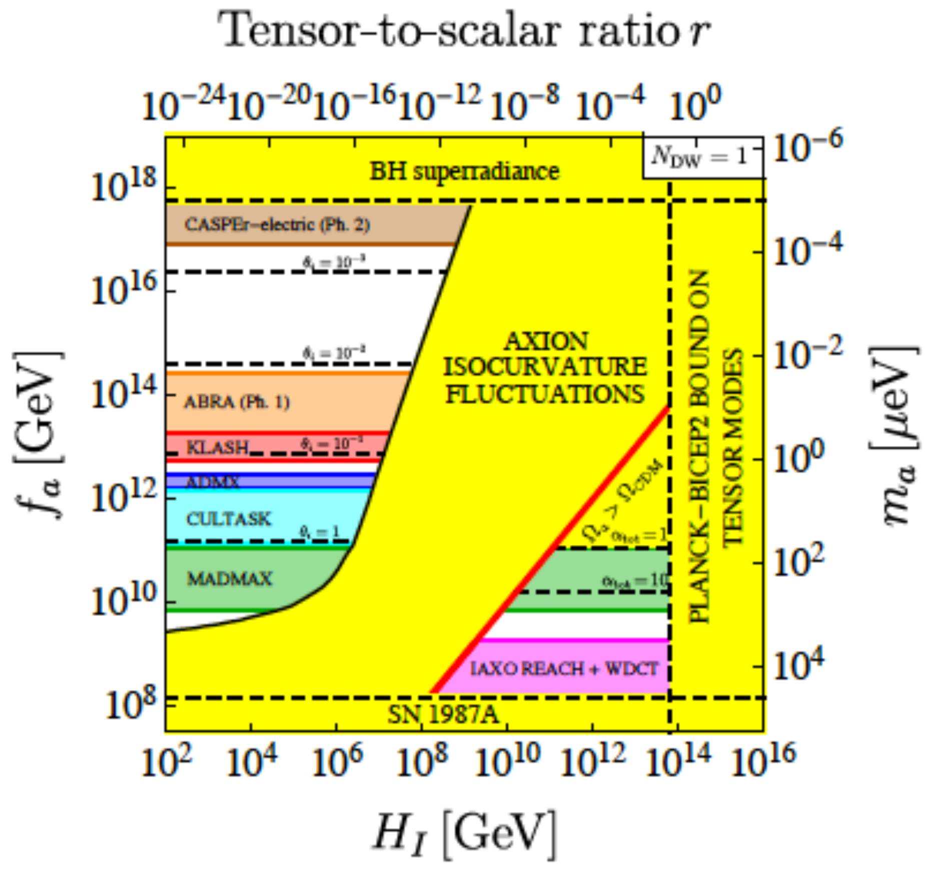

Figure 3: Region of axion parameter space where the axion constitutes the totality of the DM observed. The axion mass scale on the right corresponds to Eq. (51) for the case $N_{\rm DW} = 1$. If the PQ symmetry breaks during inflation and the axion spectates inflation ($f_a \gtrsim H_I$, pre-inflationary scenario), axion isocurvature perturbations constrain the parameter space to the region on the top left, which is marked by the values of θ_i necessary to achieve the observed CDM density for a given value of f_a. If the PQ symmetry breaks after inflation ($f_a < H_I$, post-inflationary scenario), the axion is the CDM particle only for a specific value of f_a, which takes into account the contributions from the decay of topological defects $\alpha_{\rm tot}$. The lower bound on f_a results from astrophysical considerations [33, 35, 306, 307], the upper bound on f_a relies on the non-detection in LIGO of gravitational waves associated with the super-radiance phenomenon from stellar-mass black holes [308, 309], the upper bound on H_I comes from the non-observation of tensor modes in the CMB [251, 252, 310]. The coloured transparent bands indicate future reaches of planned or ongoing experiments covering the allowed regions of the parameter space: CASPEr-Electric Phase 2 (bronze), ABRACADABRA (ABRA Ph.1, orange), KLASH (red), ADMX (blue), CULTASK (Cyan), MADMAX (green), and IAXO (magenta).

Pre-inflationary axions

For a given f_a the scale of inflation must be below some maximum value or axion produces too much isocurvature

$$H_I \lesssim 2.8 \times 10^8\,\mathrm{GeV} \times \theta_i \left(\frac{f_a}{10^{11}\,\mathrm{GeV}} \right)$$

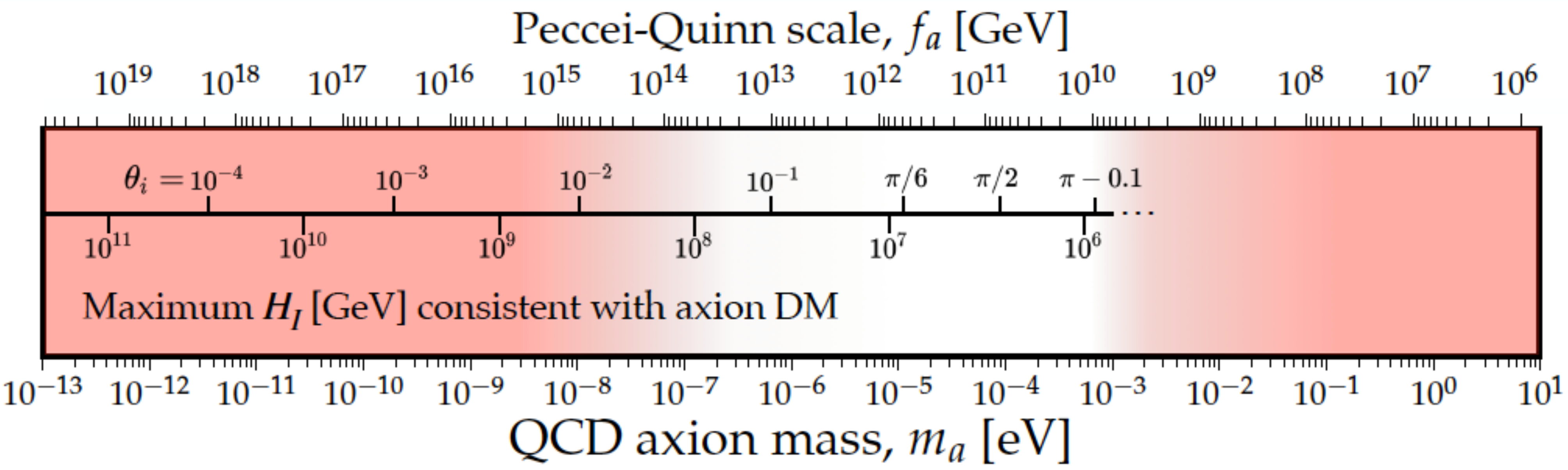

Slide dy Ciaran O’Haare

Post-inflationary scenario

- We have an ensemble of every possible θ_i sampled across our Universe.
- Stochastic average:

$$\langle\theta_i^2\rangle \approx \left(\frac{\pi}{\sqrt{3}}\right)^2 \approx (1.81)^2$$

$$\Omega_a h^2 \approx 0.12 \frac{\langle\theta_i^2\rangle}{(1.81)^2}\left(\frac{20\mu\text{eV}}{m_a}\right)^{\frac{n+6}{n+4}}$$

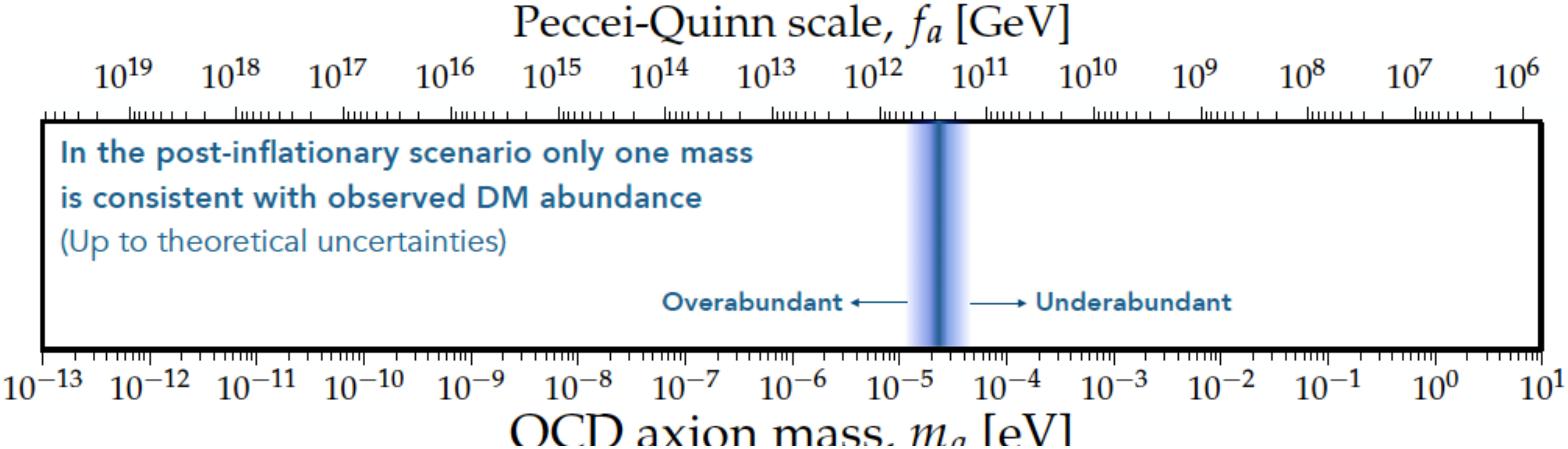

Slide dy Ciaran O'Haare

COSMIC STRINGS

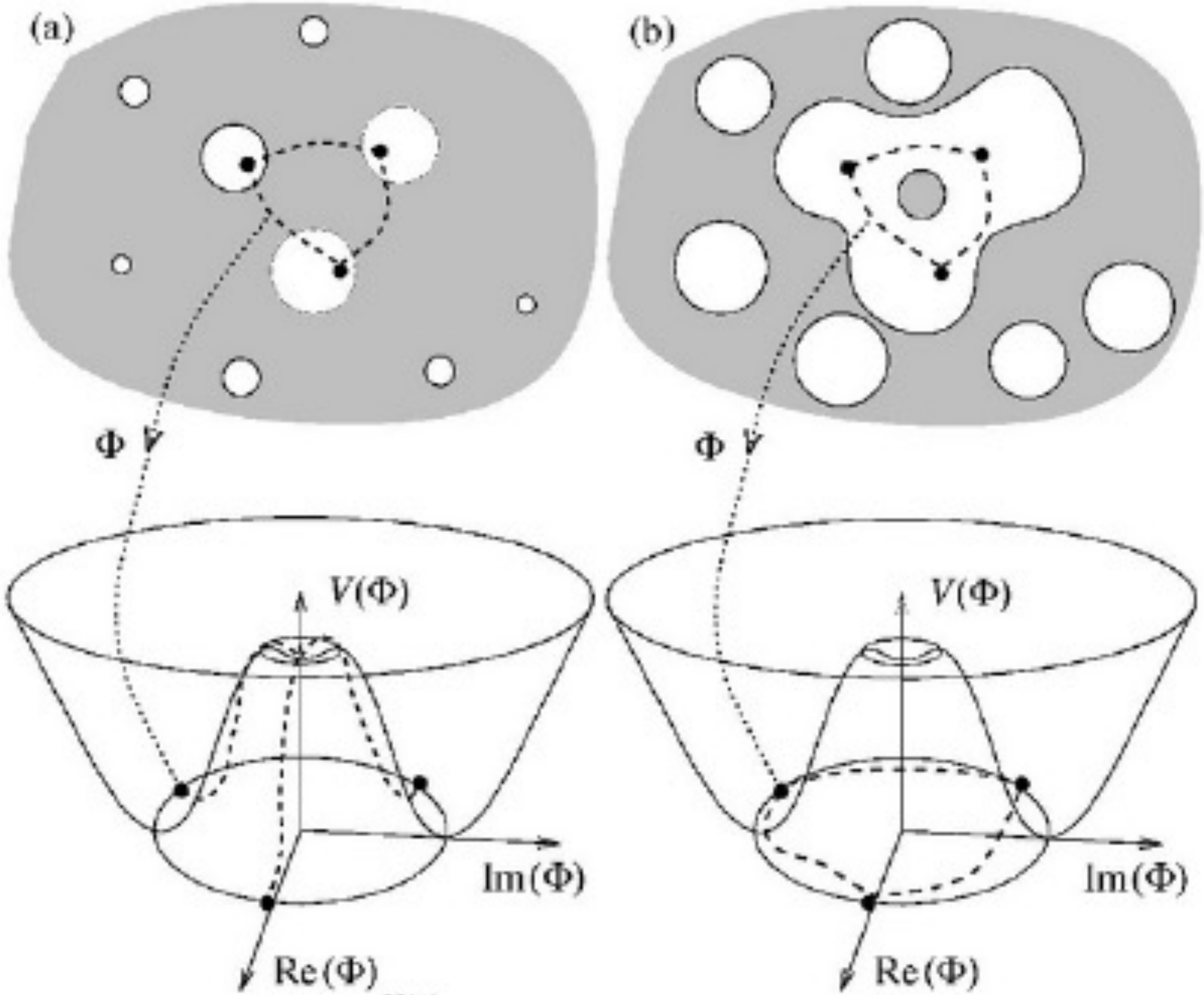

Figure 1. Kibble mechanism: $U(1)$ **symmetry breaking of a complex scalar field produces cosmic strings [1]. (a) patches with true vacuum energies start growing as the symmetry is broken. Gray region represents false vacua. (b) As the patches with true vacua merge, false vacuum regions are squeezed and form topological defects.**

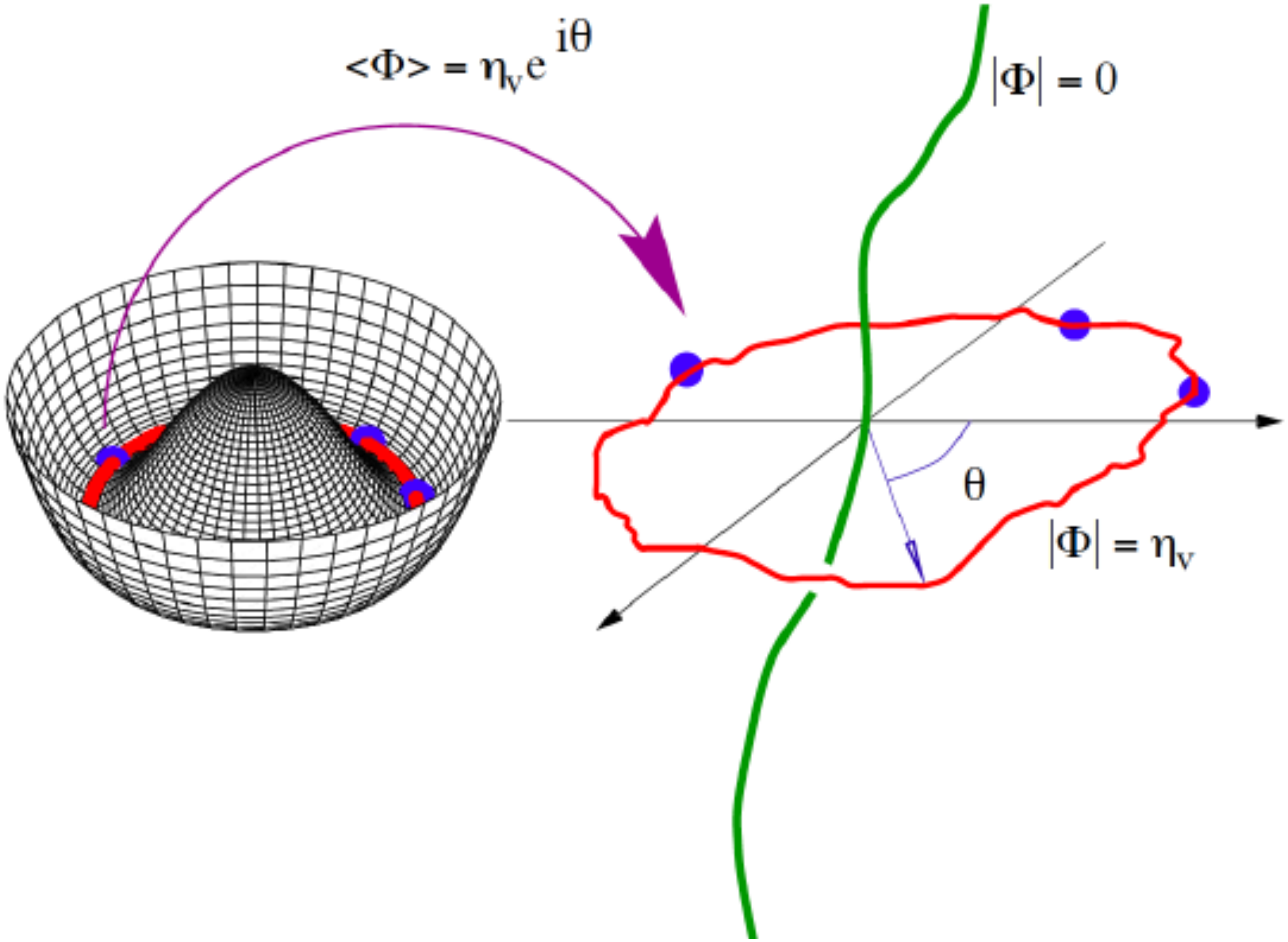

<Φ> = ηve iθ
|Φ| = 0
θ
|Φ| = ηv

AXION STRINGS

If PQ SSB afer inflation, $H_I > f_a$ axions can be produced via cosmic string decays

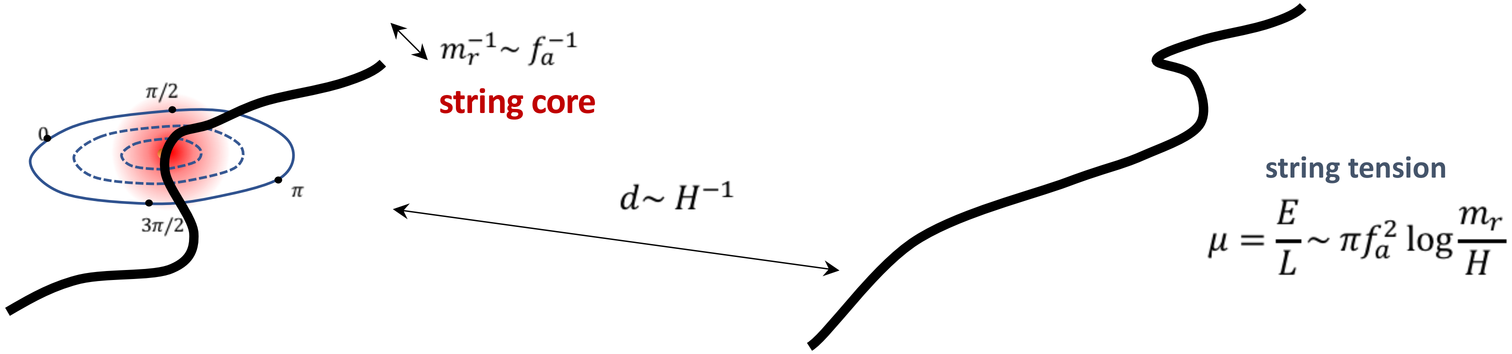

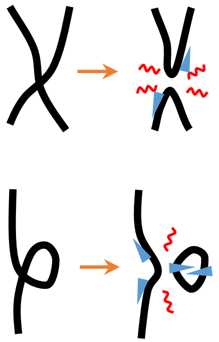

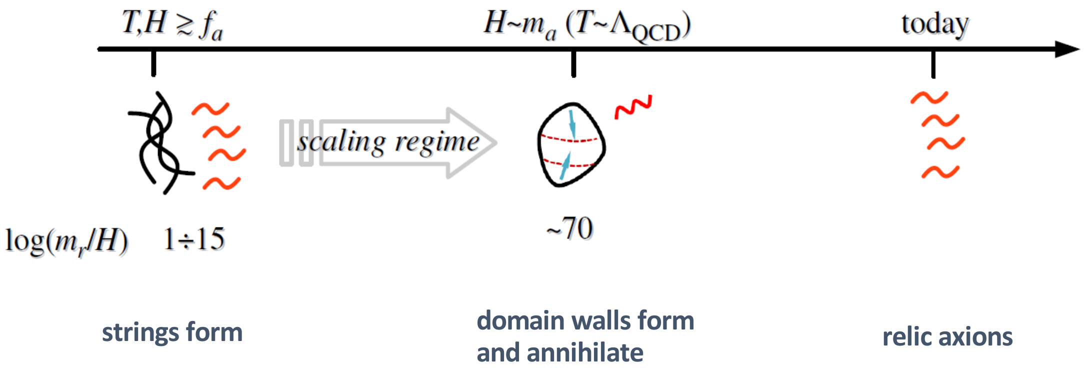

Numerical simulations are really challenging since the string size $m_r^{-1} \ll H^{-1}$

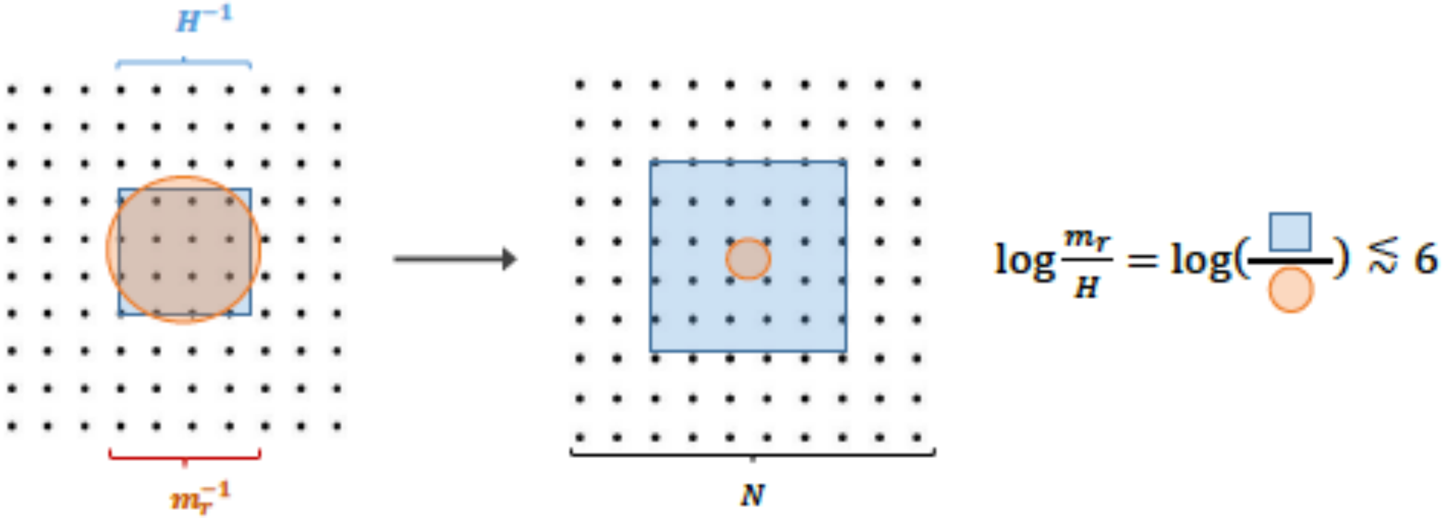

Figure 5: An illustration of how the size of a string core, shaded red, and a Hubble volume, shaded blue, evolve relative to the lattice points in our simulations, where N is the number of lattice points in a spatial dimension. Requiring that the simulation contains at least a few Hubble volumes and that a string core contains at least ~ 1 lattice point constrains the maximum scale separation that can be studied.

From: Dark matter from axion strings with adaptive mesh refinement

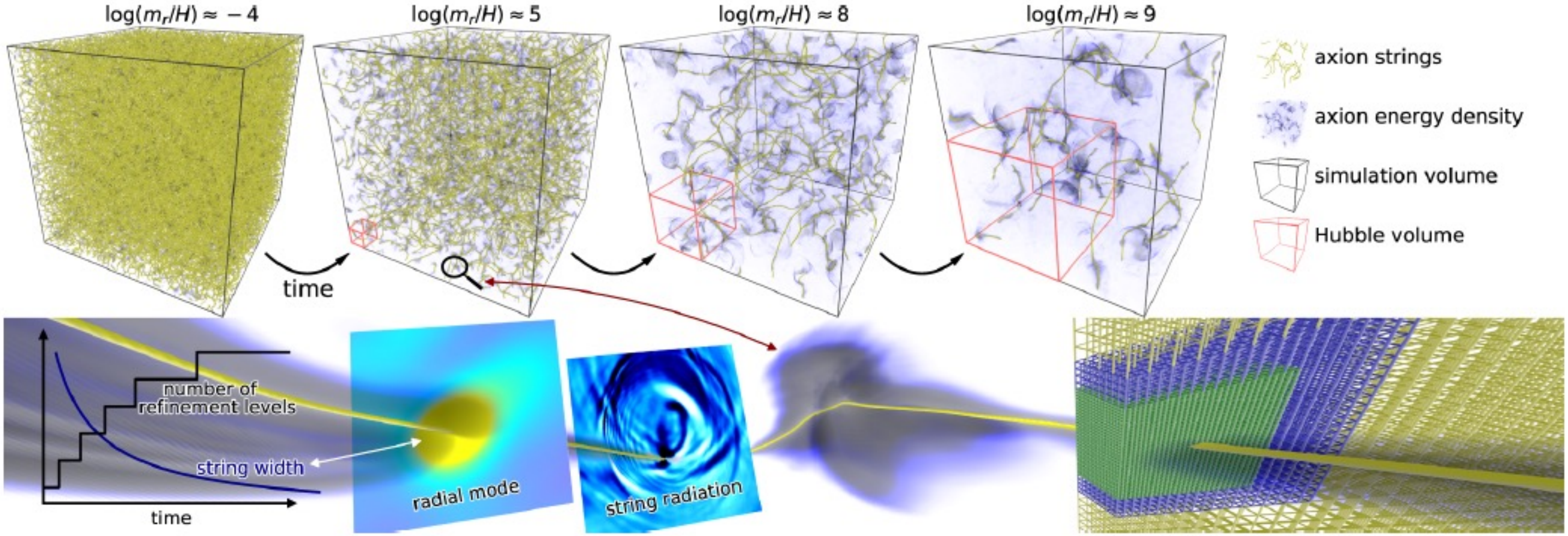

https://www.youtube.com/playlist?list=PLnDPmkb-Wddb_EmW6DKgHz6fw_mCzxF53

AXION NUMBER DENSITY FROM STRING: EXTRAPOLATION

[Gorghetto, Hardy, Villadoro, 1806.04677]

Spectrum of axions

$$\frac{d\rho_a}{dk} \sim \frac{1}{k^q}$$

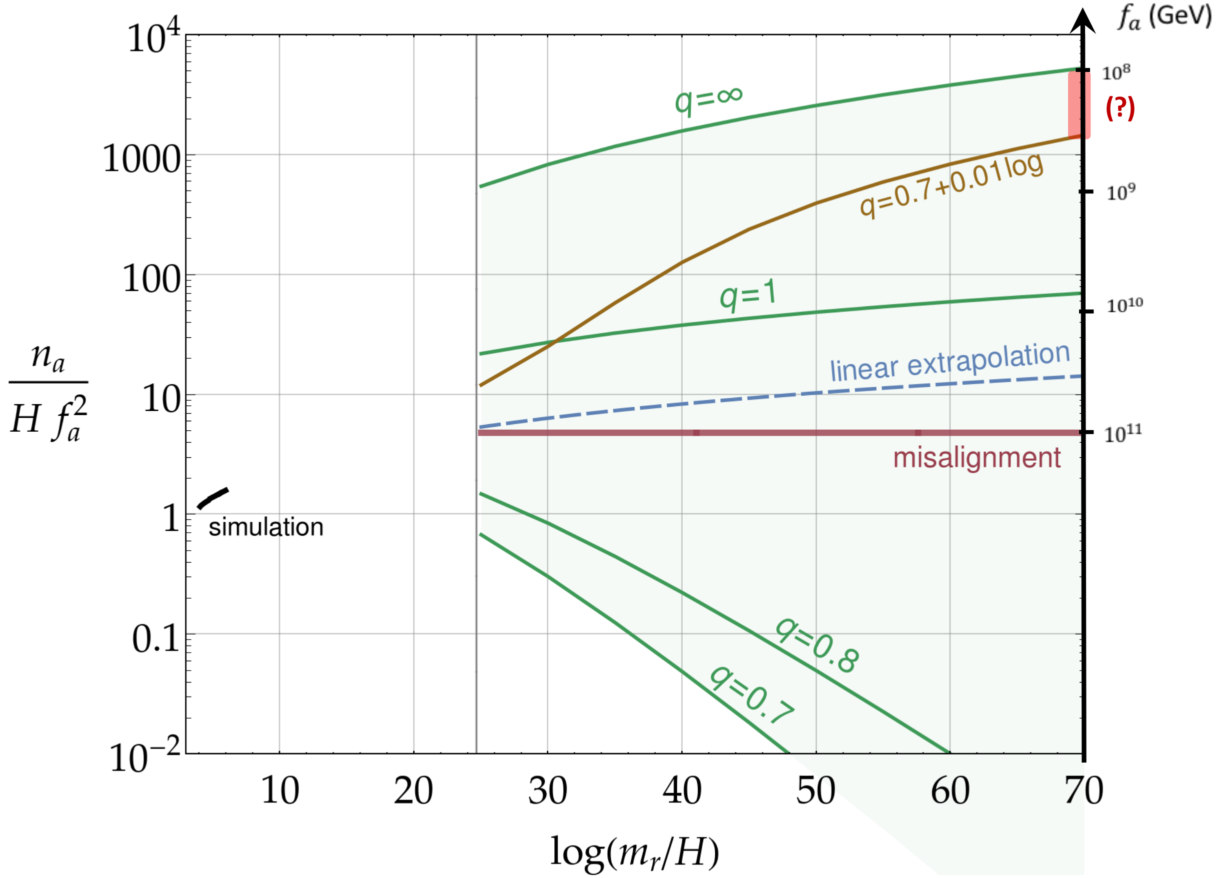

Precision determination of q(log) is needed to get a reliable extrapolation of the spectrum at late times

Axion string radiation uncertainties

Extrapolating beyond the end of the simulations could be treacherous and has large consequences for axion mass prediction

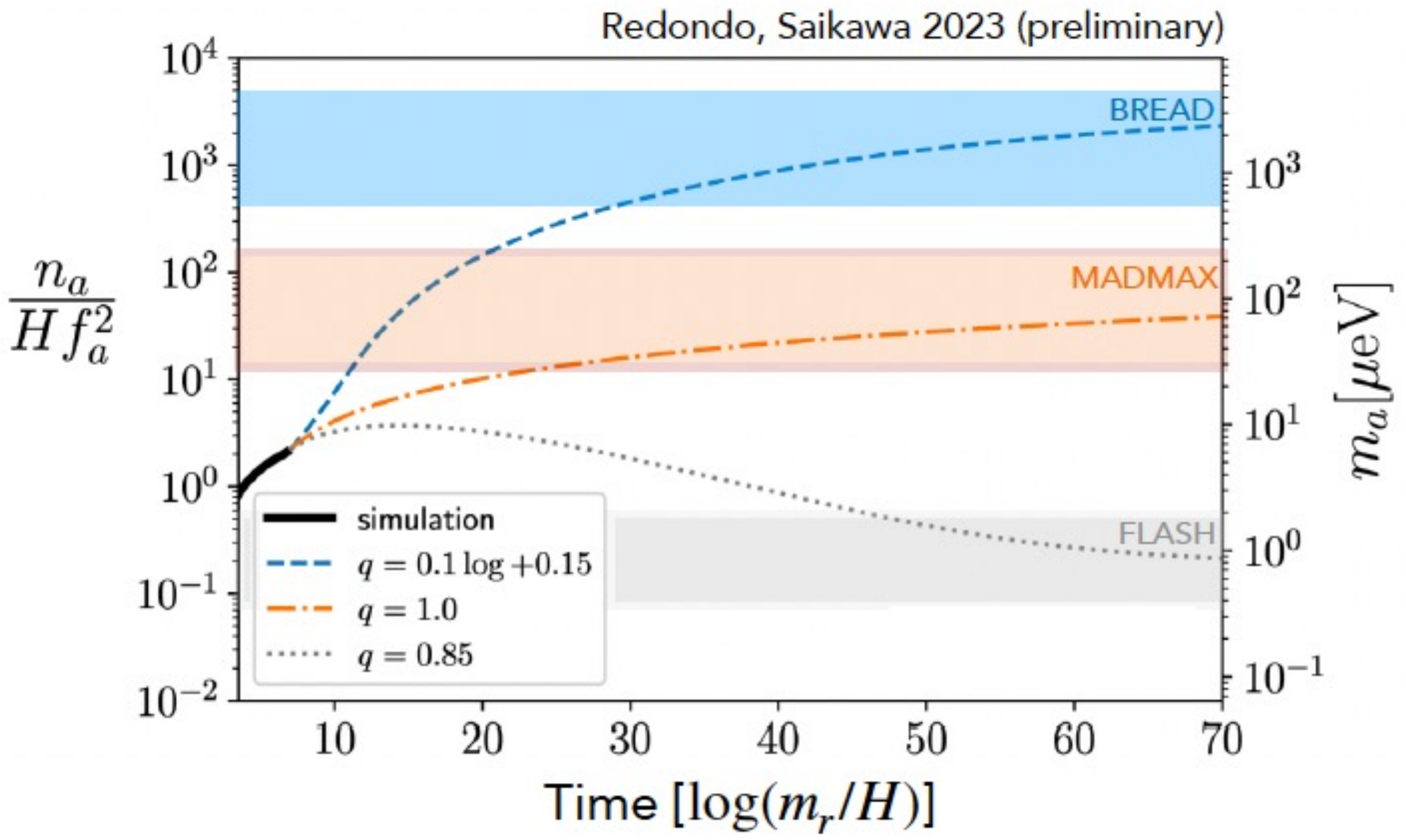

DOMAIN WALL

Before PQ transition

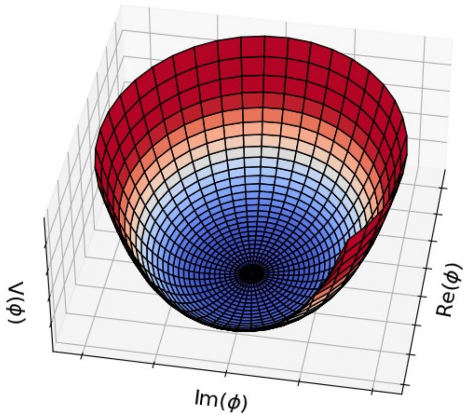

After PQ transition

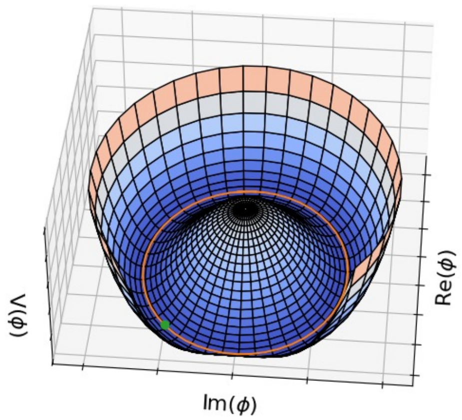

After QCD transition

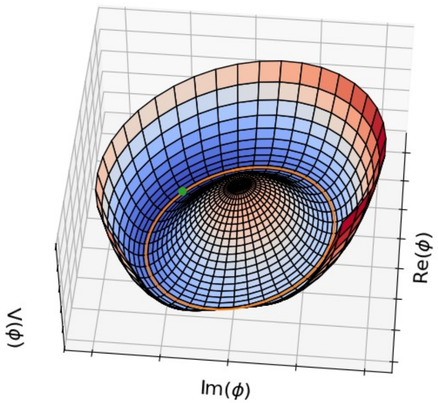

N_{DW} = 4 case

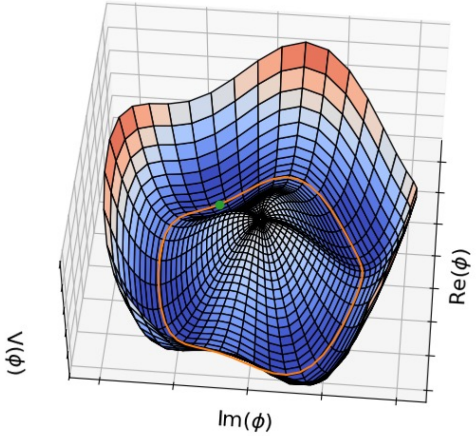

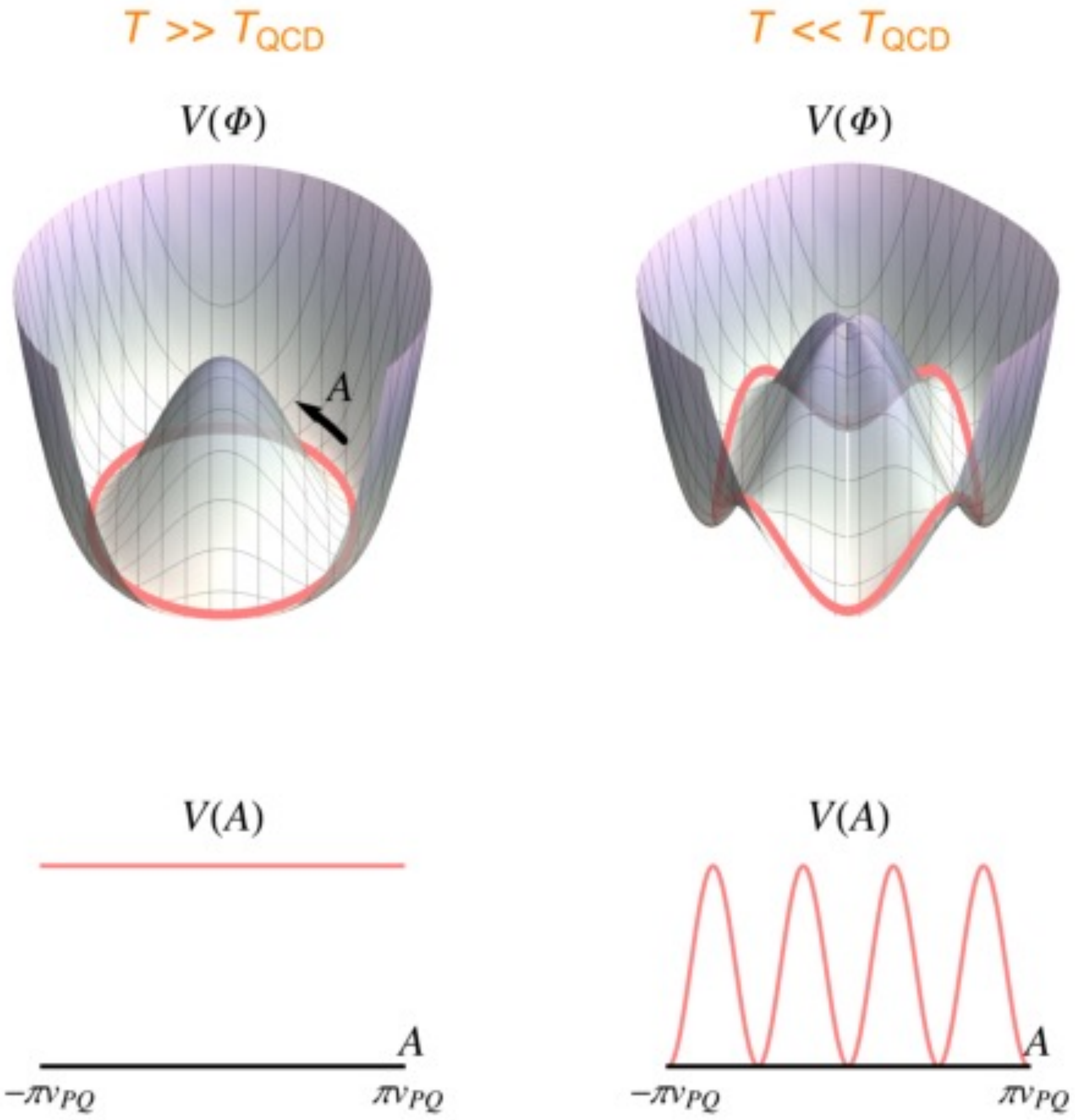

T >> T_QCD
T << T_QCD
V(Φ)
V(Φ)
A
V(A)
V(A)
A
A
−πv_PQ
πv_PQ
−πv_PQ
πv_PQ

TOP VIEW OF STRING WALL SYSTEM WITH N_{DW}=3

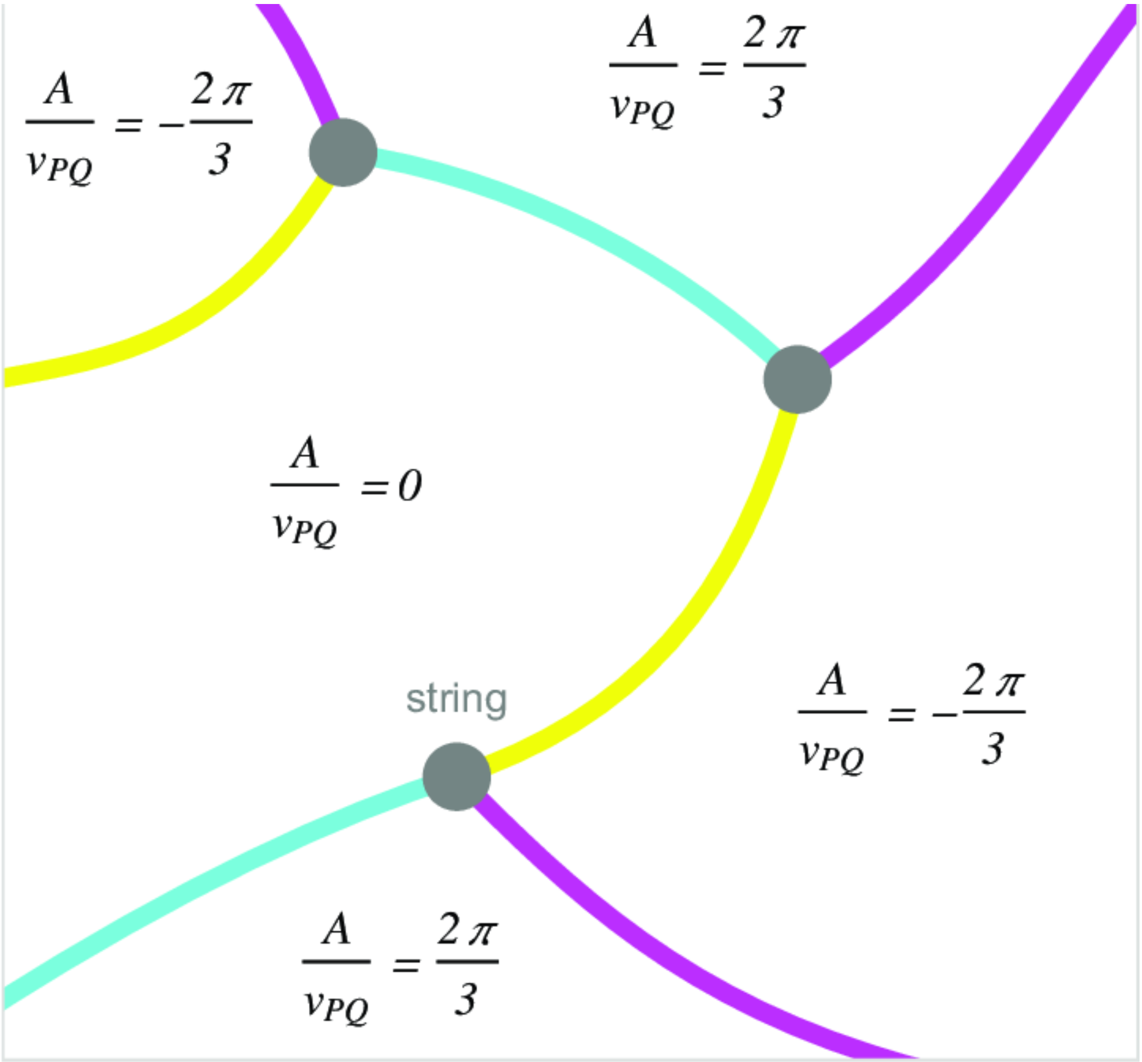

DOMAIN WALL WITH NDW=1

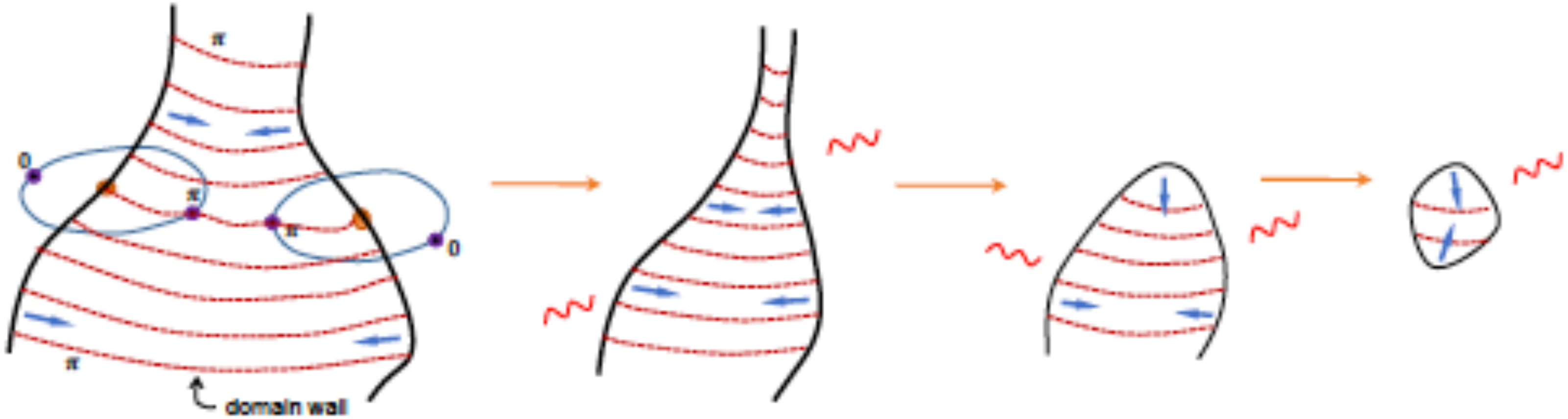

Figure 3: *Domain wall configurations with $N_W = 1$. Domain walls (in red) are attached to strings and in $O(1)$ Hubble times the full system shrinks into axion radiation.*

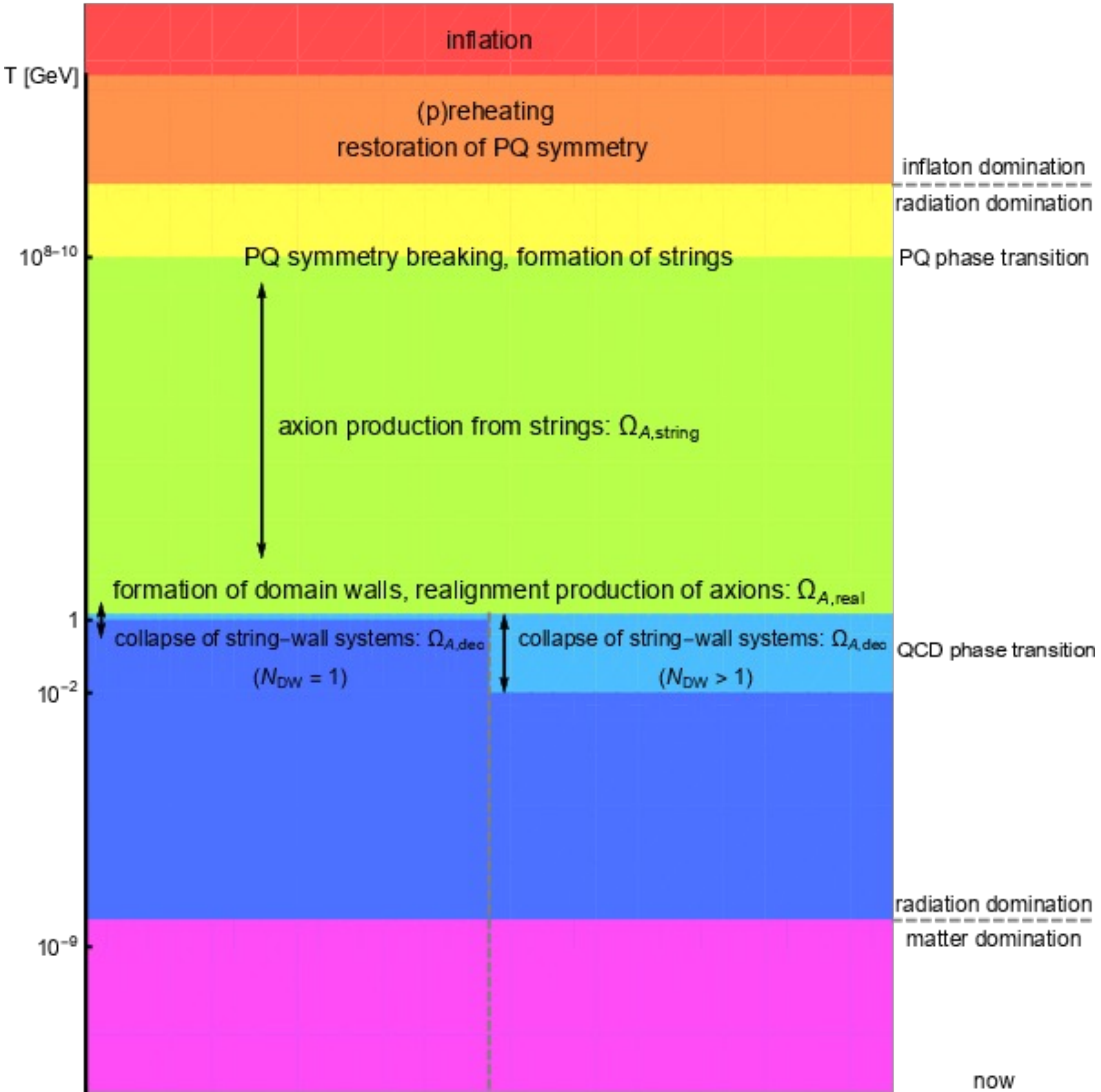

inflation
T [GeV]
(p)reheating
restoration of PQ symmetry
inflaton domination
radiation domination
10^{8-10}
PQ symmetry breaking, formation of strings
PQ phase transition
axion production from strings: $\Omega_{A,\mathrm{string}}$
formation of domain walls, realignment production of axions: $\Omega_{A,\mathrm{real}}$
1
collapse of string–wall systems: $\Omega_{A,\mathrm{dec}}$
($N_{\mathrm{DW}} = 1$)
collapse of string–wall systems: $\Omega_{A,\mathrm{dec}}$
($N_{\mathrm{DW}} > 1$)
QCD phase transition
10^{-2}
radiation domination
matter domination
10^{-9}
now

After t_{QCD} axion field forms quasi-stable solitons that lay down small-scale perturbations

These eventually form AU—mpc gravitationally bound clumps of axions with masses $M \in [10^{-15}, 10^{-9}]\ M_{\odot}$

→ **axion miniclusters**

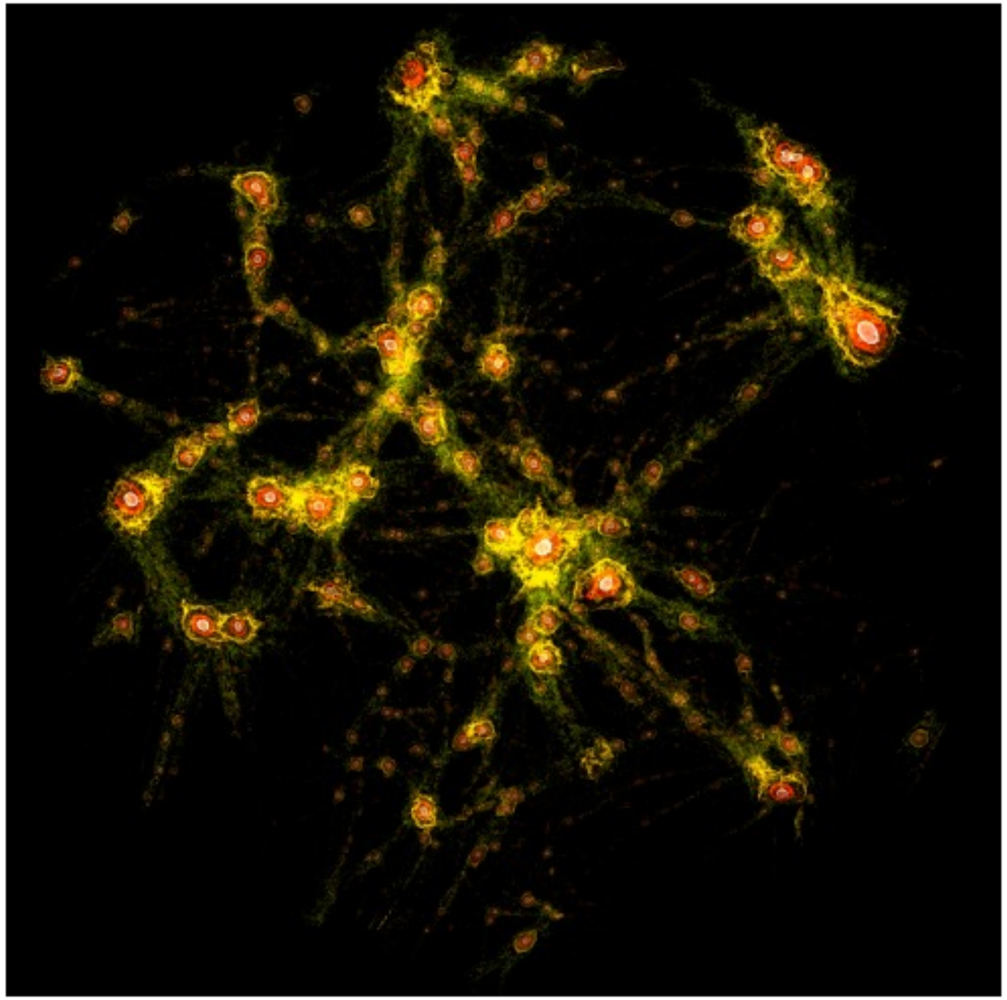

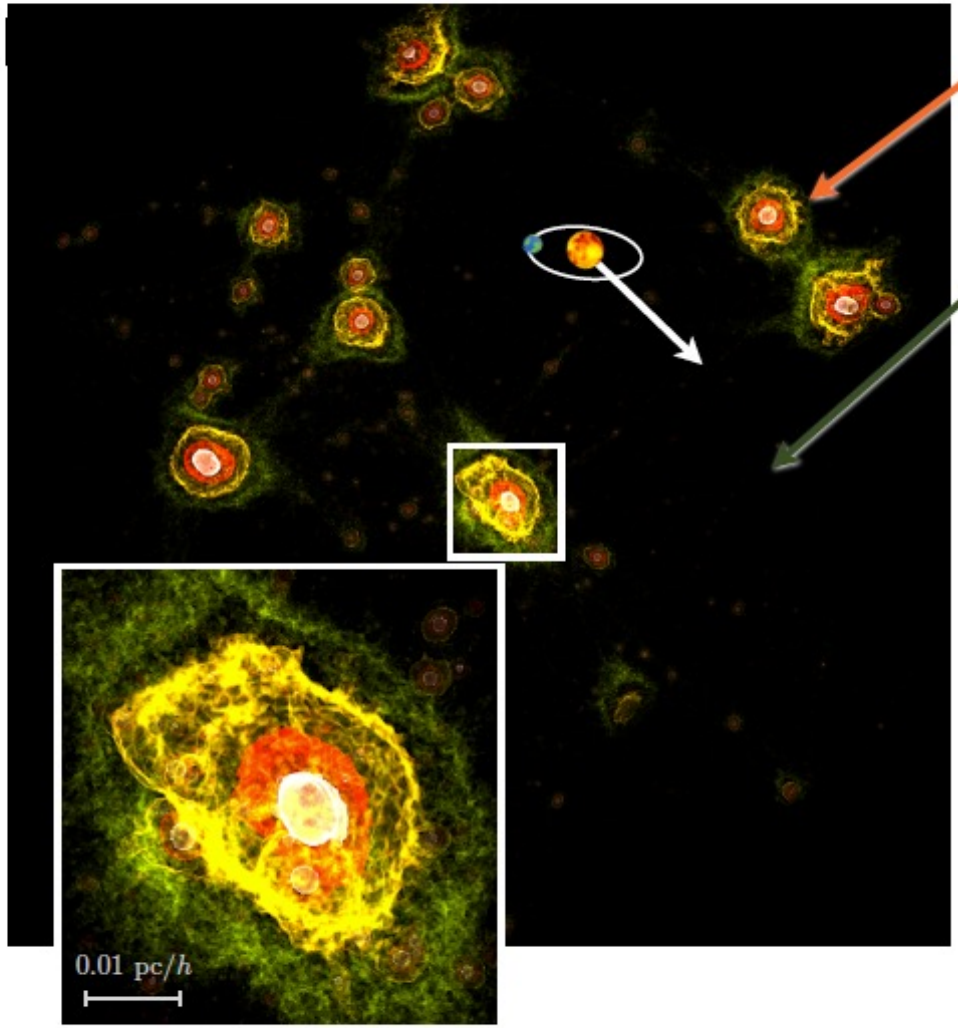

Miniclusters

Minivoids

Miniclusters contain >80% of the axions but make up <1% of the volume

Earth travels through galaxy at about 0.2 mpc per year, so experiments are much more likely to sample the mini*voids* than the mini*clusters*

Minivoids are mostly stable by final simulation time (z~100)

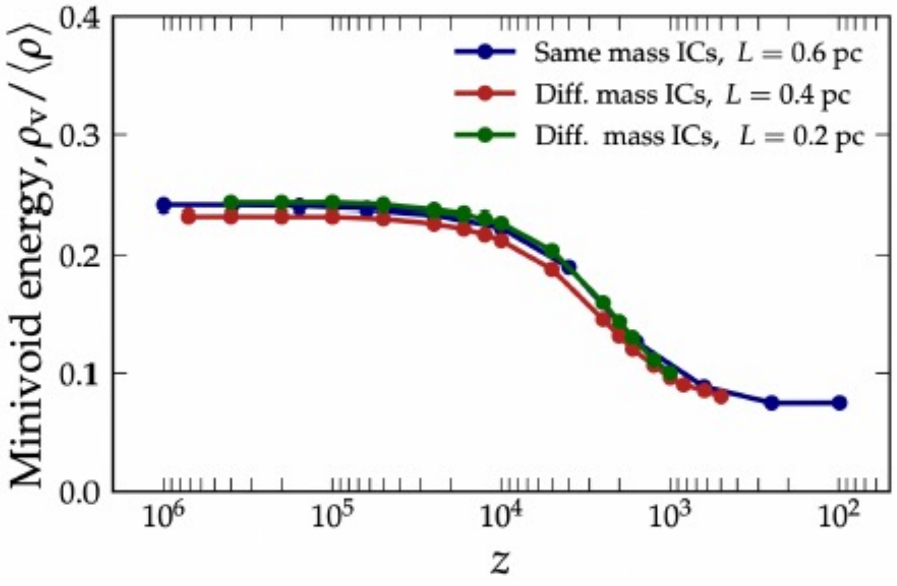

Typical "worst case scenario" density would be inside the minivoids ~10% of large-scale average density

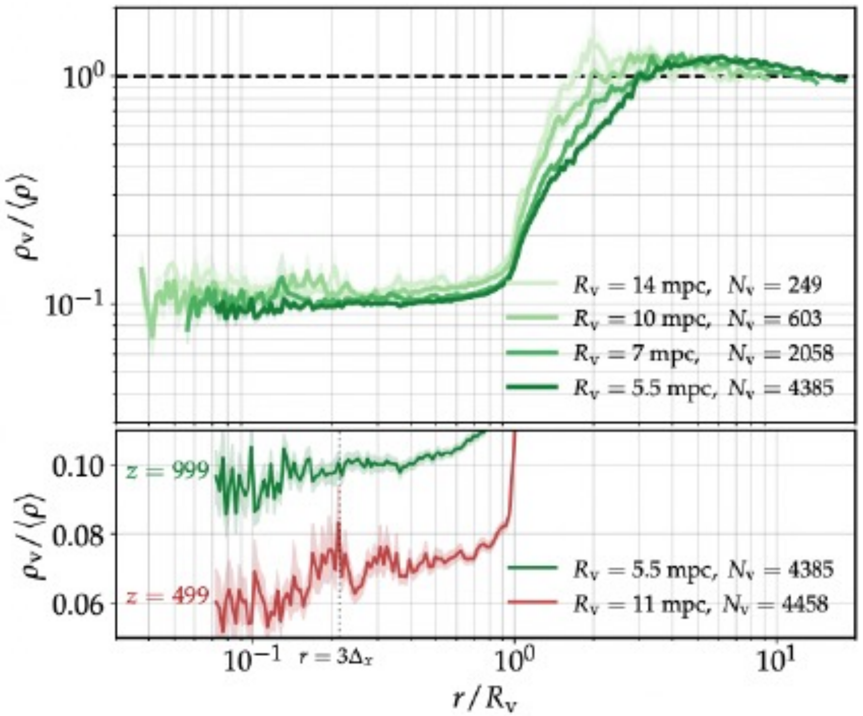

Eggemeier, CAJO+ [2212.00560]

Eggemeier et al. 2212.00560.

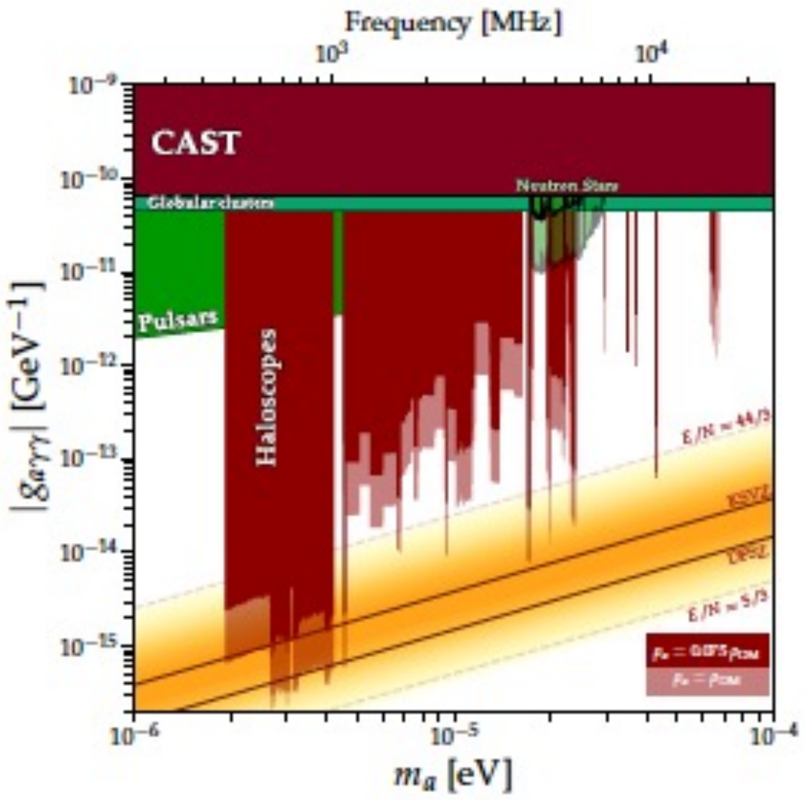

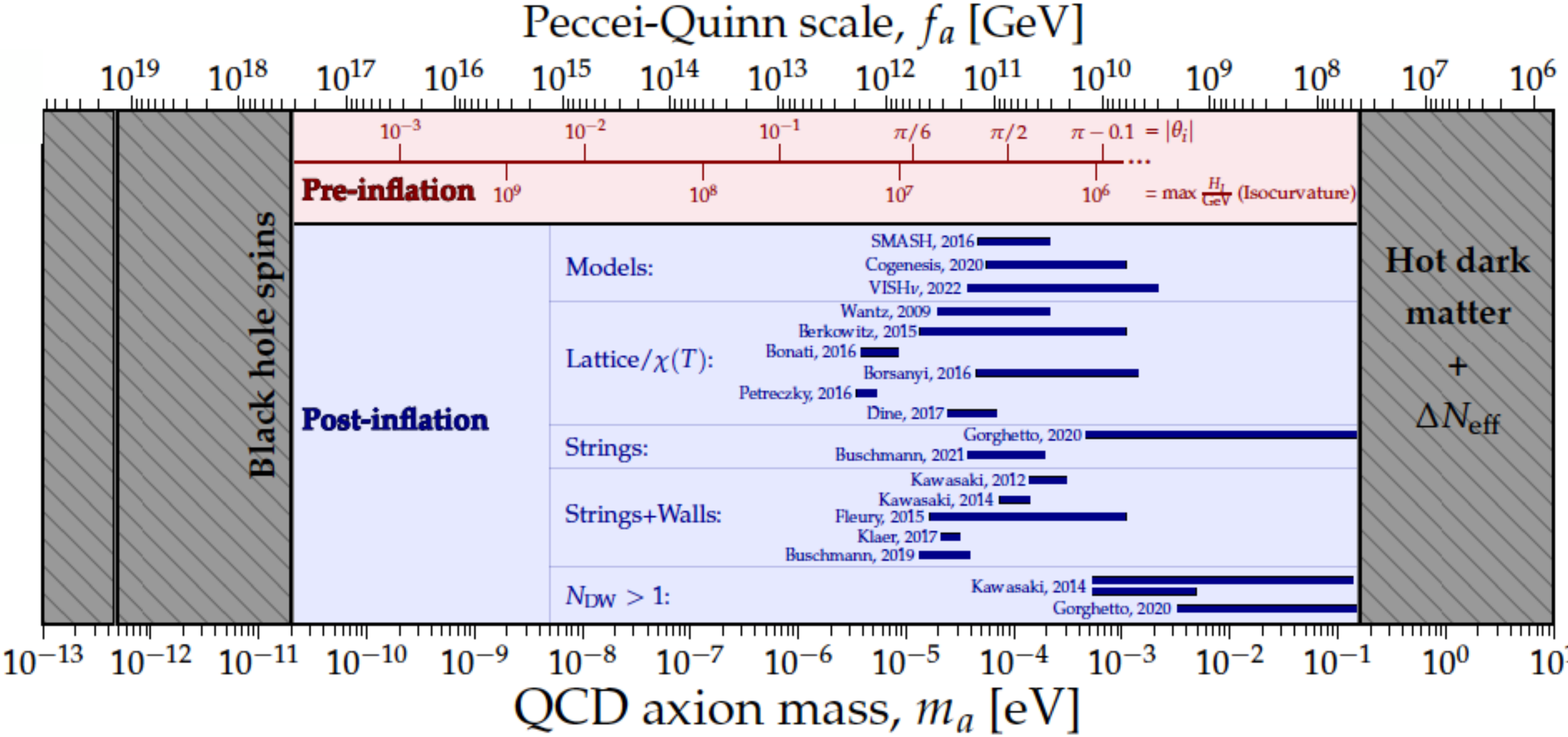

github.com/cajohare/AxionLimits

1502.03325

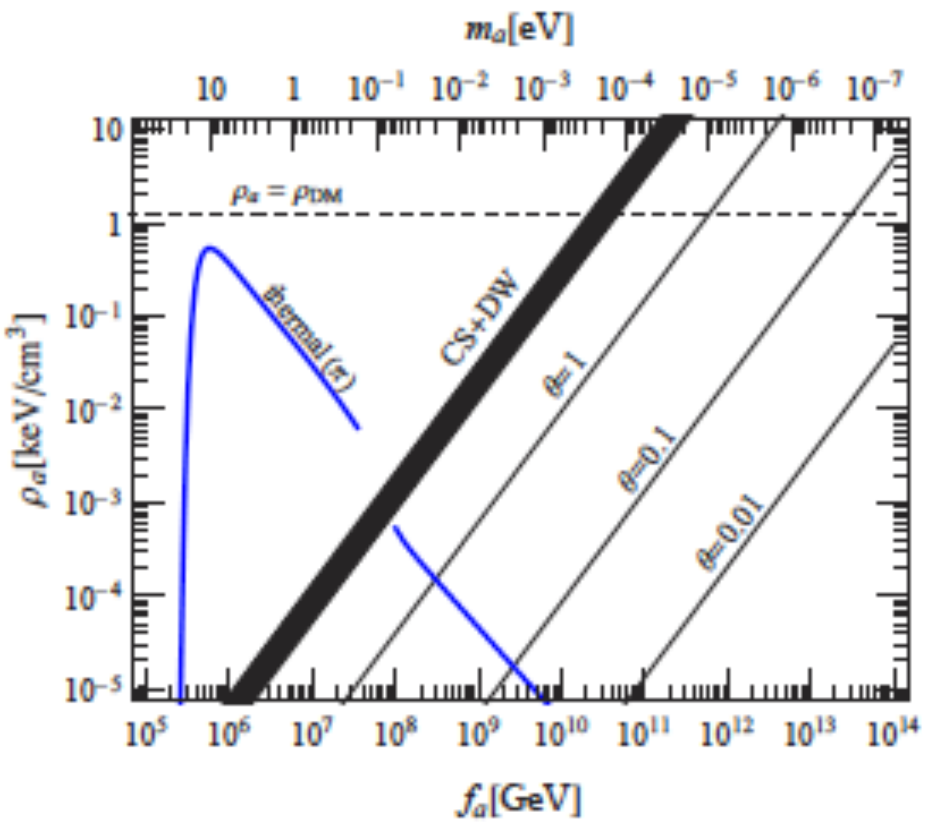

Figure 1. Present-day axion dark matter density as a function of m_a. The thermal axion population, which forms hot dark matter, is represented by the thick blue line. The thick black line denotes the cold axion population in the scenario in which Peccei-Quinn symmetry breaking occurs after inflation so that the visible universe contains many patches of different initial axion-field misalignment angles Θ_i; the energy density shown here subsumes both contributions from the re-alignment mechanism and from cosmic string (CS) and domain-wall (DW) decay according to reference [42]. The thin black lines pertain to the case in which Peccei-Quinn symmetry breaking occurs before inflation so that one single initial misalignment angle Θ_i pervades the entire visible universe; the cold axion populations for several different values of Θ_i as indicated at the lines are shown. (Figure adapted from one supplied by Javier Redondo.)

ALP DM

Arias et al, 1201.5902

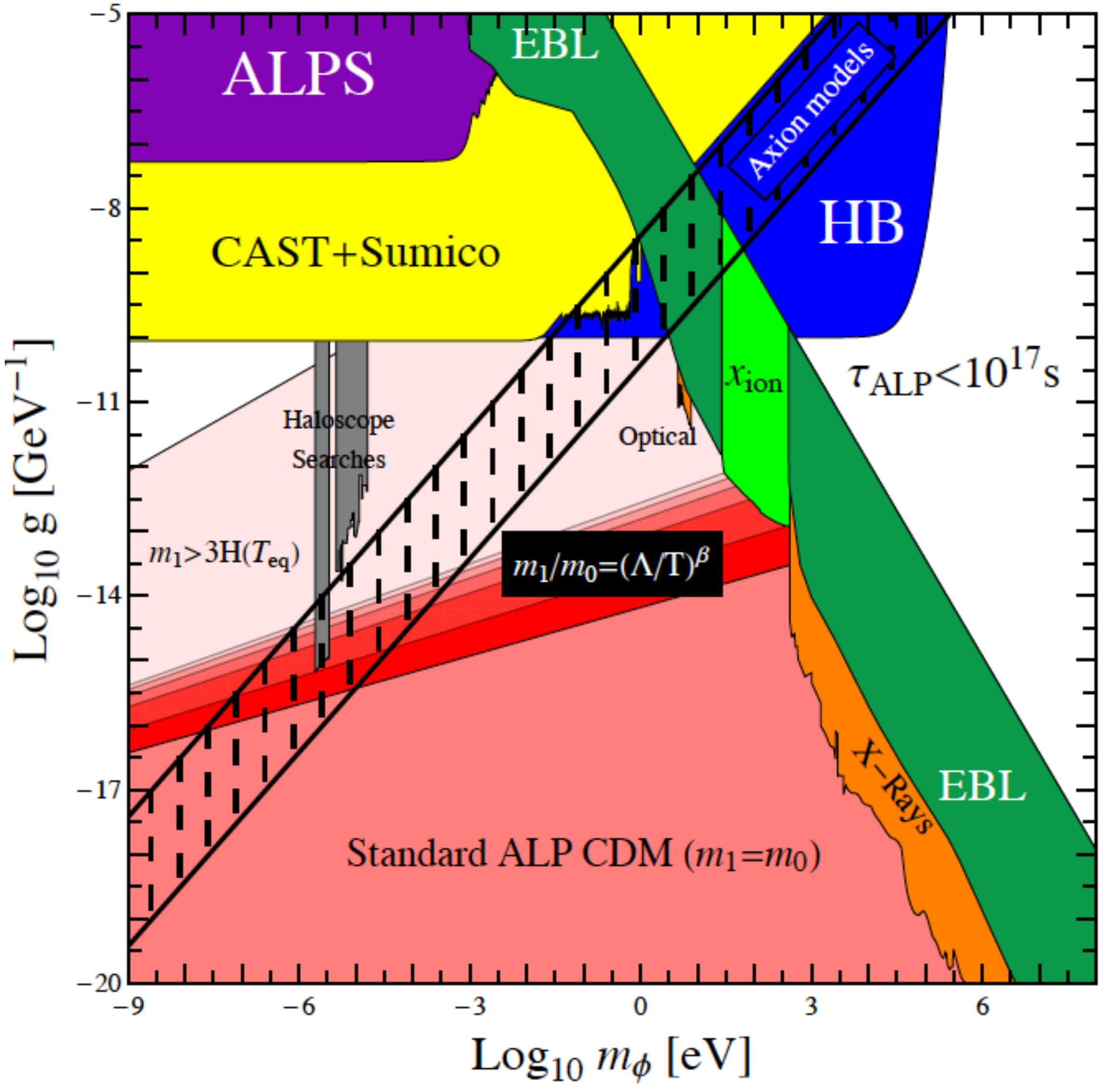

SCHEME OF AN HALOSCOPE

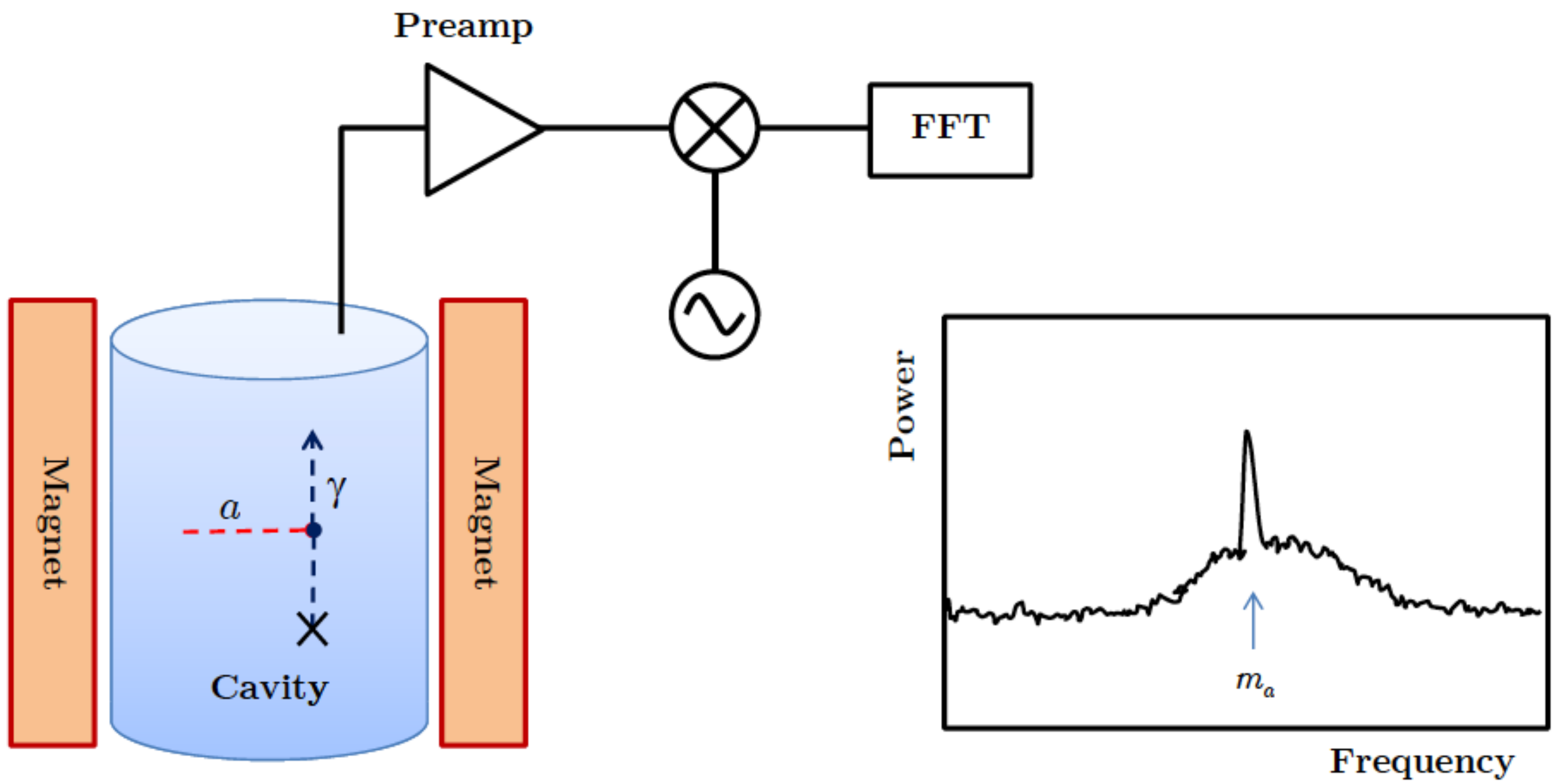

HALOSCOPE SENSITIVITY

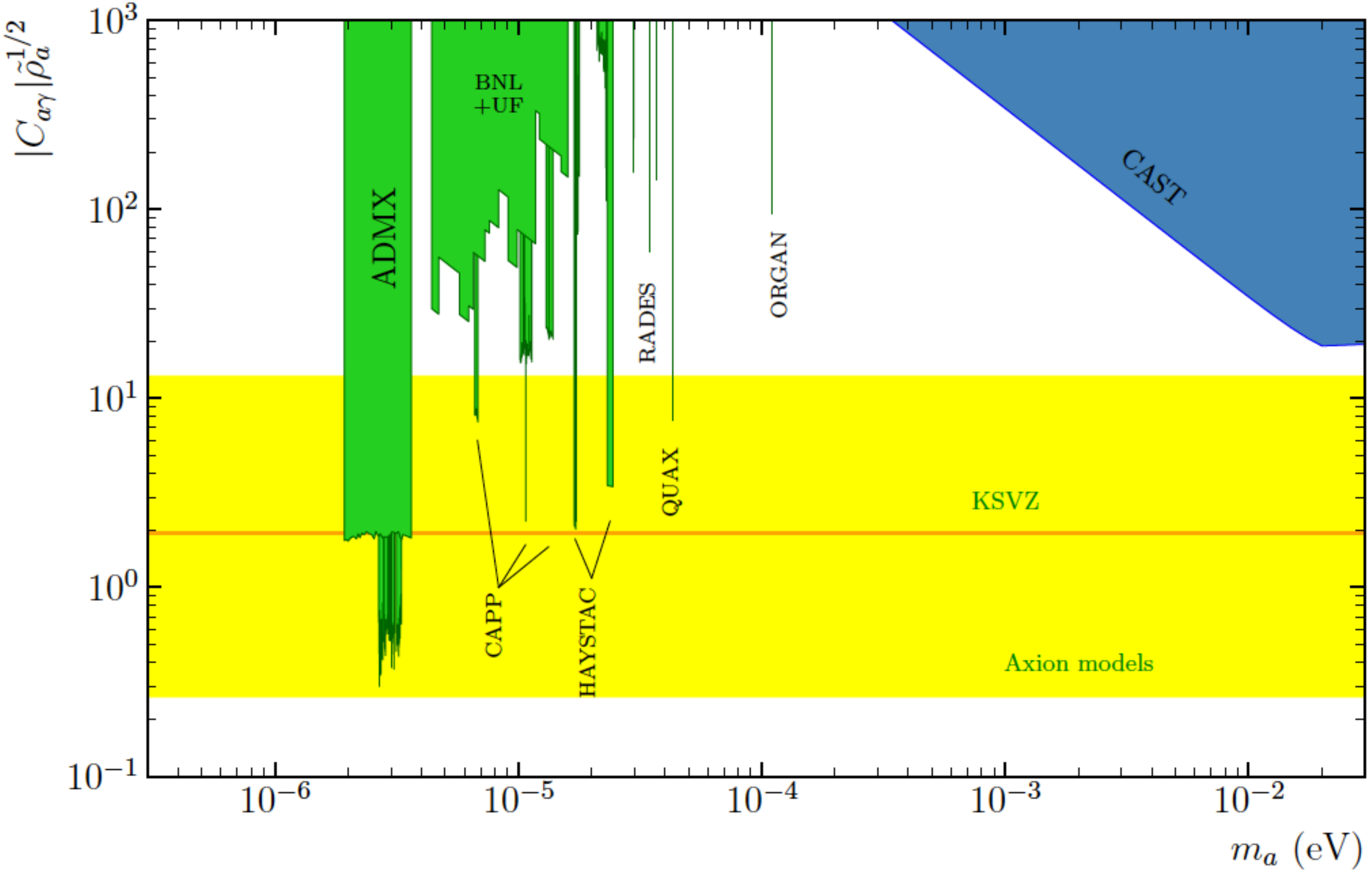

MADMAX: A DIELECTRIC HALOSCOPE

[Caldwell et al., 1611.05865]

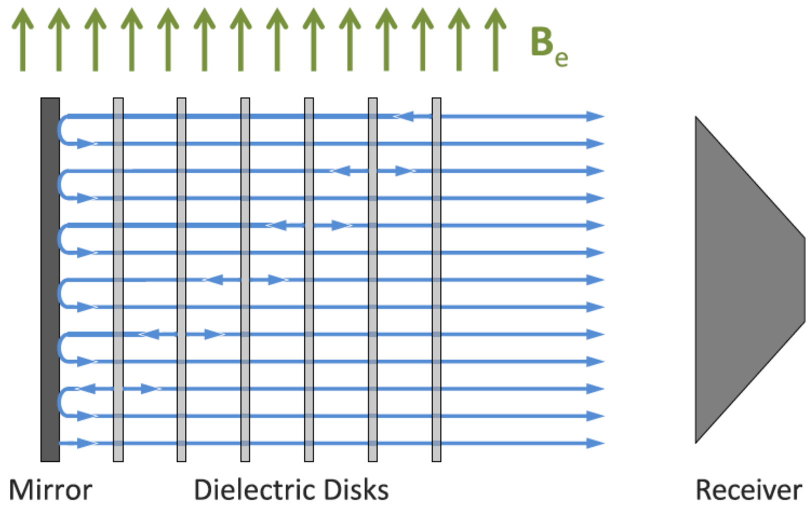

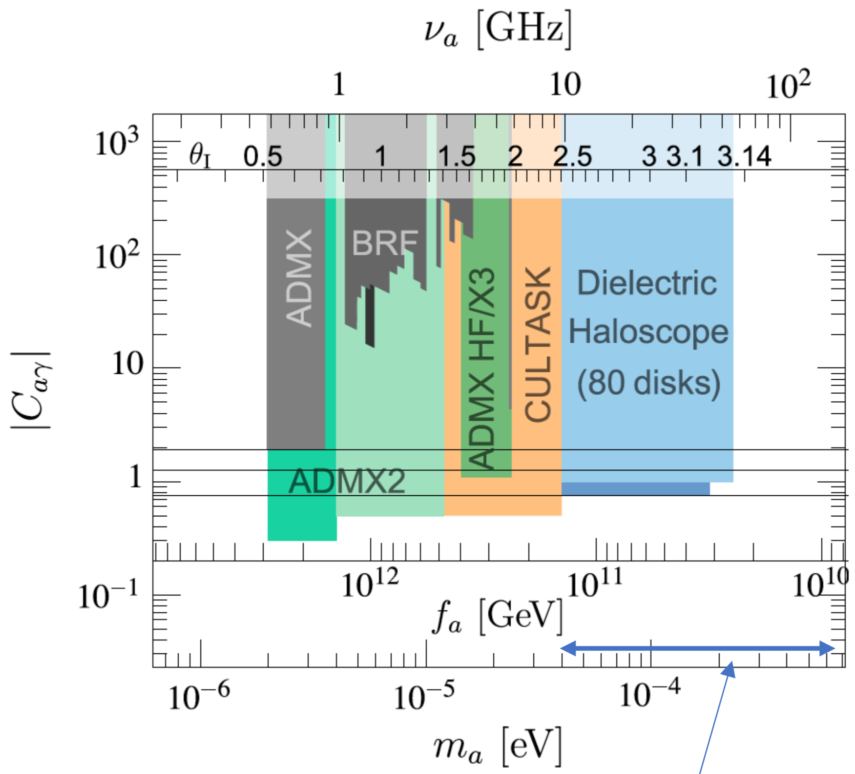

- In an external **B-field** the **axion** sources an oscillating **E-field**

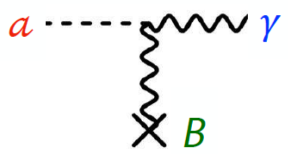

$$E_a = -\frac{g_{a\gamma\gamma} B_e}{\epsilon} a$$

- At surfaces with transition of $\epsilon_1 \neq \epsilon_2$: E-field must be continuous
  → **Emission of photons**

Sensitivity to QCD axion in the post inflation scenario

SEARCHES FOR AXION DM

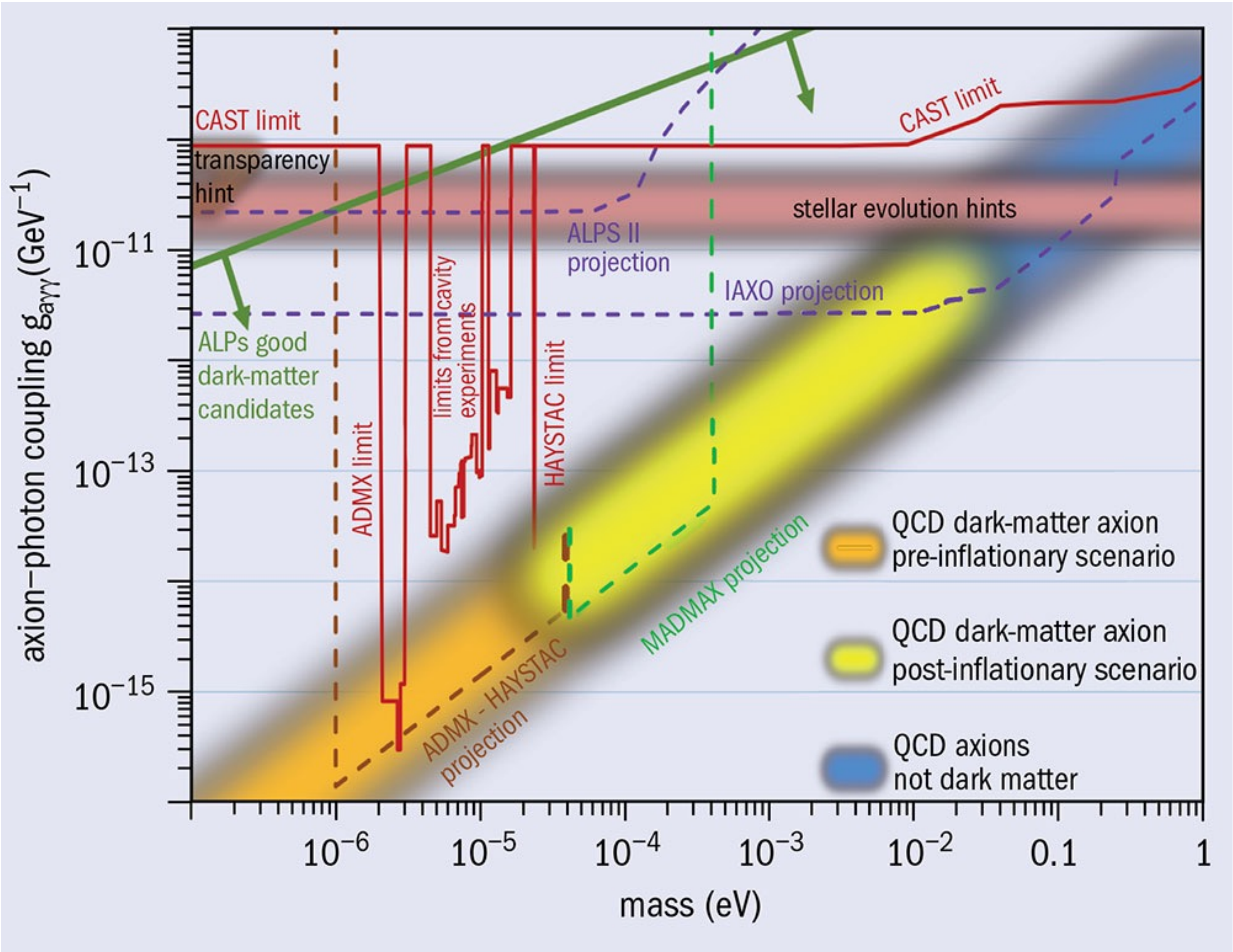

DM EXPERIMENTS

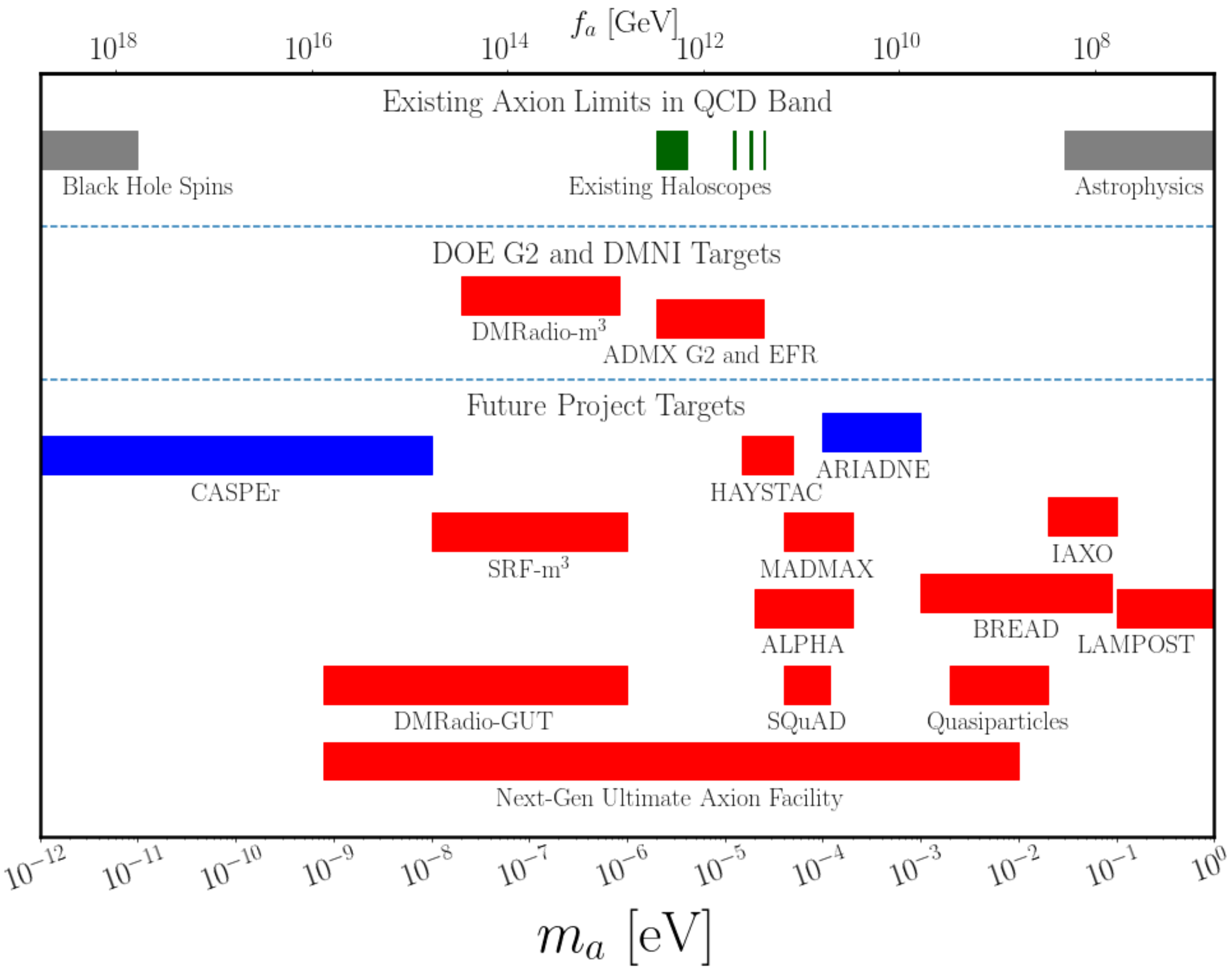

SOLAR MODELS

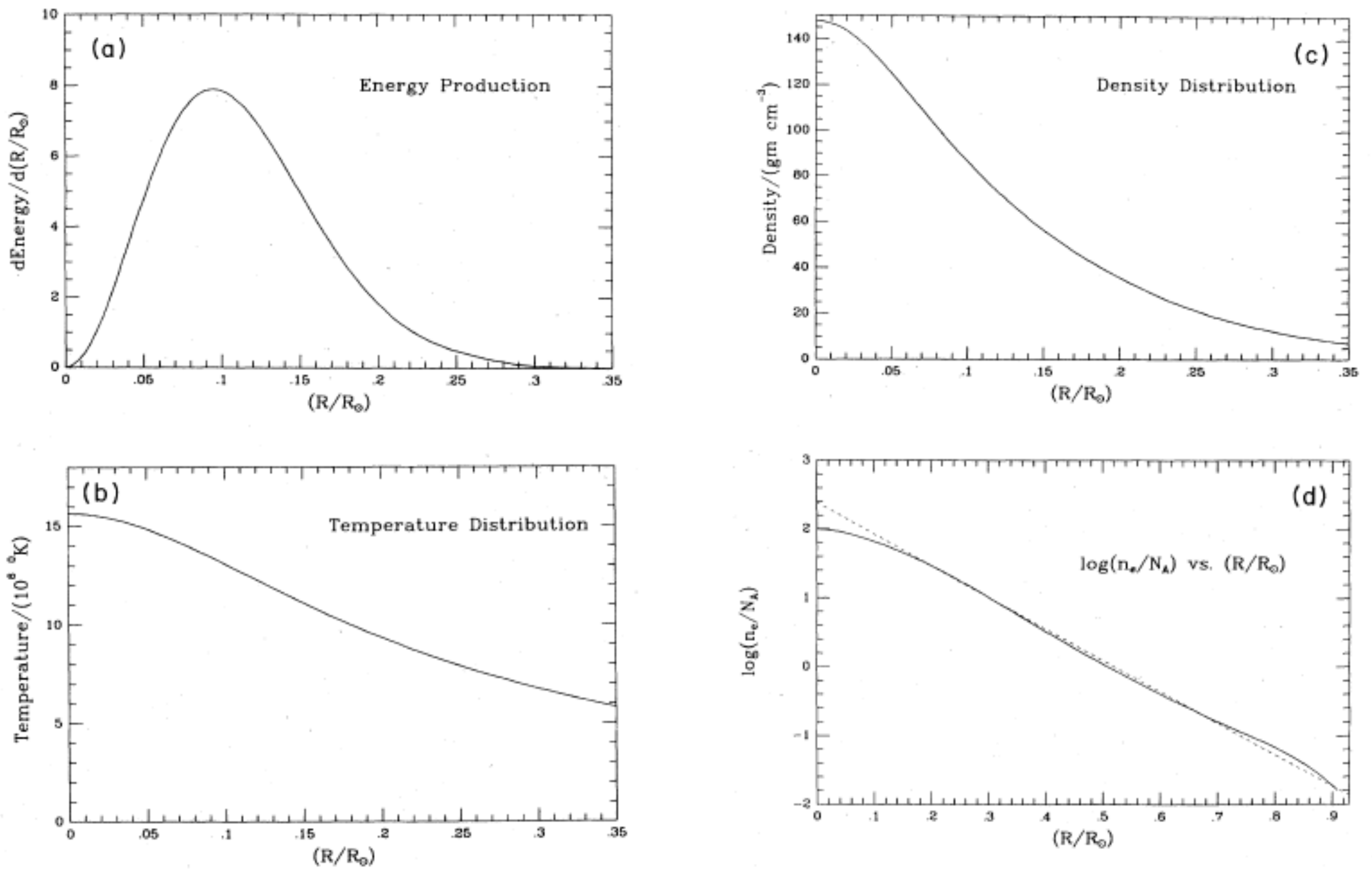

FIG. 6. Energy production, temperature, density, and electron density: (a) the fraction of the energy generation that originates in a given fraction of the solar radius as a function of position in the sun; (b) temperature distribution in the sun; (c) density distributions in the sun; (d) solid line, the logarithm of the electron number density N_e, divided by Avogadro's number N_A, as a function of solar radius; dotted line, exponential fit to the density distribution, the parameters of which are given in the text. These results are obtained from the standard solar model described in Sec. V.B and Tables X and XI.

SOLAR AXION FLUX

hep-ex/0702006

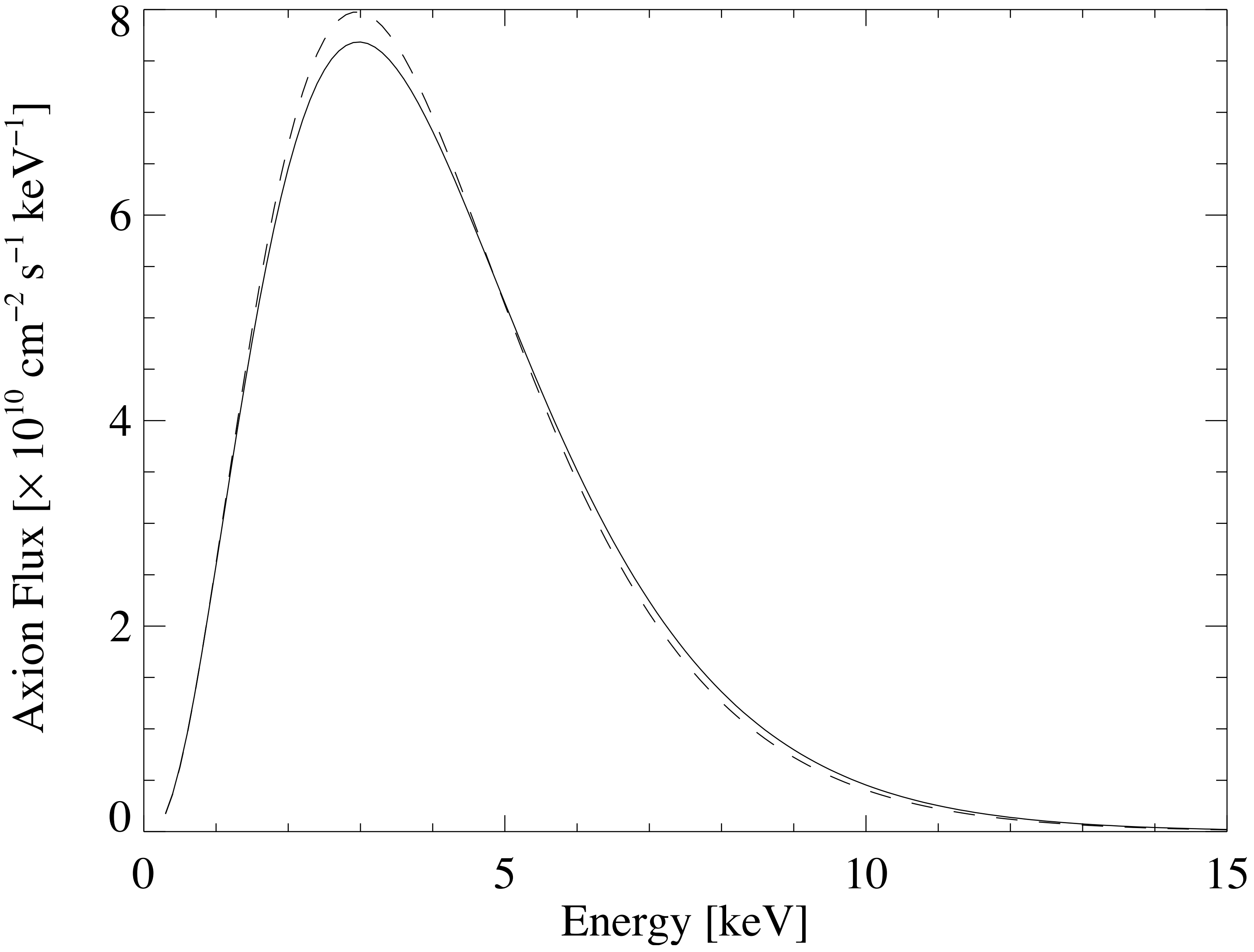

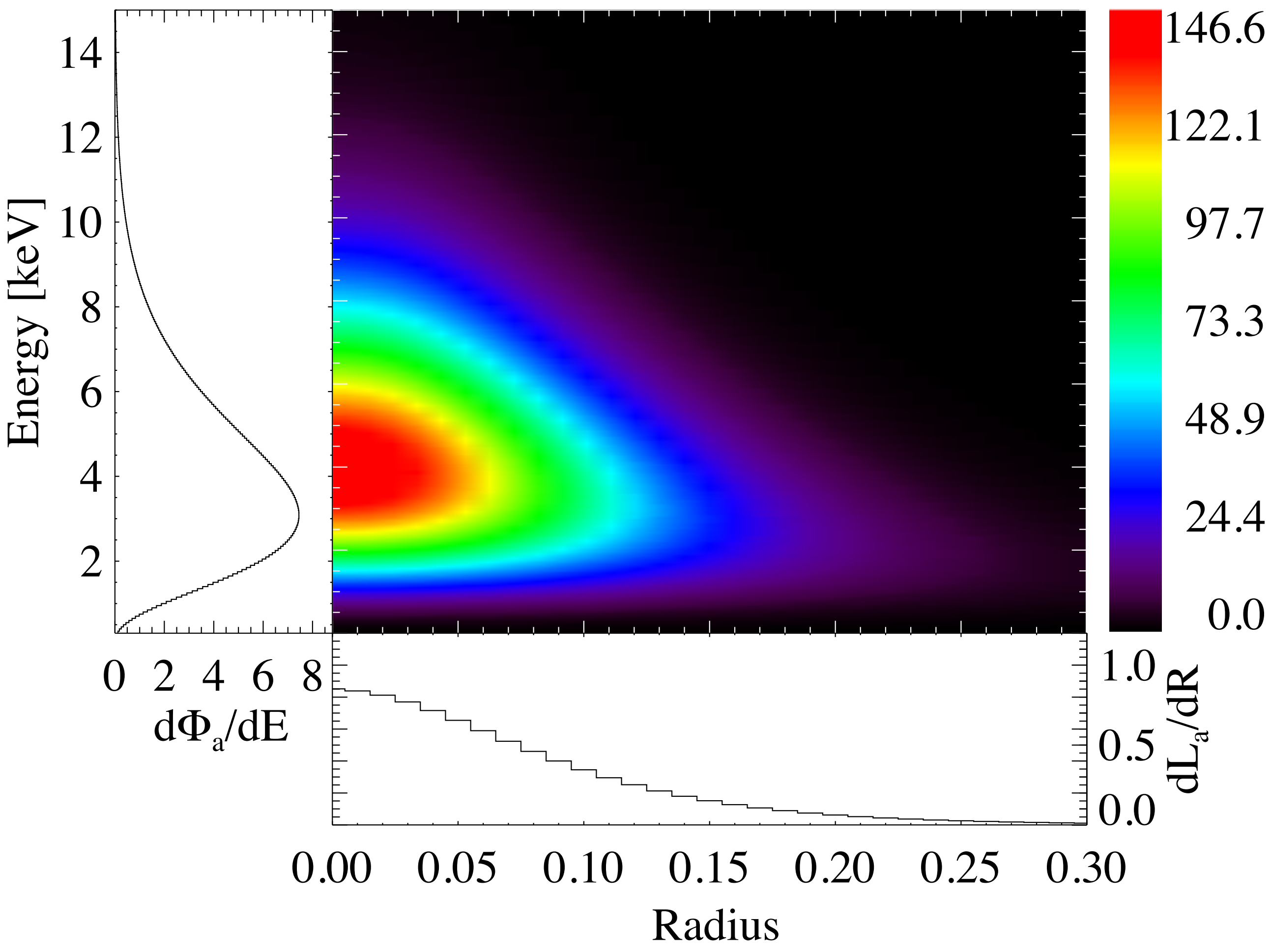

Energy [keV]
14
12
10
8
6
4
2
0 2 4 6 8
dΦa/dE
146.6
122.1
97.7
73.3
48.9
24.4
0.0
1.0
0.5
0.0
dLa/dR
0.00 0.05 0.10 0.15 0.20 0.25 0.30
Radius

HELIOSCOPES

Searches for solar axions: Axion helioscopes

Primakoff process **Axion-photon oscillation**

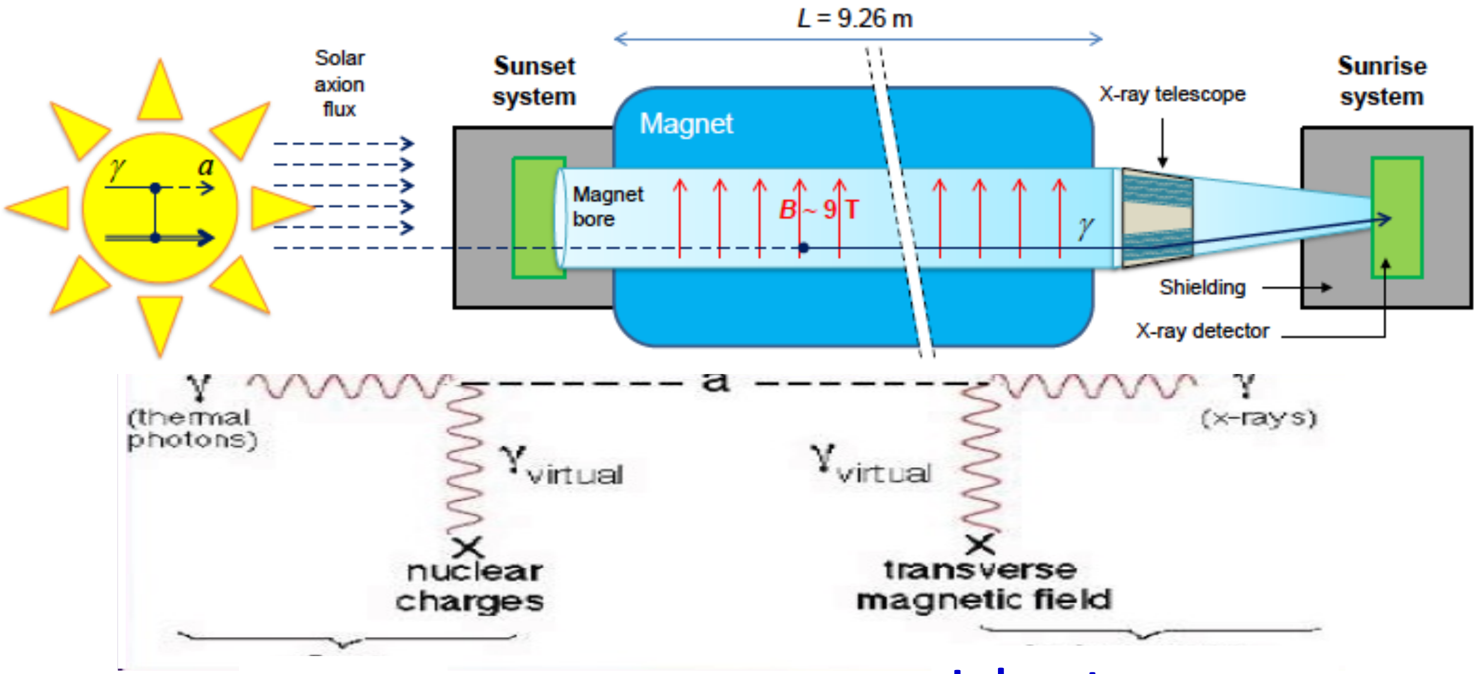

Sun **Laboratory**

- 1° generation: Brookhaven ⟶ 1992. Just a few hours of data
- 2° generation: Tokyo axion helioscope (SUMICO) ⟶ Results since 1998
- 3° generation: CERN Axion Solar Telescope (CAST) ⟶ Data since 2003

CAST @ CERN

Axion-Photon Conversion in CAST

$$P(a \to \gamma) = \left(\frac{g_{a\gamma}BL}{2}\,\frac{\sin(qL/2)}{qL/2}\right)^2 = \left(\frac{g_{a\gamma}B}{2}\right)^2 \times \begin{cases} L^2 & \text{for } qL \ll 1 \\ 1/2q^2 & \text{for } qL \gg 1 \end{cases}$$

Momentum transfer $q = (m_a^2 - m_\gamma^2)/2\omega$

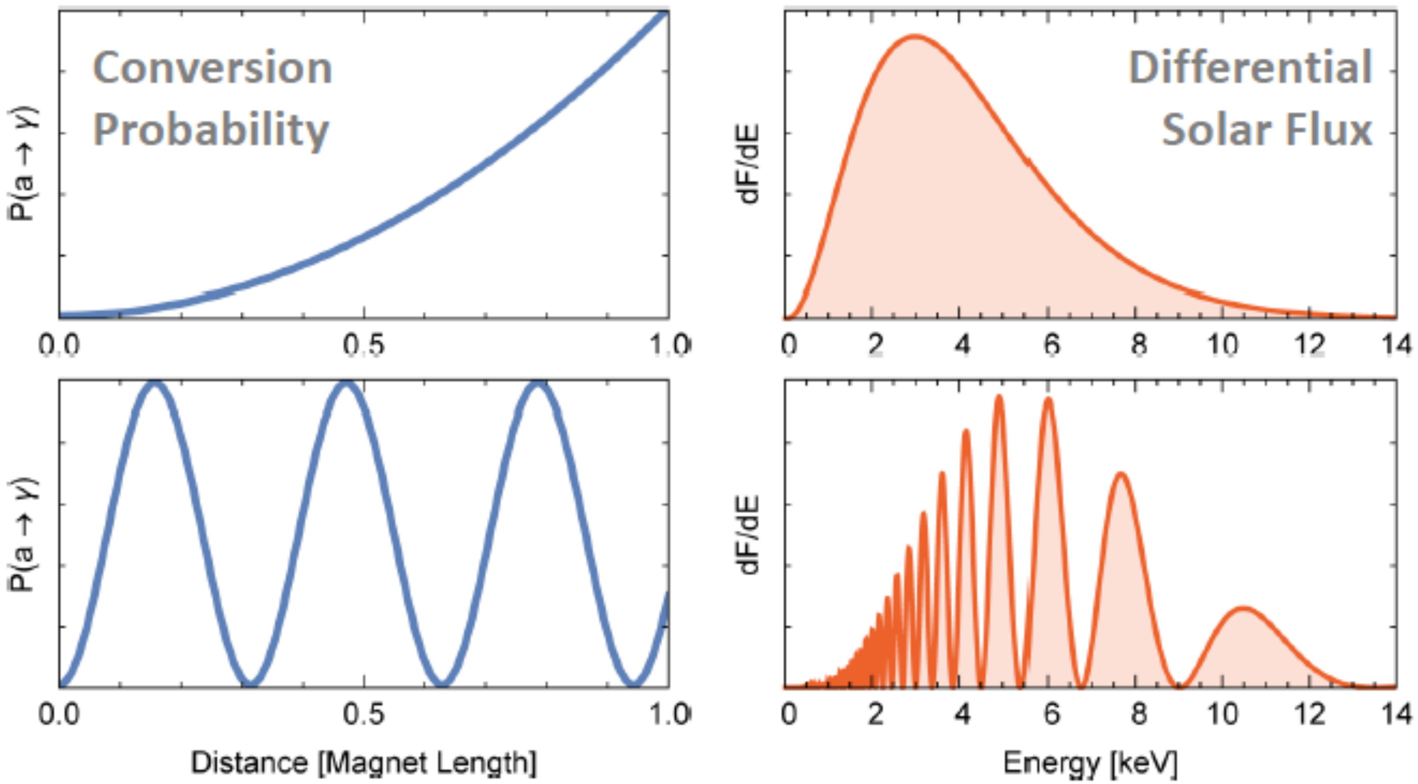

Small mass ("coherent")

Large mass ("incoherent")

Can "weigh" axions arXiv:1811.09290

Helioscope Limits

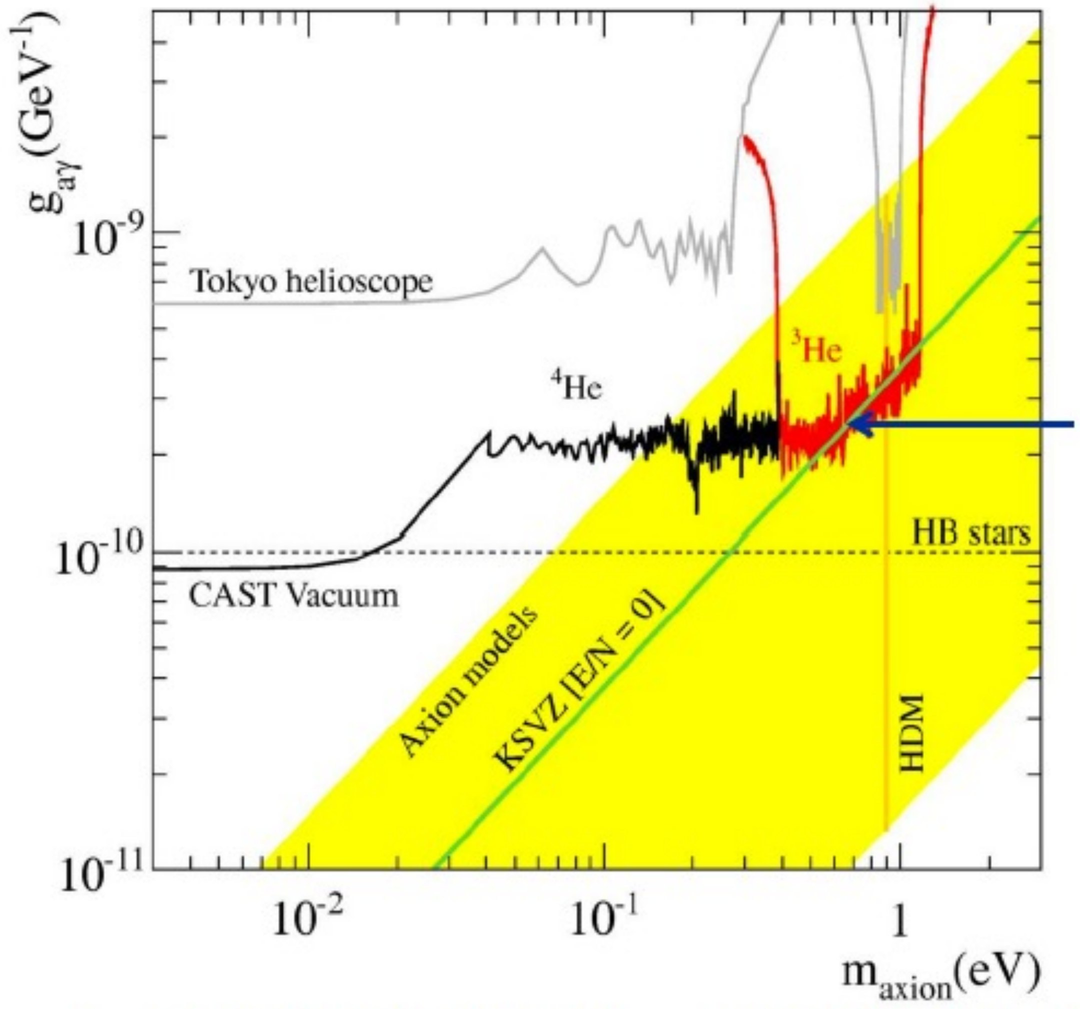

First experimental crossing of the KSVZ line

CAST-I results: PRL 94:121301 (2005) and JCAP 0704 (2007) 010
CAST-II results (He-4 filling): JCAP 0902 (2009) 008
CAST-II results (He-3 filling): PRL 107: 261302 (2011) and PRL 112, 091302 (2014)

CAST LIMIT

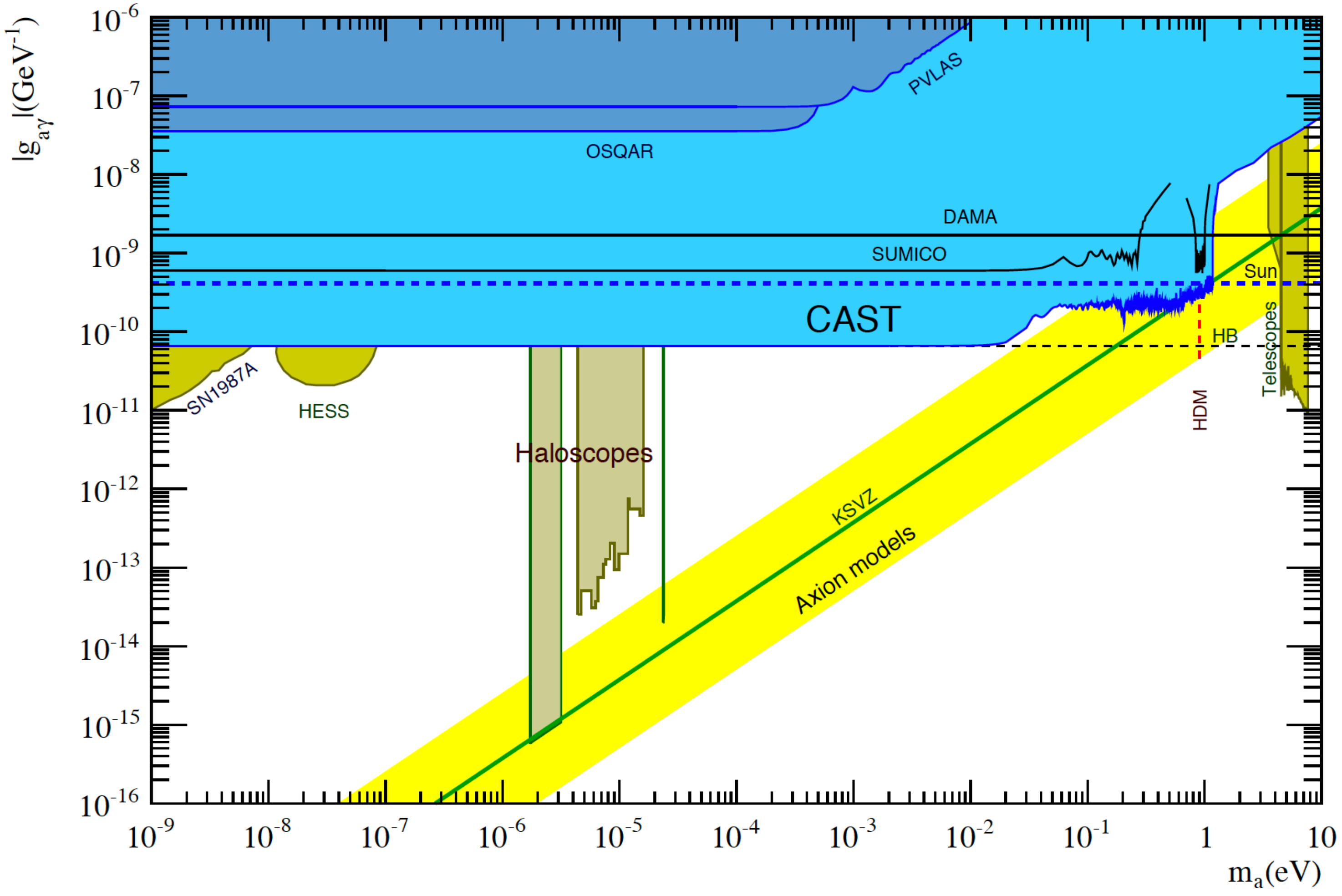

[1705.02290]

4^{th} Generation: An Enhanced Axion Helioscope

Enhanced axion helioscope: JCAP 1106, 013 (2011)

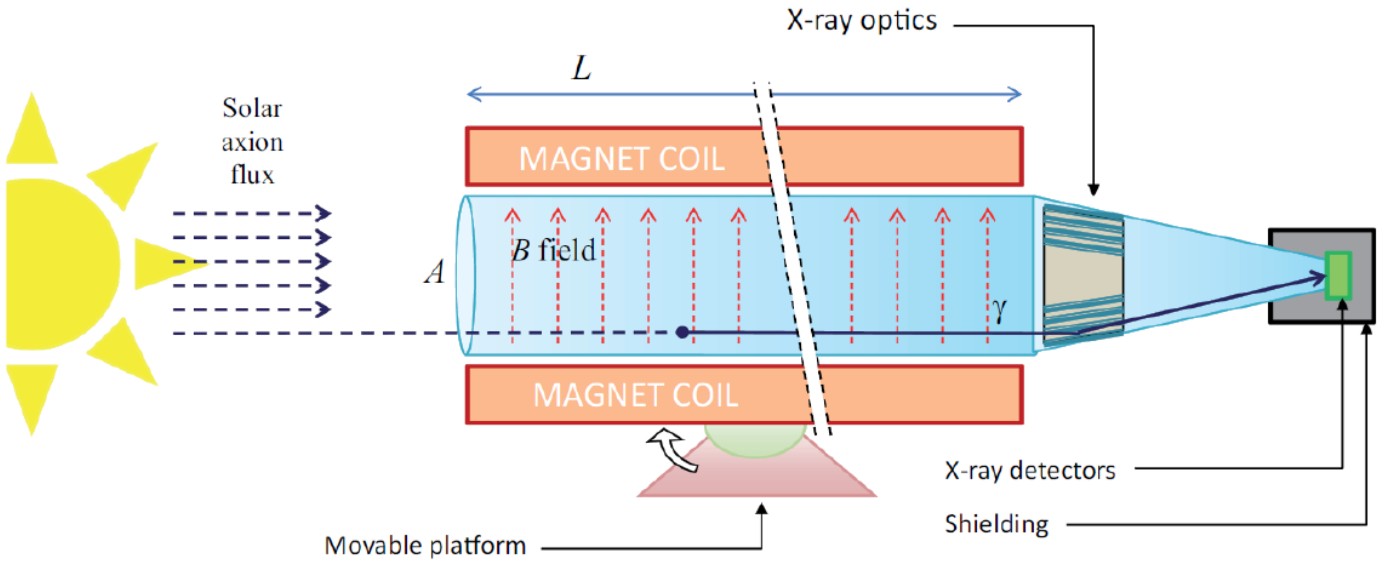

Measure of sensitivity to axion-photon interaction:

$$g_{a\gamma}^{4} \propto \underbrace{(BL)^{-2} A^{-1}}_{\textit{magnet}} \times \underbrace{t^{-1/2}}_{\textit{exposure}} \times \underbrace{s^{1/2} \varepsilon_0^{-1}}_{\textit{optics}} \times \underbrace{b^{1/2} \varepsilon^{-1}}_{\textit{detectors}}$$

magnet
- B = magnetic field
- L = magnet length
- A = cross-sectional area

exposure
- t = time

optics
- s = spot size
- ε_0 = efficiency

detectors
- b = background
- ε = efficiency

The smaller $g_{a\gamma}$ the better!

Slide by Julia Vogel

Expected improvement over CAST with IAXO:
1–1.5 orders of magnitude in sensitivity to $g_{a\gamma}$ (factor of 10000-20000 in S/N)

THE INTERNATIONAL AXION OBSERVATORY (IAXO)

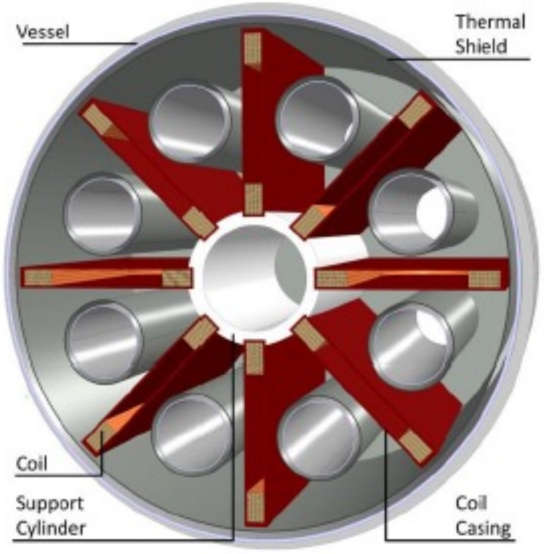

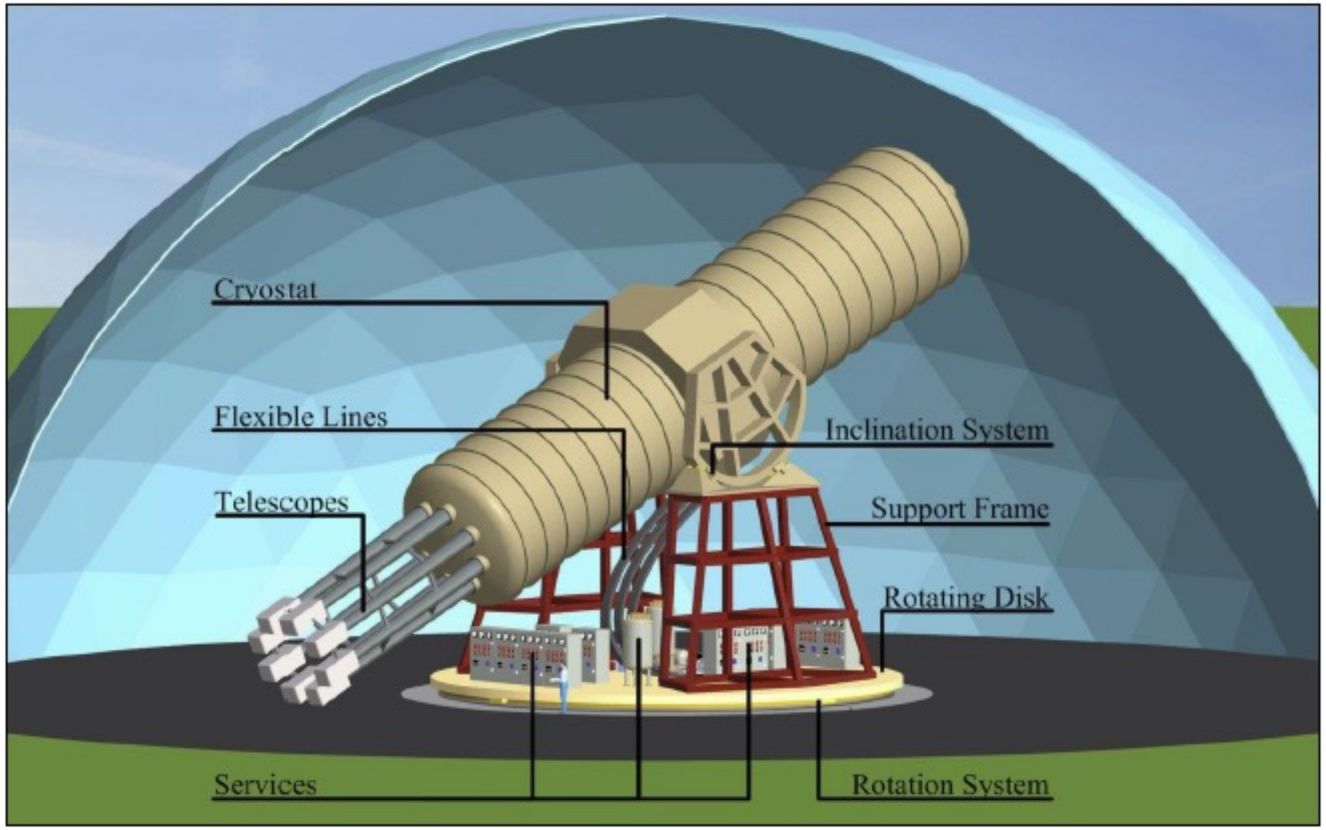

Need new magnet w/
- Much bigger aperture: $\sim$1 m^2 per bore
- Lighter (no iron yoke)
- Bores at T_{room}

- Irastorza et al.: Towards a new generation axion helioscope, arXiv:1103.5334
- Armengaud et al.: Conceptual Design of the International Axion Observatory (IAXO), arXiv:1401.3233

BABY-IAXO AND IAXO PHYSICS REACH

IAXO will probe:

- QCD axions in meV to eV mass band
- Astrophysically hinted regions invoked to solve stellar cooling anomaly
- Cosmologically interesting regions
  - Viable QCD axion DM models
  - ALP DM+inflation models
- Large generic unexplored ALP space
  - Down to $g_{a\gamma}$ ~ few 10^{-12} GeV^{-1}
  - Down to g_{ae} ~ few 10^{-13}
  - Including ALP region astrophysically invoked to solve the transparency anomaly

→ All, independent of the axion as DM

→ No other competing technique: IAXO unique

→ BabyIAXO will already have relevant intermediate physics potential!

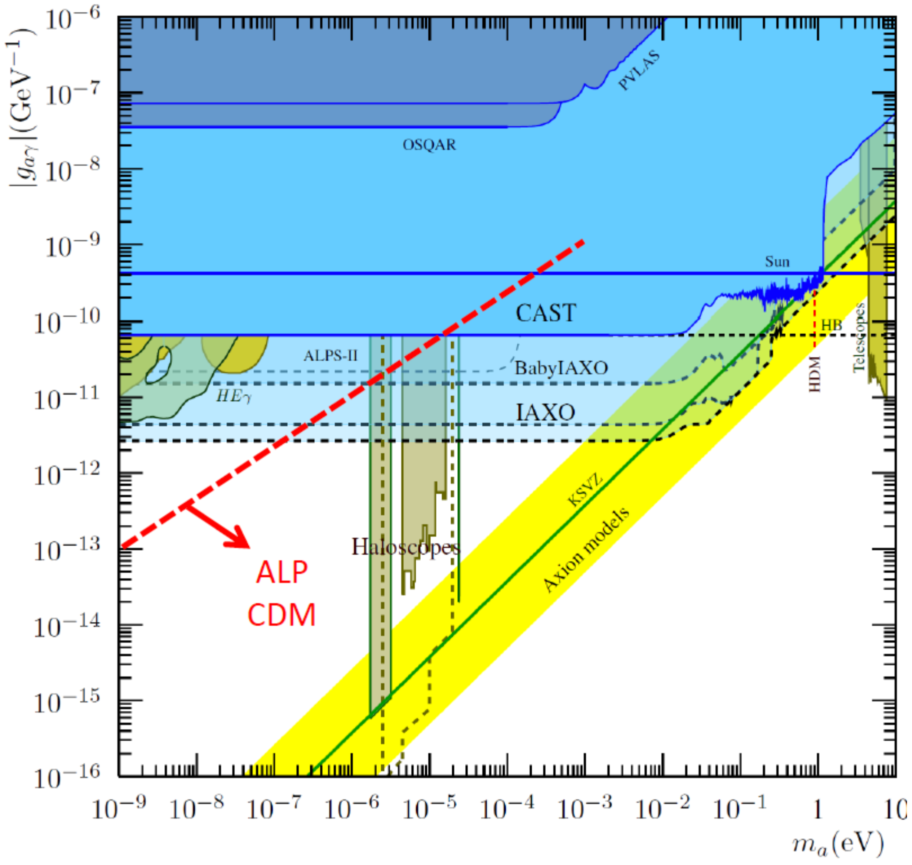

Review of Physics potential of IAXO arXiv:1904.09155

EVOLUTION "TRACKS" ON THE H-R DIAGRAM

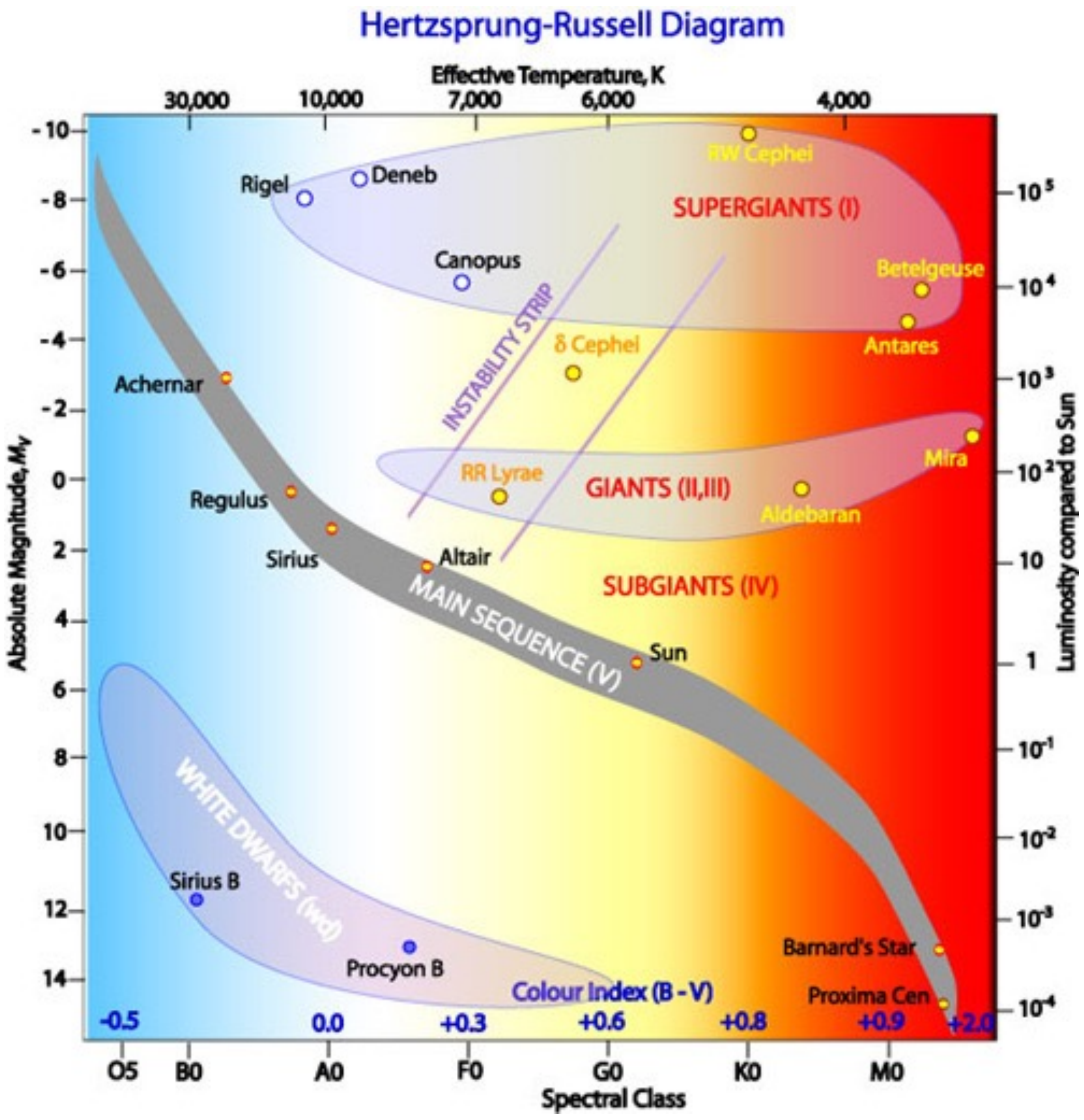

For animations look at: http://rainman.astro.illinois.edu/ddr/stellar/index.html

HYDROGEN EXHAUSTION

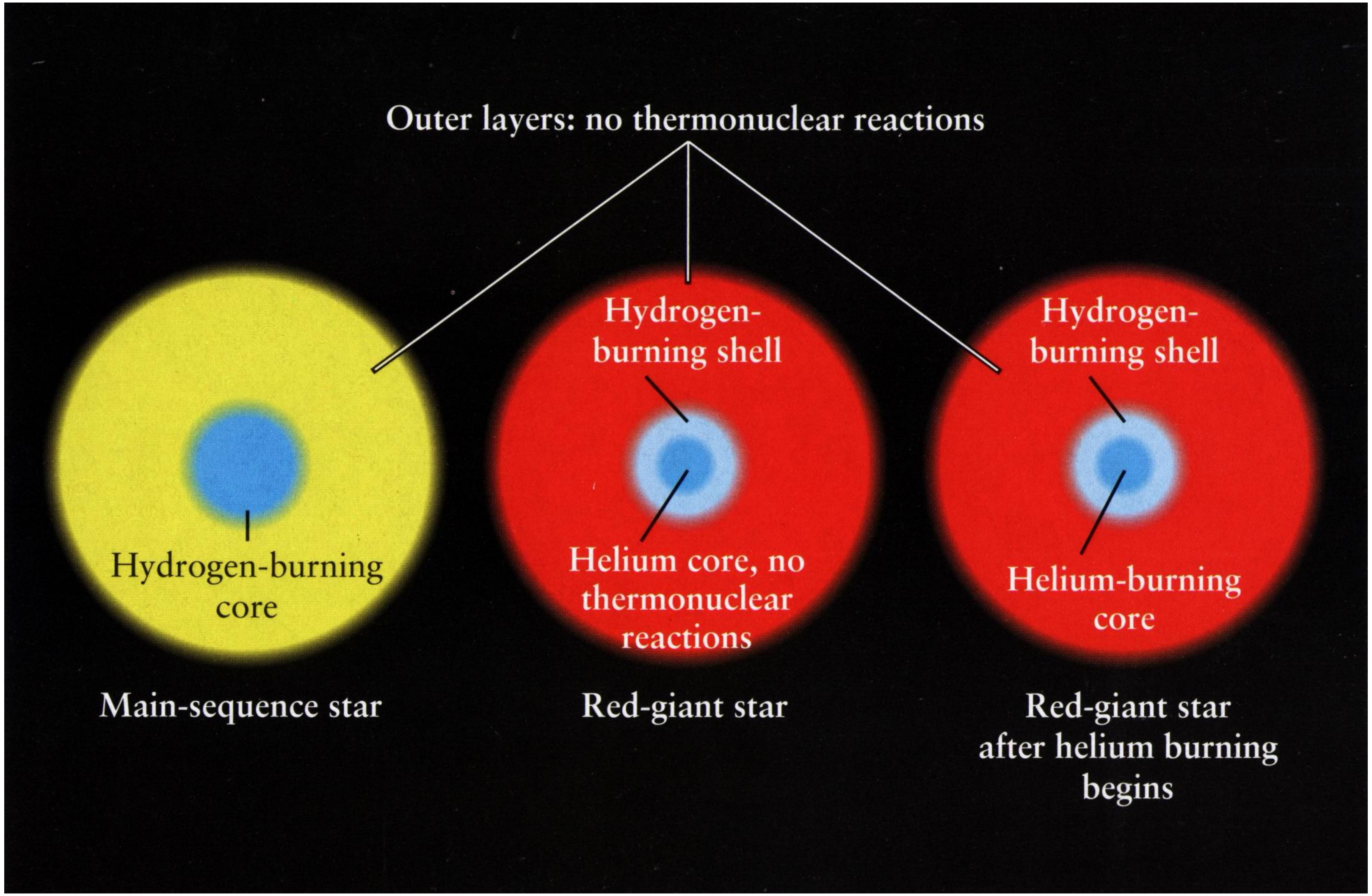

Evolution of Stars

$M \;□\; 0.08\, M_{sun}$	Never ignites hydrogen → cools ("hydrogen white dwarf")		Brown dwarf
$0.08 \;□\; M \lesssim 0.8\, M_{sun}$	Hydrogen burning not completed in Hubble time		Low-mass main-squence star
$0.8 \lesssim M \lesssim 2\, M_{sun}$	Degenerate helium core after hydrogen exhaustion		• Carbon-oxygen white dwarf • Planetary nebula
$2 \lesssim M \lesssim 5\text{–}8\, M_{sun}$	Helium ignition non-degenerate		
$5\text{–}8\, M_{sun} \lesssim M \;□\; ???$	All burning cycles → Onion skin structure with degenerate iron core	Core collapse supernova	• Neutron star (often pulsar) • Sometimes black hole? • Supernova remnant (SNR), e.g. crab nebula

GLOBULAR CLUSTERS

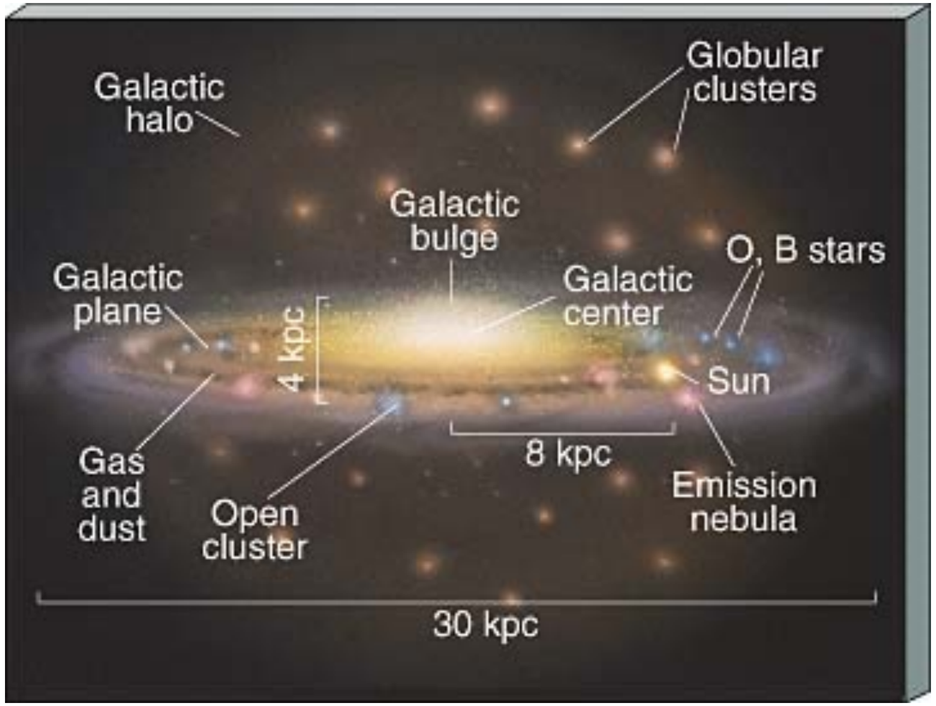

- Globular clusters are gravitationally bound associations of typically 10^6 stars
- The low metallicity is one indicator for their great age
- All stars in a given cluster are coeval; they differ only in their mass

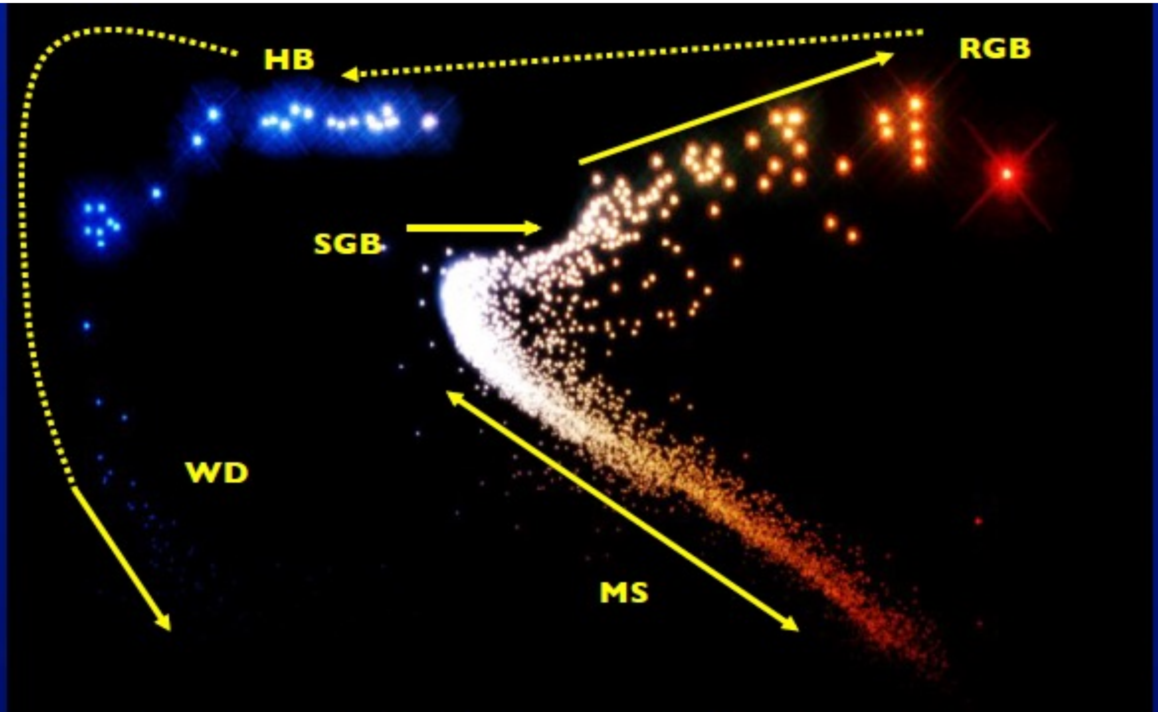

Since a star's color and brightness tell us its evolutionary phase, we can easily identify stars by phase in the image.

COLOR MAGNITUDE DIAGRAM FOR GLOBULAR CLUSTER

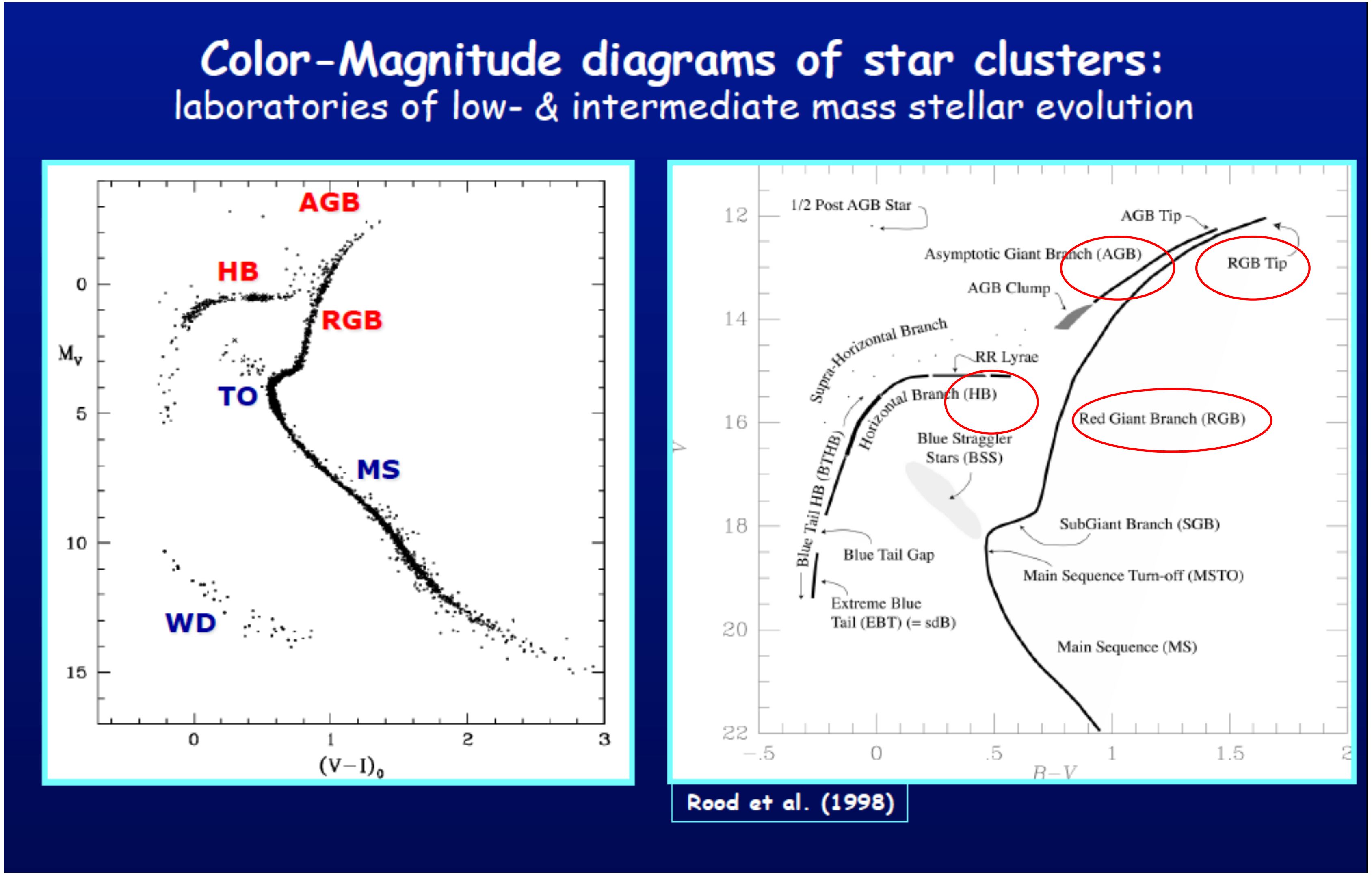

The color-magnitude diagram of a globular cluster represents an "isochrone" of a stellar population. Locus of coeval stars with different initial masses.

SENSITIVITY TO AXION EMISSION

$R = N_{HB}/N_{RG}$

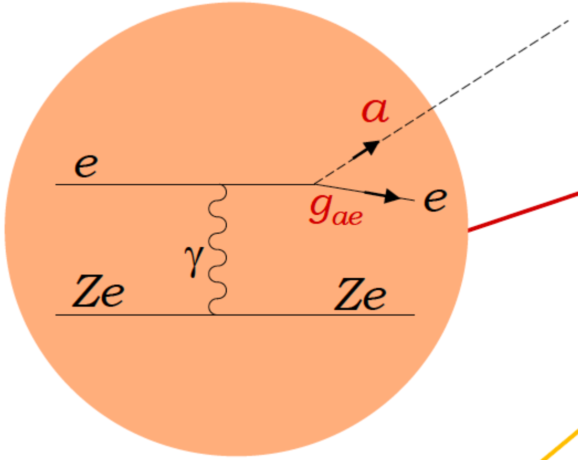

RGB: Very dense.
Sensitive to g_{ae}

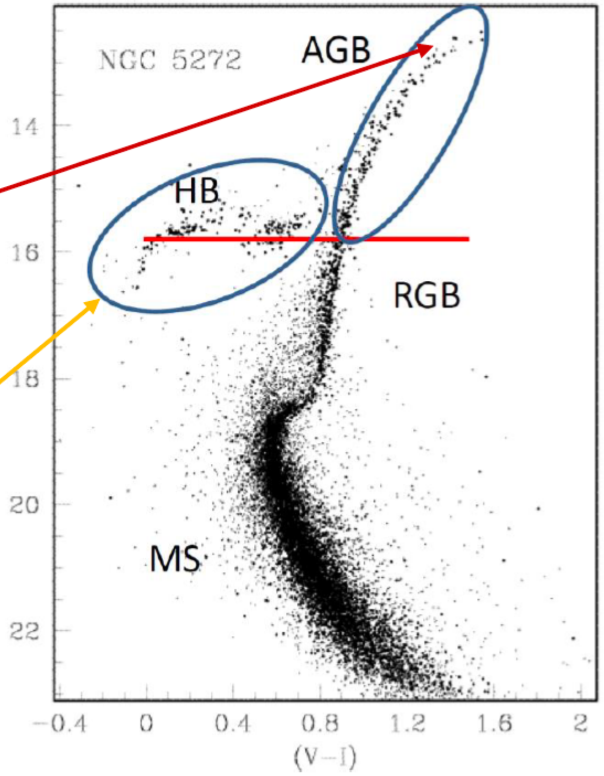

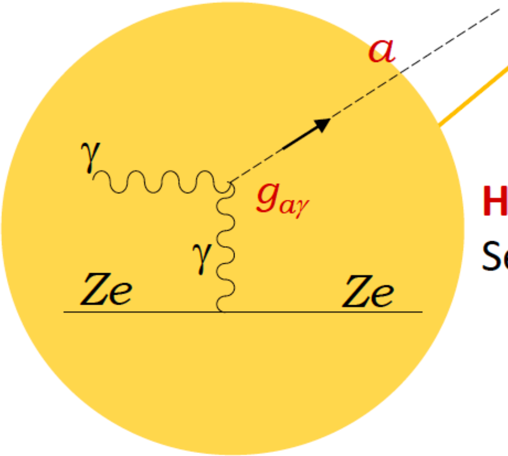

HB: Not very dense.
Sensitive to $g_{a\gamma}$

Straniero (proc. of XI Patras Workshop, 2015)

M.G., Irastorza, Redondo, Ringwald (2015)

HELIUM BURNING LIFETIME OF HB STARS

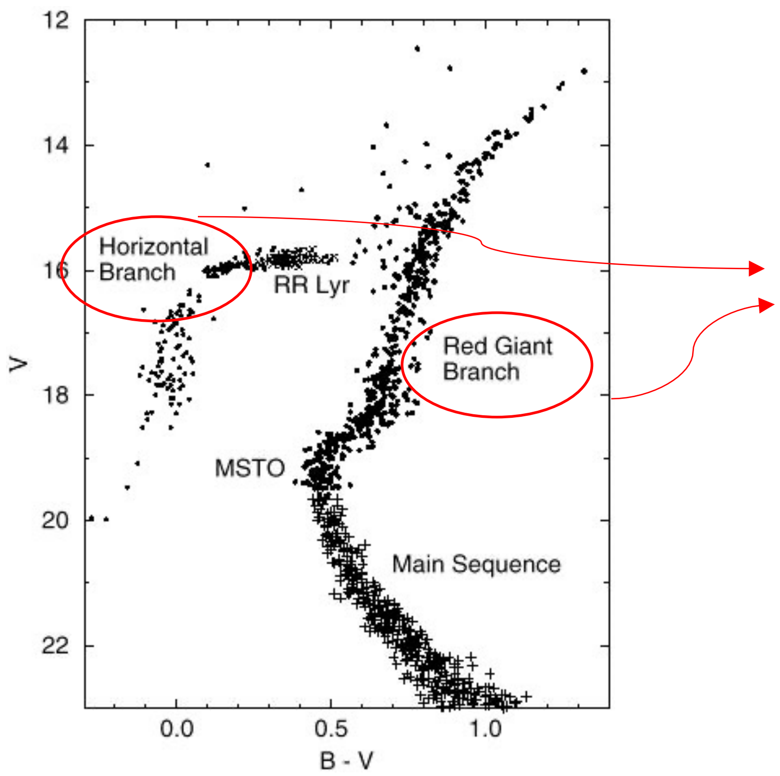

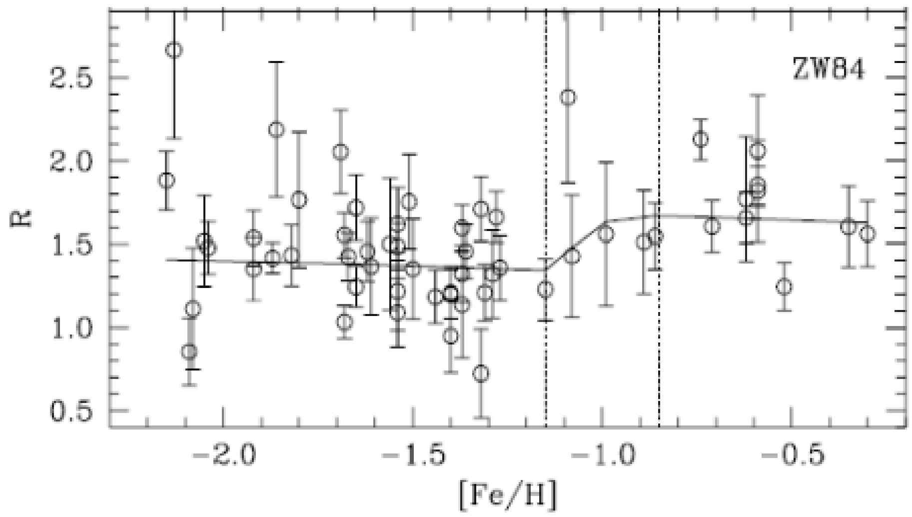

[Salaris et al., astro-ph/0403600]
57 GCs

$$R = \frac{N_{HB}}{N_{RGB}}$$

Well reproduced, within 30 %, by models of GC without axions

Axions would reduce the lifetime of stars in HB, while producing negligible change in RGB evolution (Primakoff rate suppressed in degenerate RGB core).
[Raffelt & Deaborn, PRD 36, 2211 (1987)]

AXION BOUND FROM HB vs CAST

[*Ayala, Dominguez, Giannotti, A.M., Straniero, 1406.6053*]

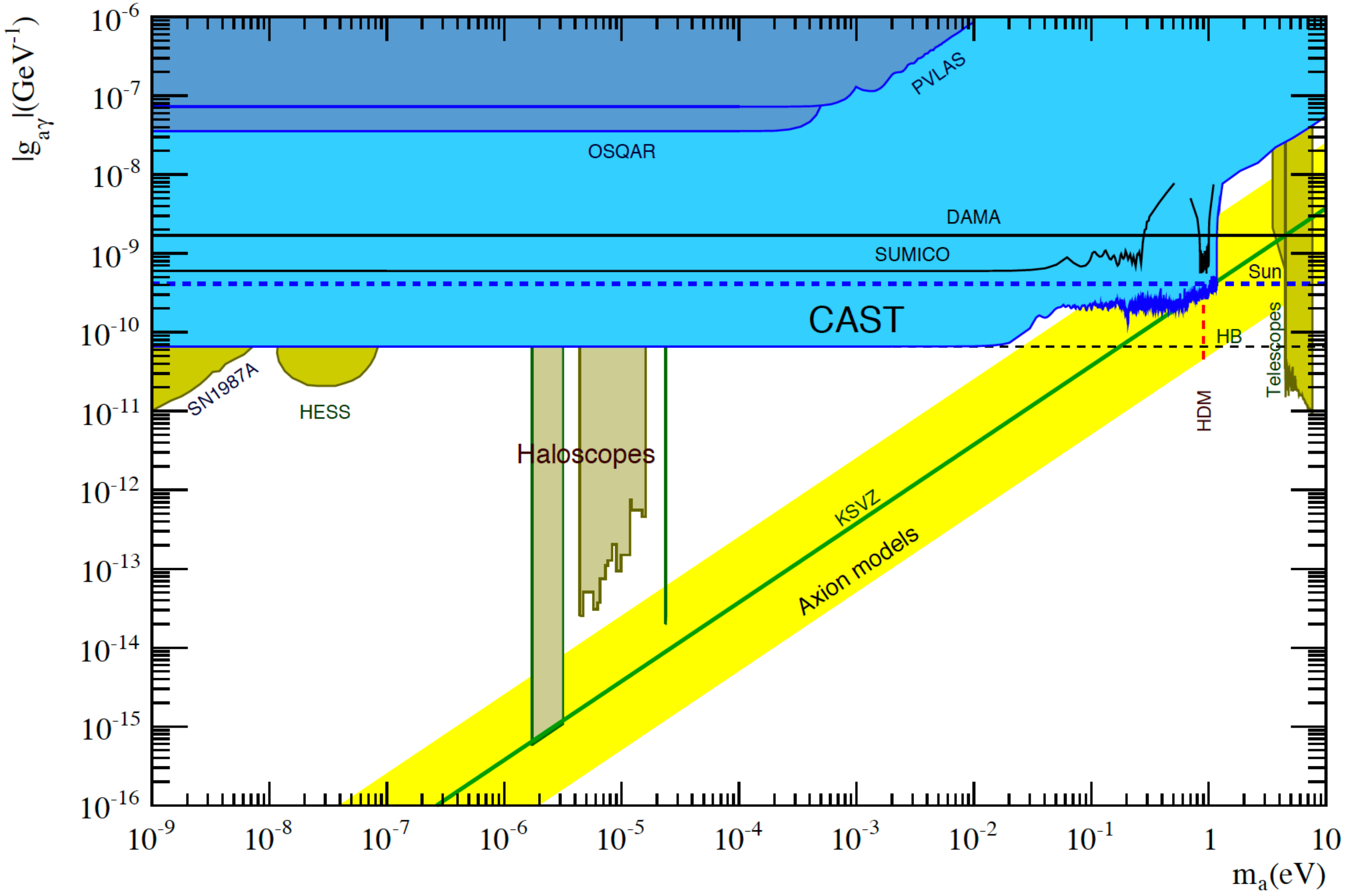

$$g_{a\gamma} < 0.66 \times 10^{-10} GeV^{-1} \quad (95\,\%\ CL)$$

The strongest bound on $g_{a\gamma}$ comparable with CAST one *[1705.02290]*

A COSMOLOGICAL PUZZLE: HOW TRANSPARENT IS THE UNIVERSE?

VHE photons from distant sources (hard) scatter off background photons (soft) thereby disappearing into electron-positron pairs.

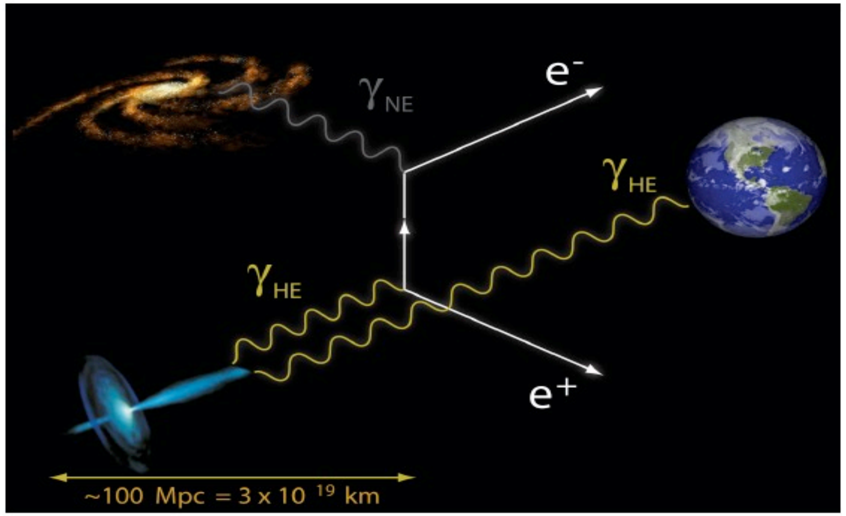

The dominant contribution to cosmic opacity comes from the extragalactic background light (EBL) produced by galaxies. Stellar evolution models + deep galaxy counts yield the spectral density of the EBL

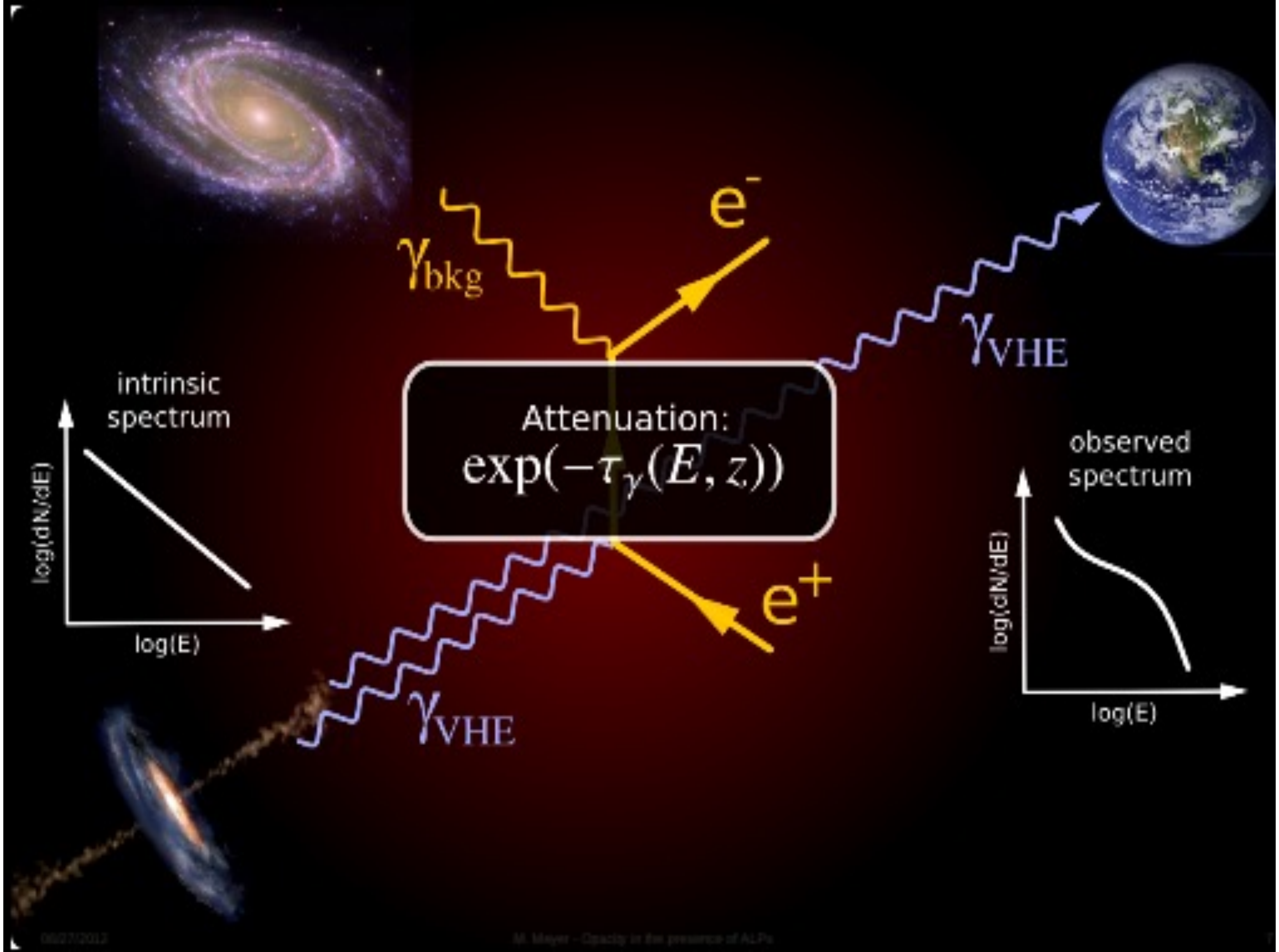

γbkg
e-
e+
γVHE
γVHE
Attenuation:
exp(−τγ(E, z))
intrinsic spectrum
log(dN/dE)
log(E)
observed spectrum
log(dN/dE)
log(E)

VHE EMISSION FROM GRB221009A

- On 11/10/2022 the LHAASO experiment has reported the observation of the Gamma Ray Burst GRB221009A [z=0.151] with more than 5000 very-high-energy (VHE) photons up to around 18 TeV

- On 12/10/2022 the Carpet-2 at Baksan Neutrino Observatory has detected – still from the gamma ray burst GRB221009A – an air shower consistent with being caused by a photon of energy 251TeV

These VHE photons cannot reach us from the assumed GRB redshift z = 0.151 unless unconventional particle physics is involved.

- Are ALPs at work?

[Galanti, Roncadelli, Tavecchio, 2210.05659, Baktash, Horns, Meyer, 2210.07172, Troitsky, 2210.09250, Carenza & Marsh, 2211.01010,..]

THE ALP (AXION-LIKE PARTICLE) HYPOTHESIS

If photon-ALP oscillations take place in intergalactic (or galactic) magnetic fields, photons can reach the observer even if distance from source >> mean free path, since ALPs are not absorbed !!

[De Angelis, Mansutti & Roncadelli, arXiv: 0707.4312, Simet, Hooper, Serpico, arXiv:0712.2825]

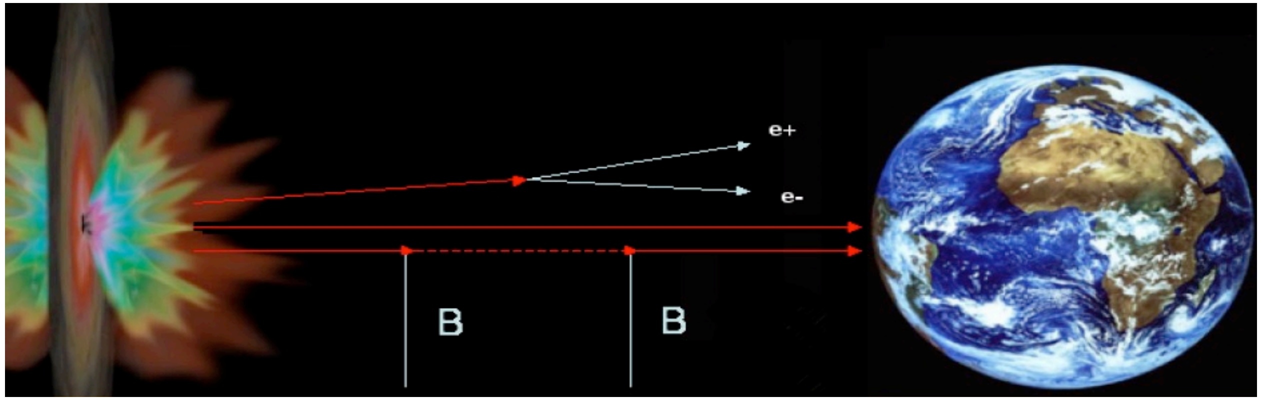

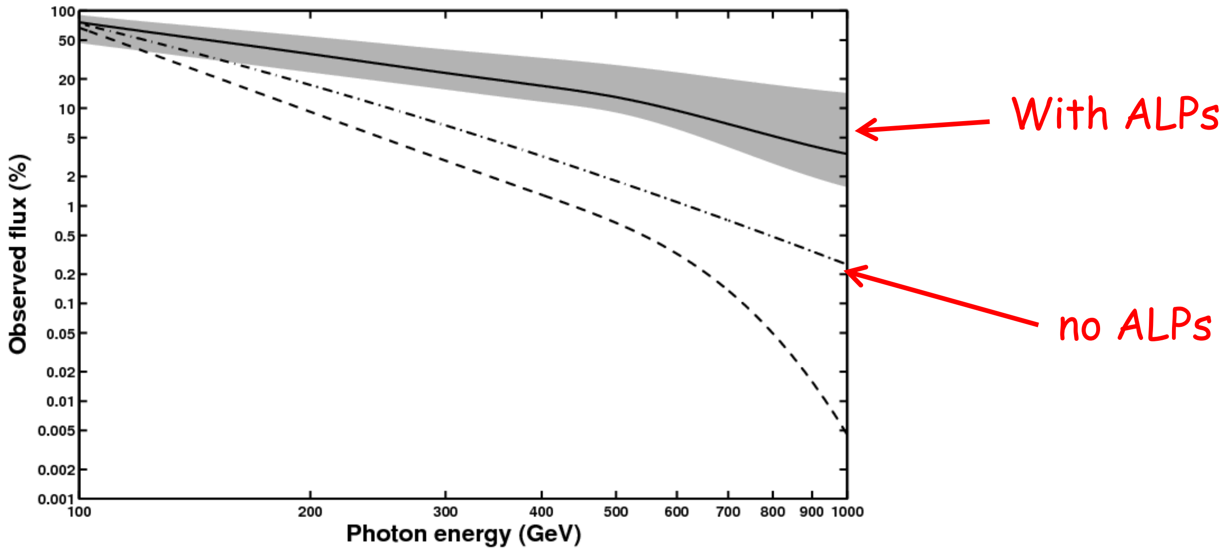

SENSITIVITY ON $g_{a\gamma}$ FROM VHE PHOTONS

[Meyer, Horns, Raue, arXiV:1302.1208, Conrad & Meyer, arXiV:1410 1556]

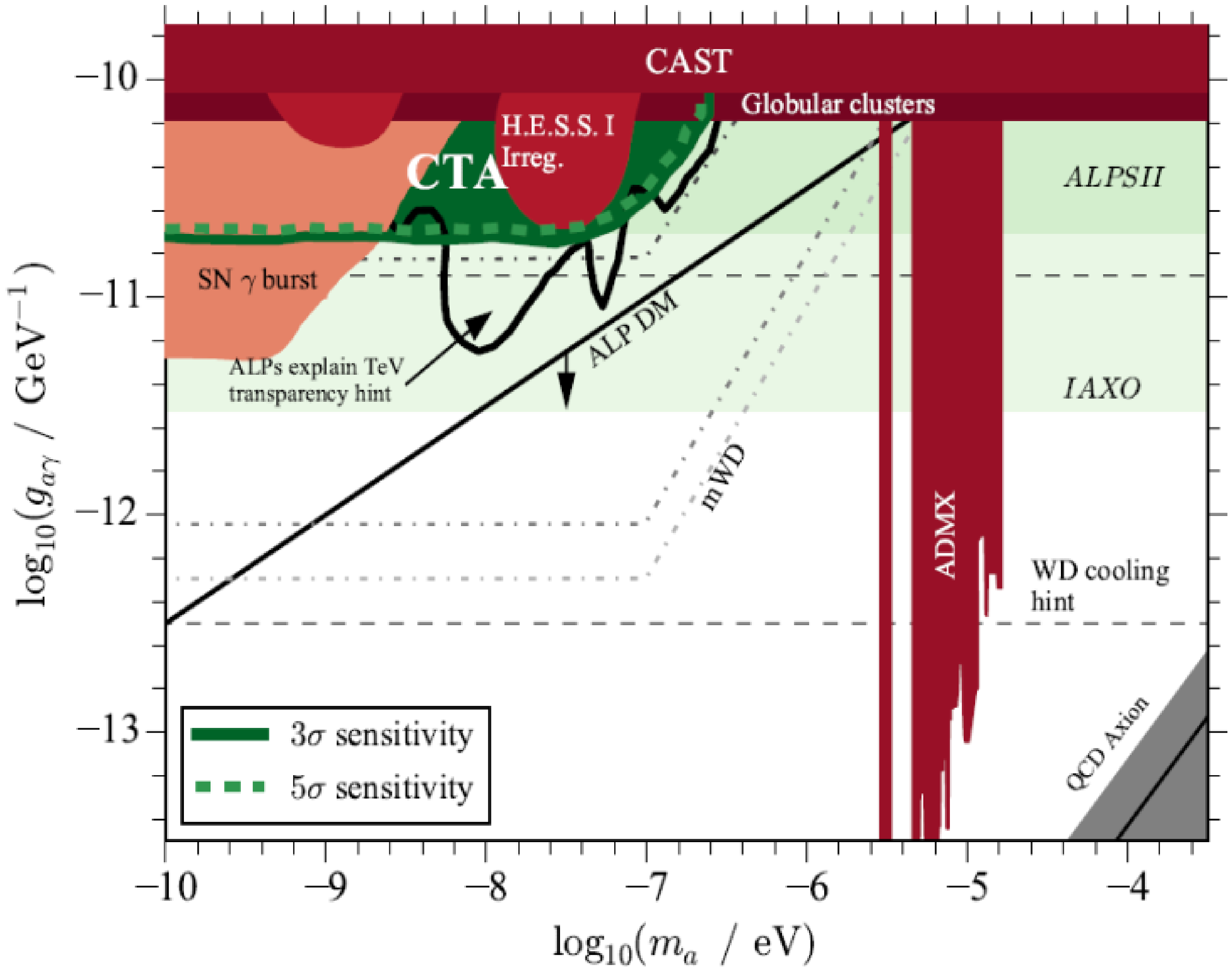

CONSTRAINING THE MODEL

[Dessert, Dunsky, Safdi, 2203.04319]

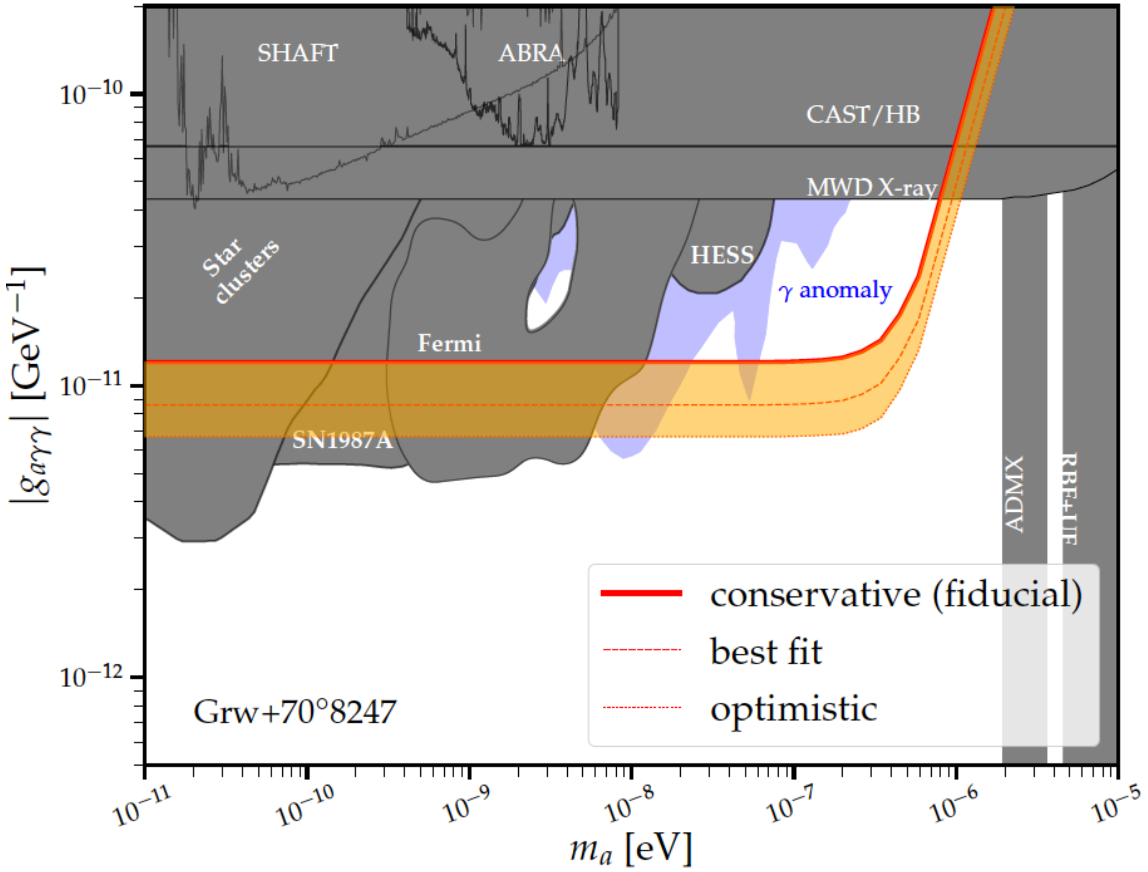

Fermi-LAT analysis of γ-spectrum of NGC 1275 in Perseus cluster [*Fermi collab., 1603.06978*] + SN 1987A bound + magnetic white dwarf polarization [Dessert, Dunsky & Safdi, 2203.04319] strongly constrain the parameter space for the model

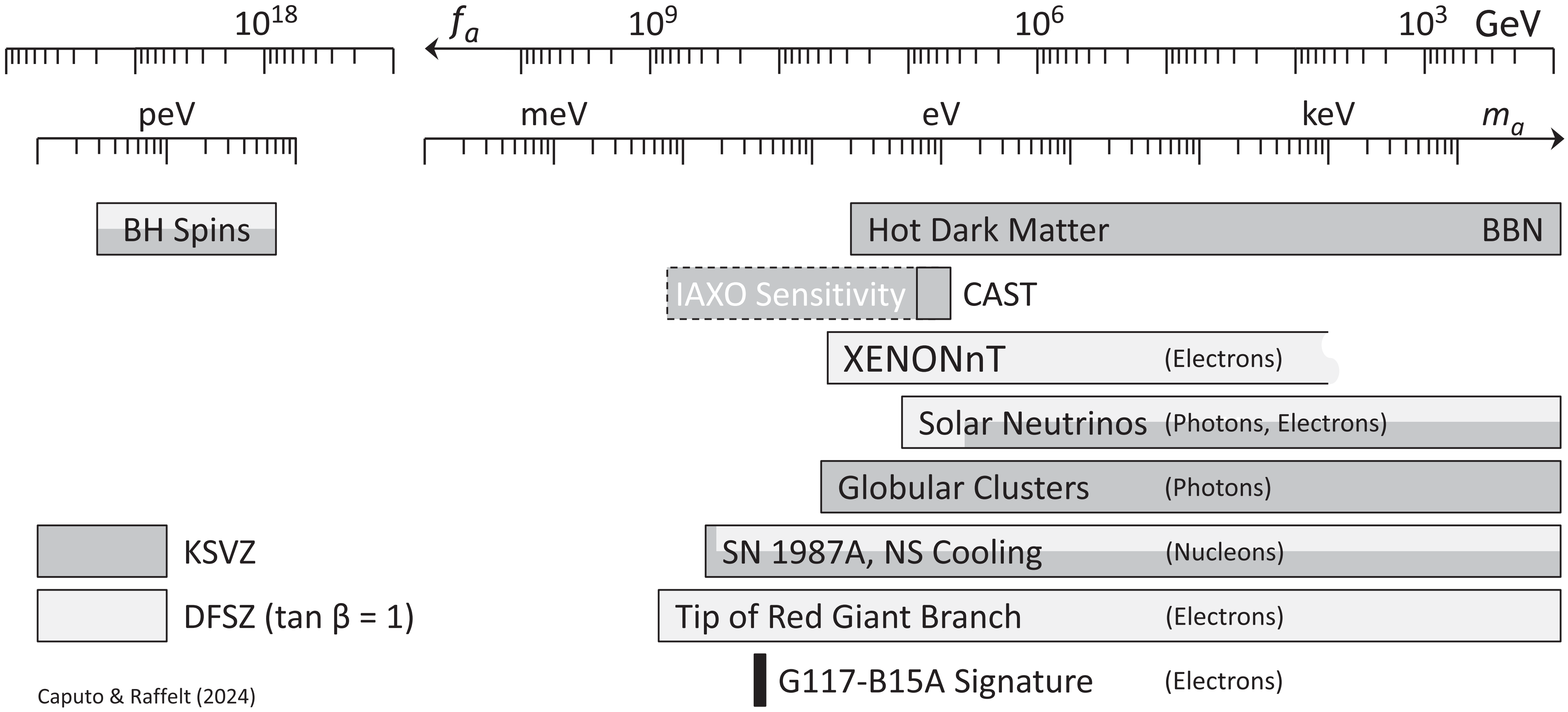

10^{18}
f_a
10^9
10^6
10^3 GeV
peV
meV
eV
keV
m_a
BH Spins
Hot Dark Matter
BBN
IAXO Sensitivity
CAST
XENONnT
(Electrons)
Solar Neutrinos
(Photons, Electrons)
Globular Clusters
(Photons)
KSVZ
SN 1987A, NS Cooling
(Nucleons)
DFSZ (tan β = 1)
Tip of Red Giant Branch
(Electrons)
G117-B15A Signature
(Electrons)
Caputo & Raffelt (2024)

2401.13728

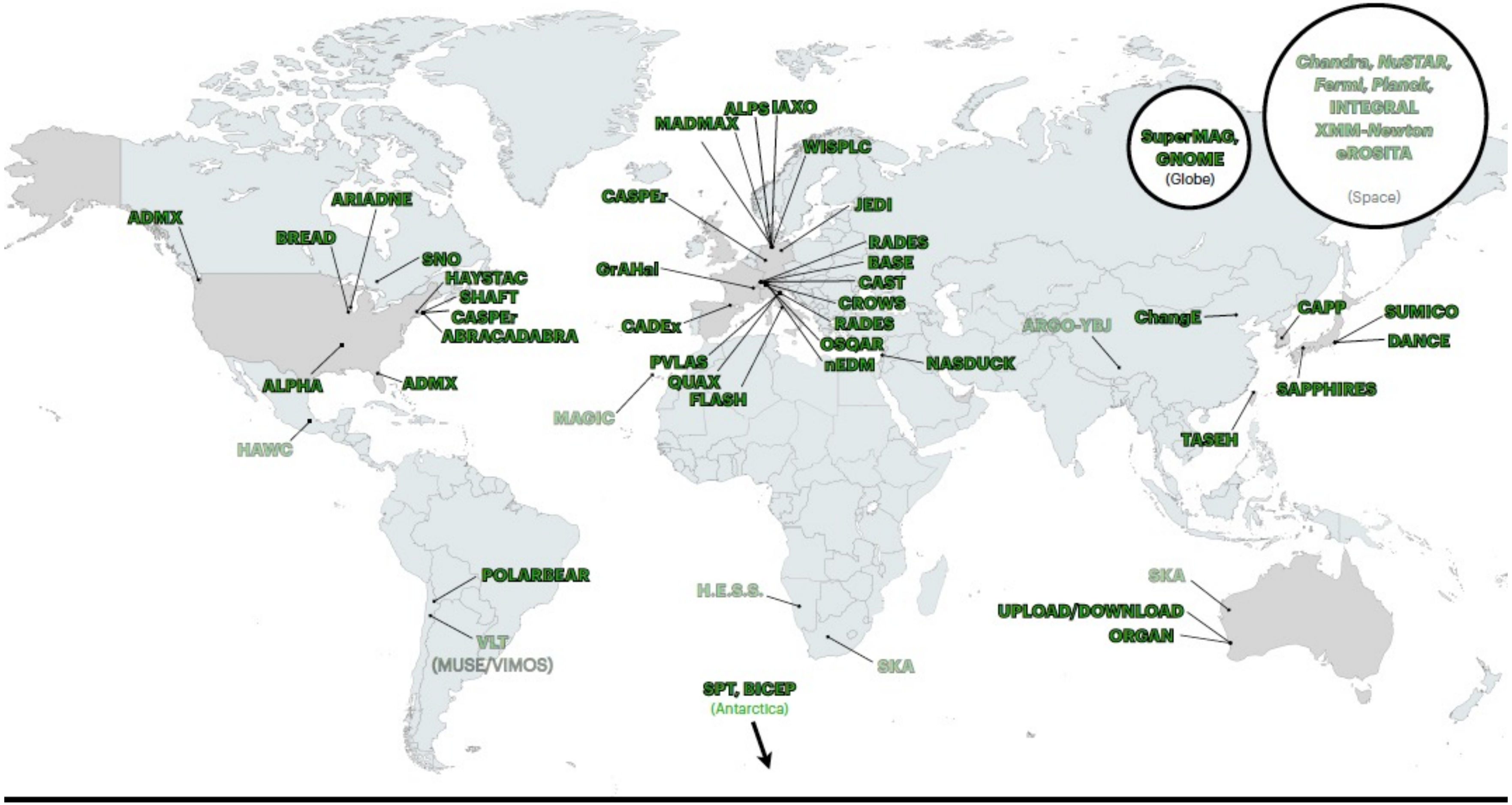
Chandra, NuSTAR, Fermi, Planck, INTEGRAL XMM-Newton eROSITA
(Space)
SuperMAG, GNOME
(Globe)
ALPS
IAXO
MADMAX
WISPLC
CASPEr
JEDI
RADES
BASE
GrAHal
CAST
CROWS
CADEx
RADES
OSQAR
nEDM
NASDUCK
PVLAS
QUAX
FLASH
MAGIC
ADMX
ARIADNE
BREAD
SNO
HAYSTAC
SHAFT
CASPEr
ABRACADABRA
ALPHA
ADMX
HAWC
ARGO-YBJ
ChangE
CAPP
SUMICO
DANCE
SAPPHIRES
TASEH
POLARBEAR
VLT
(MUSE/VIMOS)
H.E.S.S.
SKA
SPT, BICEP
(Antarctica)
SKA
UPLOAD/DOWNLOAD
ORGAN

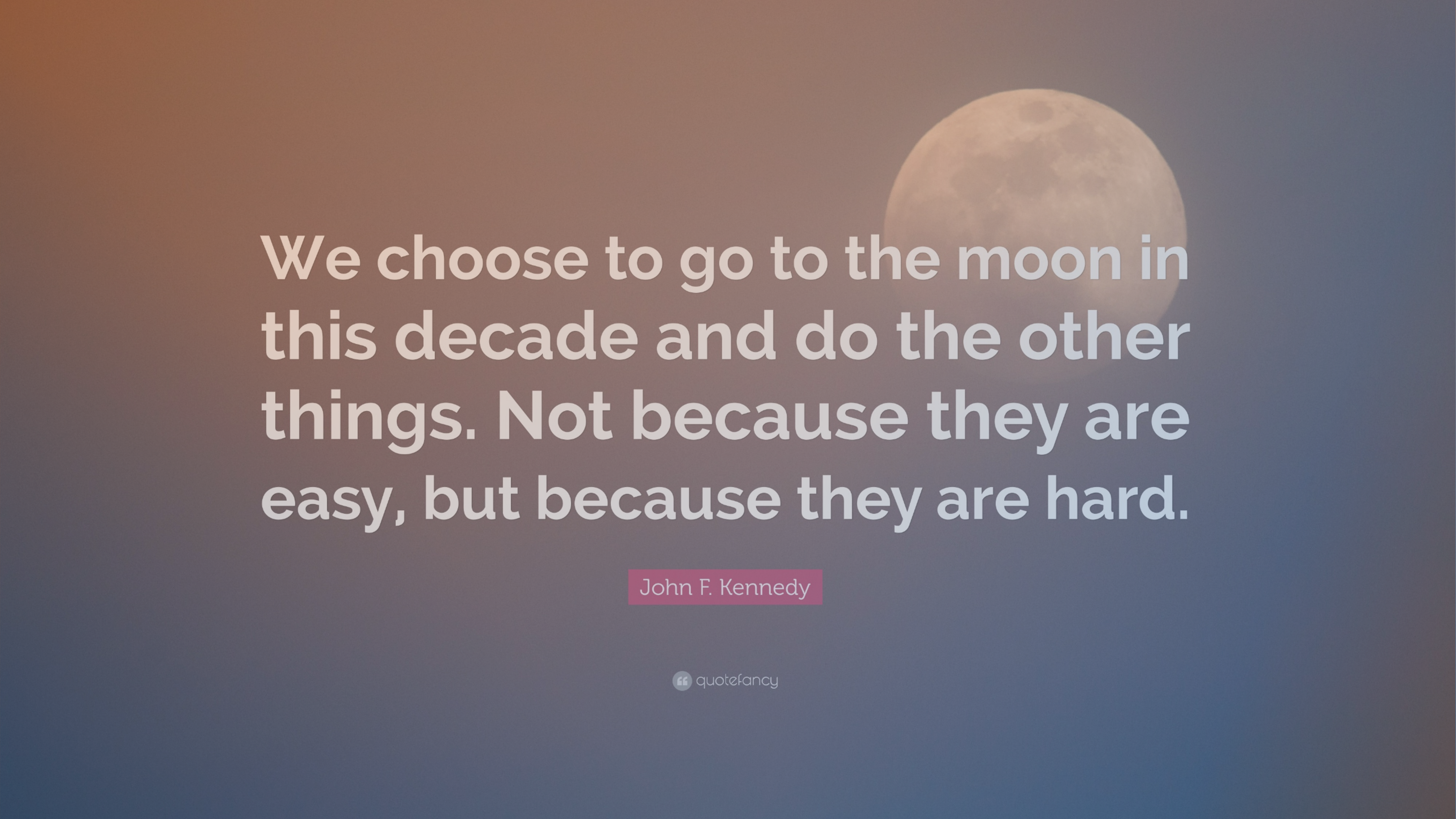
We choose to go to the moon in this decade and do the other things. Not because they are easy, but because they are hard.
John F. Kennedy
quotefancy

«Se non e' vero, e' molto ben trovato»
(Giordano Bruno's aphorism, 1582)

«Even if it is not true, it is a very good fabrication»